

Forschungszentrum Karlsruhe
Technik und Umwelt

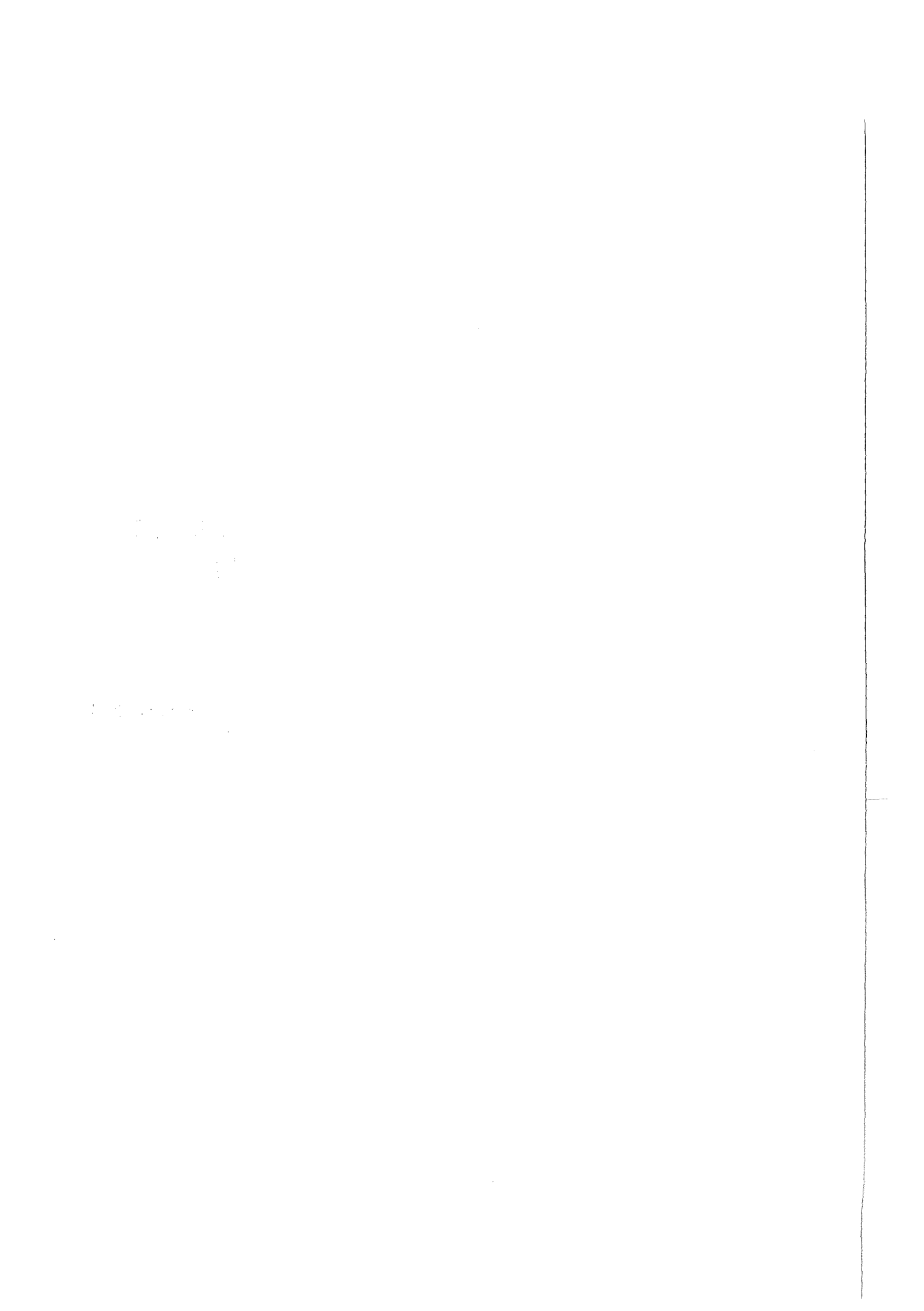
Wissenschaftliche Berichte
FZKA 6095

Thermal Properties of Transition Metals

K. Thurnay

**Institut für Neutronenphysik und Reaktortechnik
Projekt Nukleare Sicherheitsforschung**

Mai 1998



Forschungszentrum Karlsruhe

Technik und Umwelt

Wissenschaftliche Berichte

FZKA 6095

Thermal Properties of Transition Metals

K. Thurnay

Institut für Neutronenphysik und Reaktortechnik

Projekt Nukleare Sicherheitsforschung

Forschungszentrum Karlsruhe GmbH, Karlsruhe
1998

**Als Manuskript gedruckt
Für diesen Bericht behalten wir uns alle Rechte vor**

**Forschungszentrum Karlsruhe GmbH
Postfach 3640, 76021 Karlsruhe**

**Mitglied der Hermann von Helmholtz-Gemeinschaft
Deutscher Forschungszentren (HGF)**

ISSN 0947-8620

Abstract

The paper recommends mathematical descriptions for calculating vapor pressure, heat capacity, enthalpy and density in the solid and liquid states for the following transition metals: titanium, vanadium, chromium, manganese, iron, cobalt, nickel, niobium and molybdenum.

Thermische Eigenschaften der Übergangsmetalle

Zusammenfassung

Es werden mathematische Darstellungen vorgeschlagen für den Dampfdruck, die Wärmekapazität, die Enthalpie und die Dichte im festen und flüssigen Zustand der folgenden Übergangsmetalle: Titan, Vanadin, Chrom, Mangan, Eisen, Kobalt, Nickel, Niob und Molybdän.

Contents

1	Preface	1
2	Caloric properties of the transition metals	2
2.1	The properties in the solid state	2
2.2	The properties in the liquid state	3
3	The density of a transition metal	4
3.1	Density of the solid state	4
3.2	Density of the liquid state	5
3.3	The "calculated" density	5
4	Titanium	7
4.1	Phase transitions	7
4.2	Vapor pressure	8
4.3	Heat capacity and enthalpy	9
4.4	Thermal expansion and density	11
5	Vanadium	17
5.1	Phase transitions	17
5.2	Vapor pressure	19
5.3	Heat capacity and enthalpy	20
5.4	Thermal expansion and density.	21
6	Chromium	26
6.1	Phase transitions	26
6.2	Vapor pressure	28
6.3	Heat capacity and enthalpy	29
6.4	Thermal expansion and density.	30
7	Manganese	36
7.1	Phase transitions	36
7.2	Vapor pressure	37
7.3	Heat capacity and enthalpy	38
7.4	Thermal expansion and density	41

8 Iron	46
8.1 Phase transitions	46
8.2 Vapor pressure	47
8.3 Heat capacity and enthalpy	49
8.4 Thermal expansion and density	52
9 Cobalt	57
9.1 Phase transitions	57
9.2 Vapor pressure	58
9.3 Heat capacity and enthalpy	58
9.4 Thermal expansion and density	61
10 Nickel	67
10.1 Phase transitions	67
10.2 Vapor pressure	68
10.3 Heat capacity and enthalpy	69
10.4 Thermal expansion and density.	71
11 Niobium	77
11.1 Phase transitions	77
11.2 Vapor pressure	78
11.3 Heat capacity and enthalpy	79
11.4 Thermal expansion and density	81
12 Molybdenum	87
12.1 Phase transitions	87
12.2 Vapor pressure	89
12.3 Heat capacity and enthalpy	90
12.4 Thermal expansion and density	93
11 Bibliography	99
A The Debye-function	113
A.1 Heat capacity at low temperatures.	113
A.2 Expanding the functions at high temperatures	114
A.3 Expanding the functions at low temperatures	117
B Speakeasy routines to calculate caloric properties	121
B.1 Calculating the heat capacity	121
B.2 Calculating the enthalpy	123
B.3 Auxiliary routines	124

Glossary

$\alpha_L = \frac{1}{L} \frac{\partial L}{\partial T}$	coefficient of the linear thermal expansion	(1/K)
C_V	heat capacity at constant volume	(J/(molK))
C_P	heat capacity at constant pressure	(J/(molK))
$\Delta H_1, \Delta H_2, \dots$	transform heat(s) of the solid	(kJ/mol)
ΔH_{fus}	heat of fusion	(kJ/mol)
ΔH_{sub}	enthalpy of sublimation	(kJ/mol)
H	density of the enthalpy	(kJ/mol)
L	length	(m)
μ	atomic weight	(g/mol)
P	pressure	(Pascal)
p°	vapor pressure	(Pascal)
R_{gas}	Gas-Law constant	(J/(molK))
ρ	density	(kg/m ³)
ρ_{298}	standard density, $\rho(T = 25 C^\circ)$	(kg/m ³)
T	temperature	(K)
T_1, T_2, \dots	transform temperature(s) of the solid	(K)
T_B	boiling point	(K)
T_c	critical temperature	(K)
T_{Cu}	Curie temperature	(K)
T_M	meltig point	(K)
T_N	Nèel temperature	(K)
Θ_D	Debye-temperature	(K)
V	volume	(m ³)
	crystal structures	
bcc	body centered cubic	
c	cubic	
ccp	cubic close packed	
fcc	face centered cubic	
hcp	hexagonal close packed	

List of Figures

4.1	Titanium. Deviations of the vapor pressure data from the Dupré-Rankine description.	9
4.2	Titanium. Heat capacity C_P as a function of the temperature.	10
4.3	Titanium. C_P change at the $\alpha - \beta$ transition.	11
4.4	Titanium. Density as a function of the temperature.	13
4.5	Titanium. Thermal expansion as a function of the enthalpy.	14
4.6	Titanium. Enthalpy as a function of the temperature.	15
4.7	Titanium. Coefficient of the linear thermal expansion in the hcp-phase.	16
5.1	Vanadium. Deviations of the vapor pressure data from the Dupré-Rankine description.	19
5.2	Vanadium. Heat capacity C_P as a function of the temperature.	20
5.3	Vanadium. Comparison of the measured C_P -s.	21
5.4	Vanadium. Coefficient of the linear thermal expansion.	22
5.5	Vanadium. Thermal expansion as a function of the enthalpy.	23
5.6	Vanadium. Enthalpy as a function of the temperature.	24
5.7	Vanadium. Density as a function of the temperature.	25
6.1	Chromium. Vapor pressure - temperature graph	27
6.2	Chromium. Deviations of the vapor pressure data from the Dupré-Rankine description.	28
6.3	Chromium. Heat capacity C_P as a function of the temperature.	30
6.4	Chromium. Thermal expansion as a function of the enthalpy.	31
6.5	Chromium. Enthalpy as a function of the temperature.	33
6.6	Chromium. Coefficient of the linear thermal expansion.	34
6.7	Chromium. Density as a function of the temperature.	35
7.1	Manganese. Deviations of the vapor pressure data from the Dupré-Rankine description.	38
7.2	Manganese. Heat capacity in the bcc-phase.	39
7.3	Manganese. Heat capacity C_P as a function of the temperature.	40
7.4	Manganese. Coefficient of the linear thermal expansion in the bcc-phase.	41
7.5	Manganese. Enthalpy as a function of the temperature.	43
7.6	Manganese. Density as a function of the temperature.	44
7.7	Manganese. Thermal expansion as a function of the enthalpy.	45
8.1	Iron. Deviations of the vapor pressure data from the Dupré-Rankine description.	48
8.2	Iron. C_P change at the Curie-point.	49
8.3	Iron. Coefficient of the linear thermal expansion in the bcc-phase.	50

8.4 Iron. Density in the liquid state.	51
8.5 Iron. Thermal expansion as a function of the enthalpy.	52
8.6 Iron. Heat capacity C_P as a function of the temperature.	54
8.7 Iron. Enthalpy as a function of the temperature	55
8.8 Iron. Density as a function of the temperature.	56
9.1 Cobalt. Deviations of the vapor pressure data of Hultgren from the Dupré-Rankine description.	59
9.2 Cobalt. Heat capacity C_P as a function of the temperature.	60
9.3 Cobalt. C_P change at the Curie-point.	61
9.4 Cobalt. Coefficient of the linear thermal expansion in the hcp-phase.	62
9.5 Cobalt. Density in the liquid state.	63
9.6 Cobalt. Thermal expansion as a function of the enthalpy.	64
9.7 Cobalt. Enthalpy as a function of the temperature	65
9.8 Cobalt. Density as a function of the temperature.	66
10.1 Nickel. Deviations of the vapor pressure data from the Dupré-Rankine description.	69
10.2 Nickel. Heat capacity C_P as a function of the temperature.	70
10.3 Nickel. C_P change at the Curie-point.	71
10.4 Nickel. Thermal expansion as a function of the enthalpy.	73
10.5 Nickel. Enthalpy as a function of the temperature	74
10.6 Nickel. Coefficient of the linear thermal expansion in the solid state.	75
10.7 Nickel. Density as a function of the temperature.	76
11.1 Niobium. Deviations of the vapor pressure data of Hultgren from the Dupré-Rankine description.	79
11.2 Niobium. Heat capacity C_P as a function of the temperature.	80
11.3 Niobium. C_P change at the melting-transition.	81
11.4 Niobium. Enthalpy change at the melting-transition	82
11.5 Niobium. Coefficient of the linear thermal expansion in the solid state.	83
11.6 Niobium. Thermal expansion as a function of the enthalpy.	84
11.7 Niobium. Enthalpy as a function of the temperature	85
11.8 Niobium. Density as a function of the temperature.	86
12.1 Molybdenum. Deviations of the vapor pressure data from the Dupré-Rankine description.	87
12.2 Molybdenum. Heat capacity C_P as a function of the temperature.	90
12.3 Molybdenum. C_P change at the melting-transition.	91
12.4 Molybdenum. Enthalpy change at the melting-transition	92
12.5 Molybdenum. Coefficient of the linear thermal expansion in the solid state.	93
12.6 Molybdenum. Thermal expansion as a function of the enthalpy.	94
12.7 Molybdenum. Enthalpy in the solid state	96
12.8 Molybdenum. Density as a function of the temperature.	97
A.1 Caloric properties of a material with $\Theta_D = 350$ K after Debye	120

List of Tables

3.1 Measuring liquid metal densities	6
4.1 Titanium. Phases and structures in the solid state	7
4.2 Titanium. Transform properties	8
4.3 Titanium. Coefficients of the density description	12
4.4 Titanium. Coefficients of the description of the lattice parameters	14
5.1 Vanadium. Transform properties	17
5.2 Vanadium. Standard density data	18
5.3 Vanadium. Coefficients of the density description	18
6.1 Chromium. Transform properties	26
6.2 Chromium. Coefficients of the density description	32
7.1 Manganese. Transform properties	36
7.2 Manganese. Phases and structures in the solid state	37
7.3 Manganese. Coefficients of the density description	42
8.1 Iron. Transform properties	46
8.2 Iron. Phases and structures in the solid state	47
8.3 Iron. Estimated critical temperatures and pressures	48
8.4 Iron. Coefficients of the density description	53
9.1 Cobalt. Phases and structures in the solid state	57
9.2 Cobalt. Transform properties	58
9.3 Cobalt. Coefficients of the density description	64
10.1 Nickel. Phases and structures in the solid state	67
10.2 Nickel. Transform properties	68
10.3 Nickel. Coefficients of the density description	72
11.1 Niobium. Measured melting points	77
11.2 Niobium. Measured heats of fusion	78
11.3 Niobium. Coefficients of the density description	84
12.1 Molybdenum. Measured melting points	88
12.2 Molybdenum. Measured heats of fusion	89
12.3 Molybdenum. Coefficients of the density description	95
A.1 The first 16 coefficients of the developement of P(x), D(x) and C(x)	119

Chapter 1

Preface

In order to describe the phenomena and the consequences of a hypothetical core disruptive accident of a nuclear reactor thermophysical properties of the stainless steel are needed at temperatures in excess of 3000 K. In calculating the development of the temperature and pressure of the steel one needs mainly the shape of the saturation line, the thermal equation of state, $P(\rho, T)$ and the caloric equation of state, $C_V(\rho, T)$. The properties in question are required as a system of temperature and density functions, covering the liquid, the gaseous and the mixed states of the steel from the melting point to the critical point.

As a first step to this aim the paper recommends - using the available experimental data - mathematical descriptions for the vapor pressures, densities and caloric properties in the saturated solid and liquid states for the commonly used steel alloying metals, namely for the titanium, vanadium, chromium, manganese, iron, cobalt, nickel, niobium and molybdenum.

There exists - for most of the metals mentioned above - critical data compilations published in recent times. P. D. Desai tabulated in different papers vapor pressure and caloric data for vanadium, iron, manganese, molybdenum, nickel and titanium, [142], [145], [149], [153] and [154]. A. F. Guillermet (and coauthors) published caloric and thermal expansion properties for molybdenum, iron, cobalt and manganese as functions of the temperature and the pressure, [136], [139] and [169]. A handbook of Touloukian and Ho, [120] from 1981 describes heat capacities, thermal expansions and thermal conductivities for most of the 3d-metals.

The present report gives an up-to-date version of the above properties in the saturated states of these metals as functions of the temperature and supplies the lacking properties for chromium and niobium taking into account most of the available papers published in the years 1960 - 1997.

To describe the heat capacities correctly at low temperatures Debye functions were used, with supplementary terms for rising T-s. The solid densities are developed from the coefficient of the linear thermal expansion, α_L . To calculate α_L again Debye-type functions were selected, to ensure, that densities and thermal expansions behave correctly at temperatures below the Debye-point.

Chapter 2

Caloric properties of the transition metals

2.1 The properties in the solid state

To calculate the heat capacity and the enthalpy of a solid substance at low temperatures one uses commonly the Debye-model (see e.g. [111]). According to this model at temperatures comparable or less than the "Debye-temperature" of the substance, Θ_D the enthalpy can be described with the help of $D(x)$, a specially adapted function as

$$H = H_D \equiv 3 R_{gas} \cdot T \cdot D\left(\frac{\Theta_D}{T}\right). \quad (2.1)$$

$D(x)$, the Debye-function is defined as

$$D(x) \equiv \frac{3}{x^3} \int_0^x \frac{dy}{e^y - 1} y^3. \quad (2.2)$$

Differentiating eq. 2.1 leads to the following expression for the heat capacity of the Debye-model:

$$C_{PD} \equiv \frac{\partial H_D}{\partial T} = 3 R_{gas} \cdot C\left(\frac{\Theta_D}{T}\right), \quad (2.3)$$

with

$$C(x) \equiv 4 D(x) - \frac{3 x}{e^x - 1}. \quad (2.4)$$

A more detailed description of the Debye-function can be found in Appendix A.

For temperatures far above the Debye-point the function C_{PD} remains constant, whereas the measured heat capacity increases, mainly by the increasing contributions of the free electrons and the vibration of the crystal-lattice. Hoch [38] proposed a supplementary T - polynomial to describe the electronic and vibrational contributions to the heat capacity:

$$C_{PH} \equiv b \cdot T + d \cdot T^3. \quad (2.5)$$

To the above C_P corresponds the following enthalpy-function:

$$H_H \equiv \frac{b}{2} T^2 + \frac{d}{4} T^4. \quad (2.6)$$

Some of the transition metals change - at a given temperature - their magnetic state or their crystal structure. In the vicinity of such transition points the heat capacity often displays a sharp increase with the temperature ("λ-points", see e.g. figure 4.3 on page 11). To describe these λ-points of the heat capacity a second supplementary function - an exponential one - is needed:

$$C_{PE} \equiv e^{(g+T \cdot h)} . \quad (2.7)$$

The enthalpy function corresponding to the exponential- C_P is

$$H_E \equiv \frac{1}{h} e^{(g+T \cdot h)} . \quad (2.8)$$

At some metals - such as the chromium and molybdenum - the melting is preceded by an intensive formation of vacancies in the lattice (s. e.g. [171]). This energy-consuming procedure leads to a sharp rise in the solid C_P , which needs also a 2.7 - type exponential term for a correct description (cf. e.g. figure 6.3 on page 30).

A typical heat capacity description in the solid state has consequently the form

$$C_P = C_{PD} + C_{PH} + C_{PE} . \quad (2.9)$$

2.2 The properties in the liquid state

The heat capacity of the liquid metals, C_{PL} remains, at reasonable temperatures, far away from the critical point constant, correspondingly the enthalpy, H_L is here a linear function of the temperature.

Chapter 3

The density of a transition metal

3.1 Density of the solid state

In developing the density for the solid state it is more convenient to begin with the coefficient of the thermal expansion, α_L and calculate from this property ρ , the density, for α_L reveals more information about the given material than the integrated property ρ . Describing the property α_L (T) itself, instead of ρ (T) ensures also, that at vanishing temperatures α_L will show the correct behaviour (s. e.g. figure 9.4 on page 62).

In constructing the thermal expansion one must at first find a satisfying description for the coefficient of the linear thermal expansion, defined as

$$\alpha_L \equiv \frac{1}{L} \frac{\partial L}{\partial T} . \quad (3.1)$$

The volumetric thermal expansion then can be calculated - at least at isotropic substances - by integrating α_L :

$$\frac{V(T)}{V(0)} = \exp [3 \int_0^T dy \alpha_L(y)] . \quad (3.2)$$

The density has a reciprocal relation to the volumetric thermal expansion:

$$\rho(T) \cdot V(T) = \rho_{298} \cdot V_{298} . \quad (3.3)$$

There is a wealth of measurements describing α_L of the transition metals. As the available data indicate, the temperature-shapes of α_L and of the heat capacities show a remarkable similarity to each other at moderate temperatures. It is therefore an obvious choice to describe α_L at low and moderate temperatures with a Debye-type function

$$c_D \equiv 3 R_{gas} \cdot C \left(\frac{\Theta_D}{T} \right) , \quad (3.4)$$

supported with a Hoch type function at higher temperatures

$$c_H \equiv b \cdot T + d \cdot T^3 . \quad (3.5)$$

If the α_L of the transition metal has λ -points - corresponding to the λ -points of the heat capacity - then a supplementary exponential function is also needed:

$$c_E \equiv \exp (g + T \cdot h) . \quad (3.6)$$

To get the right size and the right dimension ($1/K$) a scaling factor "e" completes the description:

$$\alpha_L \equiv e \cdot \{c_D + c_H + c_E\} \quad . \quad (3.7)$$

Nota. Experimental data for the thermal expansion of a material is often given as the linear expansion relative to the old standard temperature 20 grade Celsius, i.e. as

$$\frac{\Delta L}{L} \equiv \frac{L(T) - L_{293}}{L_{293}} \quad . \quad (3.8)$$

(see e.g. Tolulokian and Ho, [120]). These data can be converted to the 25 centigrade volumetric data using the formulas

$$\begin{aligned} \frac{L}{L_{298}} &= \left(1 + \frac{\Delta L}{L} \right) \cdot \frac{L_{293}}{L_{298}} \quad , \\ \frac{V}{V_{298}} &= \left(\frac{L}{L_{298}} \right)^3 \quad . \end{aligned} \quad (3.9)$$

3.2 Density of the liquid state

Dependable density data for the liquid metals are naturally much more scarce than they are for the solid state of the same metals. Only with the onset of the seventies began, for the liquid metals, the number of density measurements to increase significantly (s. table 3.1 on page 6).

Two new methods made possible to get reliable data for these high-temperature, mobile and chemically quite aggressive substances: the γ -attenuation technique and the method of isobaric expansion. The first method - Drotning, [115] gives a good description of the procedure - supplies the density-temperature-points directly, whereas with the method of the isobaric expansion - as explained for instance in [83] - one gets only a volume expansion - enthalpy dataset, which had to be translated later on into the density - temperature relation using the standard density of the metal and by inverting the corresponding $H(T)$ -equation.

3.3 The "calculated" density

The density relations, received partly by fitting the $\alpha_L(T)$ - data, partly by fitting linear $\rho(T)$ - functions to the liquid density data are described for each metal with a set of temperature-dependent polynomials:

$$\rho(T) = \sum_{k=0}^3 A_k T^k \quad . \quad (3.10)$$

Authors	Nb	Mo	Ti	V	Cr	Mn	Fe	Co	Ni
Cahill, Kirshenbaum, 1962						A		A	
Lucas, 1972							A	A	A
Frohberg, Weber, 1964							B	B	
Saito, Watanabe, 1971							B	B	
Saito, Sakuma, Shiraishi, 1969			L	L	L	L	L	L	L
Drotning, 1979 - 81							G	G	G
Basin, Kolotov, Stankus, 1979 - 93				G	G		G		
Ermachenkov, Grigoryan, Ostrovskii, Popov, 1980							G	G	G
Arkhangel'skii, Demina, Makeev, Popel', 1990					G		G		G
Gathers, Hixson, Hogson, Minichino, Shaner, Winkler, 1976 - 83	I	I	I	I					
Bauhof, Fucke, Kitzel, Seydel, Wadle, 1977 - 79		I	I	I			I	I	I
Gallob, Jaeger, Kaschnitz, Neger, Obendrauf, Pottlacher, 1985 - 94	I	I					I		I

Table 3.1: Measuring liquid metal densities

A = Archimedean method, [12], B = Bubble pressure method, [44],

L = Levitation method, [37], G = γ -attenuation technique, [115],

I = Isobaric expansion, [83].

Chapter 4

Titanium

4.1 Phase transitions

Range , T < K	Structure	Transform heat kJ/mol
1166	α - Ti , hcp	4.17
1943	β - Ti , bcc	13.75

Table 4.1: Titanium. Phases and structures in the solid state

Titanium is a lustrous, white metal. It has a low density, good strength and excellent corosions-resistance. The atomic weight of titanium is

$$\mu = 47.88 \frac{g}{mol} . \quad (4.1)$$

The enthalpy of sublimation of titanium is at T = 0 K (s. [3])

$$\Delta H_{sub} = 467.1 \frac{kJ}{mol} . \quad (4.2)$$

As the critical temperature of titanium Fortov, Dremin and Leont'ev, [74] estimate

$$T_c \sim 11\,790 \text{ K}. \quad (4.3)$$

Table 4.2 on page 8 presents recently measured data about transition points and transform heats of titanium.

Nota. The data of Hultgren, Desai, Hawkins, Gleiser, Kelley and Wagman, [56], as well as of Desai, [154] in this table are recommended values. Hultgren and Desai - a former coworker in the Hultgren group, now working at the CINDAS, Purdue University - critically evaluated various thermophysical properties of titanium - and other metals - using the existing body of measurements and recommend most probable values for them.

As the **melting point** of titanium I use the temperature measured in 1984 by Bedford, Bonnier, Mass and Pavese, [130]:

$$T_M = 1943 \text{ K} . \quad (4.4)$$

Reference			T_1 K	ΔH_1 kJ/mol	T_M K	ΔH_{fus} kJ/mol
Kohlhaas et al.,	1965	[21]	1167	4.15	-	-
Hultgren et al.,	1966	[56]	1155	4.26	1943	(15.46)
Treverton et al.,	1971	[47]	-	-	1943	13.23
Berezin et al.,	1974	[67]	-	-	1939	14.156
Kenisarin et al.,	1976	[77]	-	-	1941	-
Peletskii et al.,	1978	[90]	1155	4.36	-	-
Cezairliyan et al.,	1978	[91]	1166	4.17	-	-
Checkhovskoi et al.,	1981	[116]	-	-	1942	13.79
Bedford et al.,	1984	[130]	-	-	1943	-
P. D. Desai,	1987	[154]	1166	4.17	1945	14.55
McClure et al.,	1992	[178]	-	-	-	13.023

Table 4.2: Titanium. Transform properties

As the **heat of the fusion** I selected

$$\Delta H_{fus} = 13.75 \text{ kJ/mol} \quad (4.5)$$

consulting table 4.2.

As for the hcp \rightarrow bcc phase transition I followed Cezairliyan and Müller by setting

$$T_1 = 1166 \text{ K}, \quad \Delta H_1 = 4.17 \text{ kJ/mol} . \quad (4.6)$$

Table 4.1 on page 7 summarizes the data of the solid phases of titanium.

4.2 Vapor pressure

As the vapor pressure of titanium I use the data recommended by Desai. The data - given by him in tabulated form - can be approximated with the following Dupré-Rankine formula (p° in Pascals and T in Kelvins):

$$\log_{10} p^\circ = 17.1101 - \frac{24931.2}{T} - 1.39974 \cdot \log_{10} T \quad \text{for } T \leq T_M$$

and

$$(4.7)$$

$$\log_{10} p^\circ = 19.4704 - \frac{24689.6}{T} - 2.15530 \cdot \log_{10} T \quad \text{for } T \geq T_M .$$

The above eq. calculates

$$T_B = 3635.91 \text{ K} \quad (4.8)$$

as boiling point of titanium.

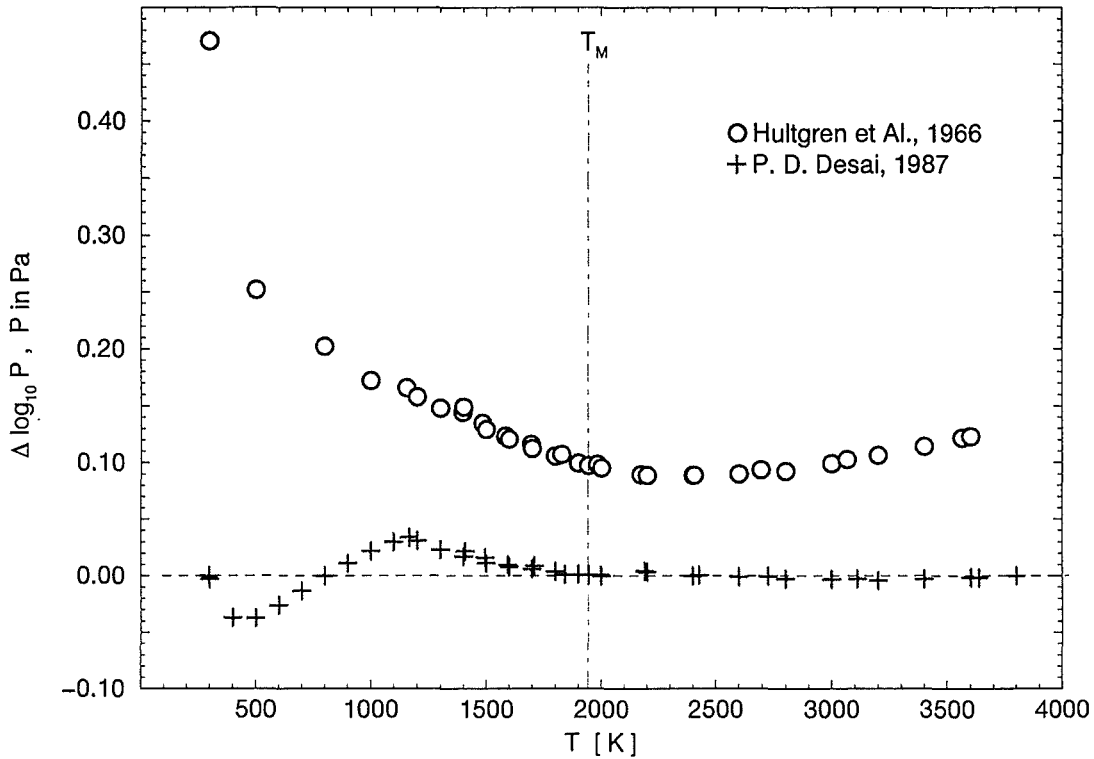


Figure 4.1: Titanium. Deviations of the vapor pressure data from the Dupré-Rankine description.

Figure 4.1 compares the vapor pressures, calculated via eq. 4.7 with the data of Desai ($\Delta P = P_{Desai} - P_{calc}$). The deviations of the data of Hultgren et al., [56] from the vapor pressure equation are also shown.

4.3 Heat capacity and enthalpy

For fitting the heat capacity of the α -Ti I selected the low-temperature data ($T \leq 300$ K) of Desai and the pre-transition points as well of Kohlhaas, Braun and Vollmer, [21] as of Peletskii and Zaretskii, [90]. Figure 4.3 on page 11 displays measured heat capacities in the vicinity of the $\alpha \rightarrow \beta$ transition. The filled resp. hollow circles of Peletskii et Zaretskii denote values, measured in different ways: in the first case the specimens were heated, in the second case they were cooled down.

The fitting resulted in the following C_P -description:

$$C_{P\alpha} = C_{PD} + C_{PH} + C_{PE} \quad \text{for } T \leq T_1 \quad (4.9)$$

with the parameters

$$\begin{aligned} \Theta_D &= 375 \text{ K} , \quad b = 0.0064 \frac{\text{J}}{\text{mol K}^2} , \quad d = 0 \\ g &= -9.2104 , \quad h = 0.0102332 \text{ 1/K} . \end{aligned} \quad (4.10)$$

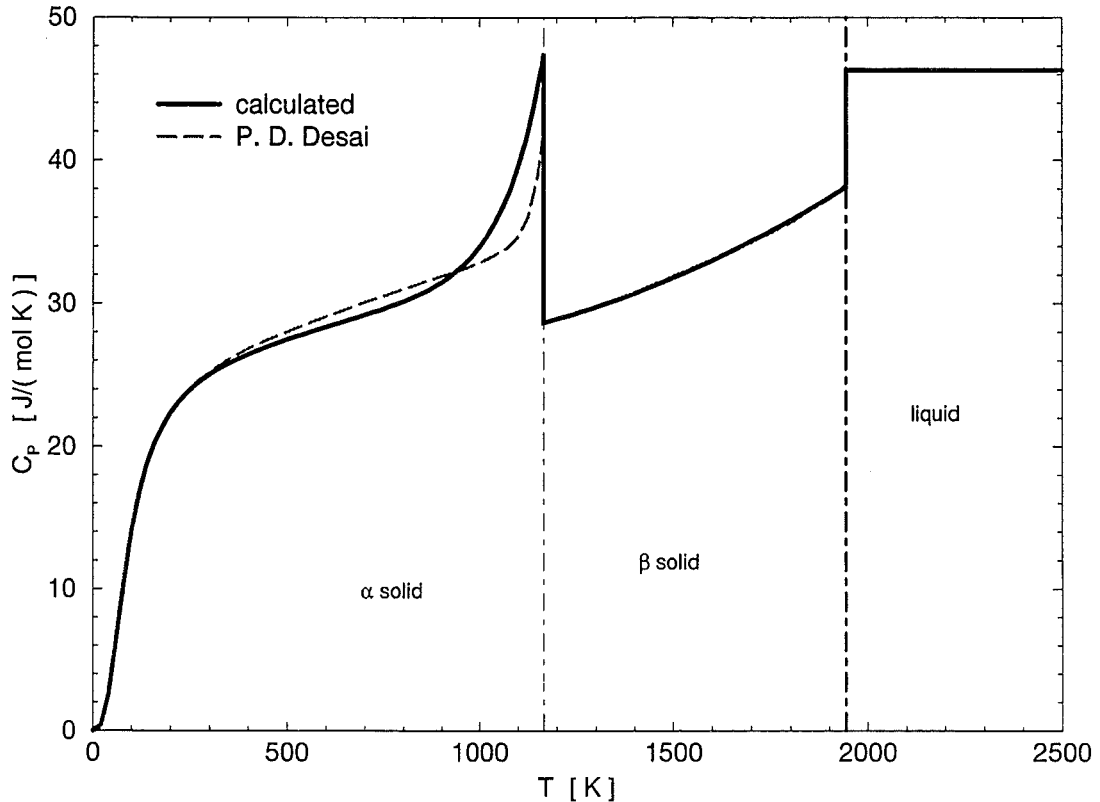


Figure 4.2: Titanium. Heat capacity C_P as a function of the temperature.

To describe the heat capacity of the β -Ti I fitted a polynomial to the data of Desai [154]:

$$C_{P\beta} [J/(mol \cdot K)] = 28.6558 - 7.27666 \cdot 10^{-3} T + 6.25205 \cdot 10^{-6} T^2$$

for $T_1 \leq T \leq T_M$. (4.11)

As the heat capacity of the liquidus I use the value recommended by Desai:

$$C_{PL} [J/(mol \cdot K)] = 46.29 \quad \text{for } T_M \leq T. \quad (4.12)$$

Figure 4.2 displays the heat capacity calculated by eq.s 4.9 - 4.12. As a comparison the recommended values of Desai are also shown.

According to eq.s 4.9 - 4.12 the enthalpy of titanium can be calculated as

$$H_\alpha(T) = H_D(T) + H_H(T) + H_E(T) \quad \text{for } T \leq T_1 \quad (4.13)$$

$$H_\beta(T) = H_\alpha(T_1) + \Delta H_1 + \int_{T_1}^T dt C_{P\beta}(t) \quad \text{for } T_1 < T \leq T_M$$

$$H_L(T) = H_\beta(T_M) + \Delta H_{fus} + C_{PL} \cdot (T - T_M) \quad \text{for } T_M < T.$$

Figure 4.6 on page 15 displays the calculated enthalpy. $H(T)$ is normalized to 298.15 K, the

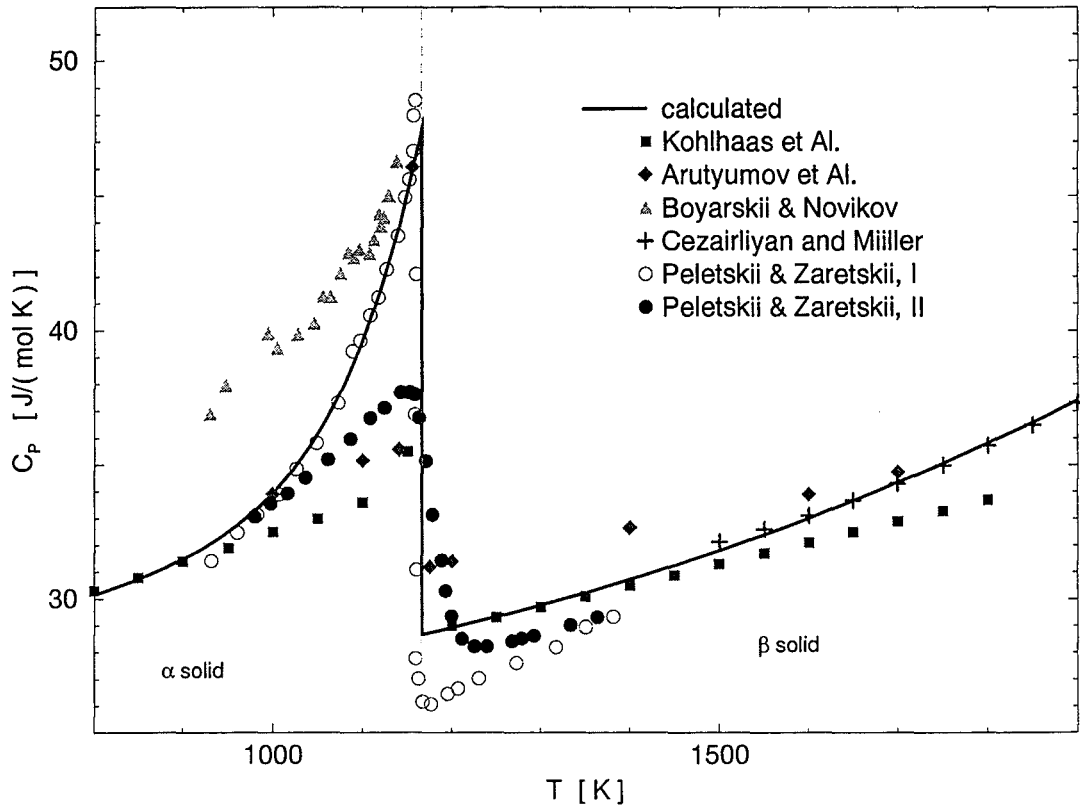


Figure 4.3: Titanium. C_P change at the $\alpha - \beta$ transition.

zero-point enthalpy being $H_0 = -4.79136 \text{ kJ/mol}$. The enthalpy data of Berezin et al., [67], Treverton and Margrave, [47] and of S. A. Kats, [95] are also shown on the figure.

4.4 Thermal expansion and density

In evaluating the density of titanium I used the data recommended by Touloukian, Kirby, Taylor and Desai in [69] for the solid phases and the data of Saito, Shiraishi, Sakuma, [37] for the liquid state.

Touloukian and Coauthors present thermal expansion data

for α - Ti, parallel to the main surface of the hcp-crystal
 for α - Ti, perpendicular to the the main surface
 and for polycrystalline α and β - Ti

as a relative expansion $\Delta L/L$, with the zero-point of ΔL at $T = 293 \text{ K}$. For the polycrystalline states they also tabulate the coefficients of the thermal expansion directly.

To describe the density of solid titanium I used the polycrystalline data of Touloukian et al..

In the α -solid I have taken not the $\Delta L/L$ -values for fitting, but the α_L - data, to get the correct density-behaviour at vanishing temperatures. To these points I fitted a Debye-type and

A_0	A_1	A_2	A_3
T \leq 200 K			
4535.63	0.0186272	$-5.10013 \cdot 10^{-4}$	$5.68528 \cdot 10^{-7}$
200 K < T \leq 1166 K			
4546.26	-0.105568	$-3.47491 \cdot 10^{-5}$	$8.16976 \cdot 10^{-9}$
1166 K < T \leq 1943 K			
4471.86	0.0406497	$-1.14497 \cdot 10^{-4}$	$2.03179 \cdot 10^{-8}$
1943 K < T			
4580.00	-0.2260	0.0	0.0

Table 4.3: Titanium. Coefficients of the density description

a Hoch-type function

$$\alpha_L = e \cdot (c_D + c_H) \quad \text{for } T \leq T_1 , \quad (4.14)$$

with a scaling factor of

$$e = 3.65 \cdot 10^{-7} \frac{\text{mol}}{J} . \quad (4.15)$$

In the fitting I used the same "Debye"- and "Hoch"-parameters, as in the C_P -description, i.e.

$$\Theta_D = 375 \text{ K} , \quad b = 0.0064 \frac{J}{\text{mol K}^2} , \quad d = 0.0 \quad (4.16)$$

(cf. eq. 4.10).

Fig. 4.7 on page 16 compares the data of Touloukian et al. with the function, calculated by eq.s 4.14 - 4.16. Measurements of Schmitz-Pranghe and Dünner, [35], Lesnaya, Volotkin, and Kashchuk, [81] and Yaggee et al., [36] are also shown. Schmitz-Pranghe and Dünner measured the thermal expansion of the lattice parameters a_{\parallel} resp. c_{\perp} . The functions shown on the figure resulted by fitting

$$a(T) = \sum_{k=0}^3 A_k T^k \quad (4.17)$$

type polynomials to their data (s. table 4.4 on page 14 for the coefficients) and building the derivatives according to eq. 3.1 in chapter 3.

Integrating the α_L function 4.14 (s. eq. 3.2) gives the volumetric thermal expansion, V/V_0 in the α - solid. V/V_{298} - displayed on fig. 4.5 - is normalized to have unit value at the standard temperature, 298 K.

In the β - solid I have taken simply the $\Delta L/L$ - polynomial supplied by Touloukian, calculated the L/L_{298} function and from this the volumetric thermal expansion as described in chapter 3.

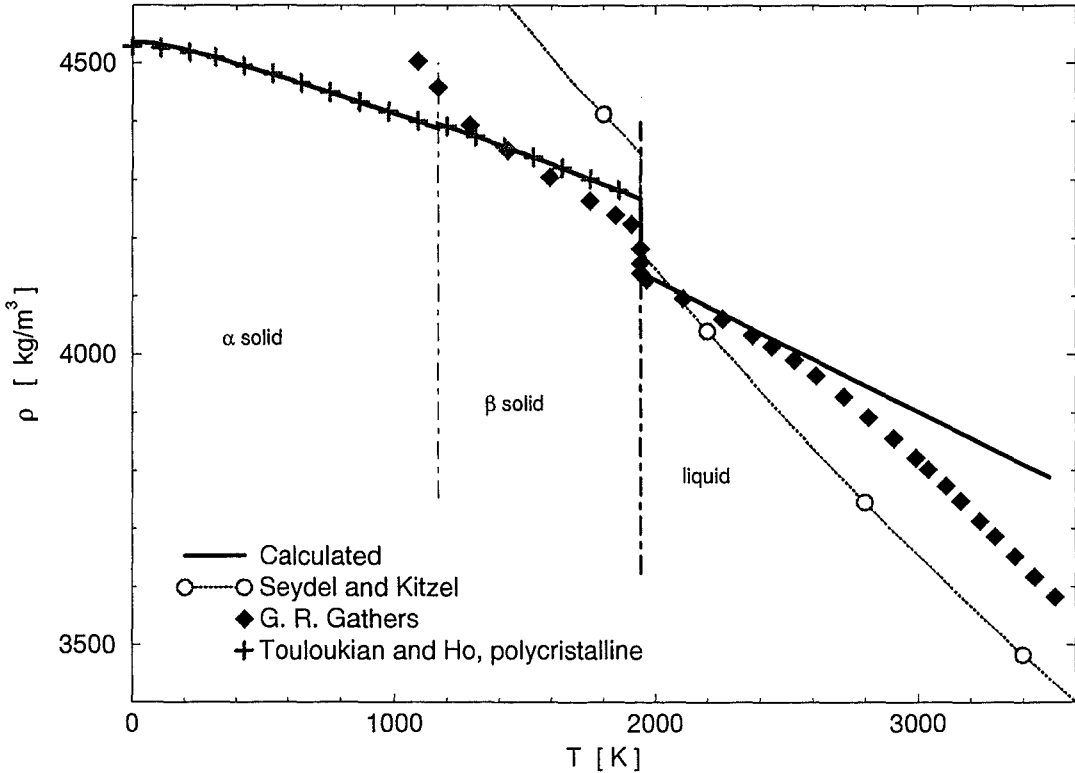


Figure 4.4: Titanium. Density as a function of the temperature.

The density of solid titanium can now be calculated from the volumetric thermal expansion by eq. 3.3. The standard density of titanium - which is also needed here - I have taken from Yaggee et al., [36] as

$$\rho_{298} = 4512 \text{ kg/m}^3 . \quad (4.18)$$

To simplify the calculation of titanium density three $\rho(T)$ polynomials were fitted to the density calculated above.

In liquid titanium I use the density polynomial of Saito et al.

Table 4.3 on page 12 collects all the coefficients of the polynomials describing the density in the different phases of titanium.

Figure 4.4 displays the density of titanium in the temperature dependence. The thermal expansion - enthalpy measurements of Seydel and Kitzel, [99] and of G. R. Gathers, [129] are also shown, converted to a $\rho(T)$ - function with the standard density and with the $H(T)$ - function 4.13.

Seydel and Kitzel present their volumetric thermal expansion as an enthalpy polynomial

$$\frac{V}{V_{298}} = 0.8762 + 0.1318 \cdot \Delta H + 4.953 \cdot 10^{-3} \cdot \Delta H^2$$

with $\Delta H \equiv H - H_{298}$ in $\frac{MJ}{kg}$. (4.19)

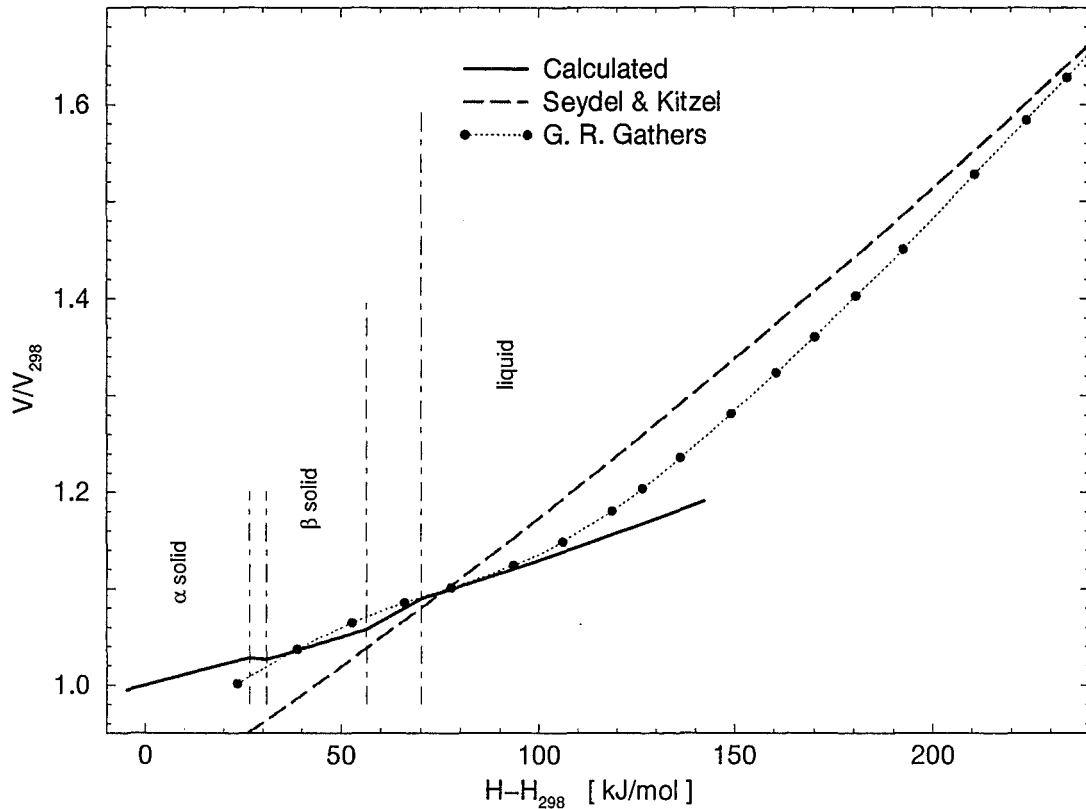


Figure 4.5: Titanium. Thermal expansion as a function of the enthalpy.

The data of Gathers I have taken from a picture. The points presented in fig. 4.4 are values from a smoothed function.

Figure 4.5 compares directly the thermal expansion - enthalpy measurements of Seydel & Kitzel and those of Gathers with the corresponding calculated property. The limiting enthalpy-values indicated in the figure are (in kJ/mol): 26.772, 30.942, 56.401, 70.151.

-	$a \parallel$ Å	$c \perp$ Å	a Å
A_0	2.9454	4.6736	3.2539
A_1	0.0	0.0	$4.7619 \cdot 10^{-5}$
A_2	$4.00 \cdot 10^{-8}$	$8.80 \cdot 10^{-8}$	0.0
A_3	$-2.80 \cdot 10^{-11}$	$-4.67 \cdot 10^{-11}$	0.0
A_4	$1.15 \cdot 10^{-14}$	$9.35 \cdot 10^{-15}$	0.0

Table 4.4: Titanium. Coefficients of the description of the lattice parameters

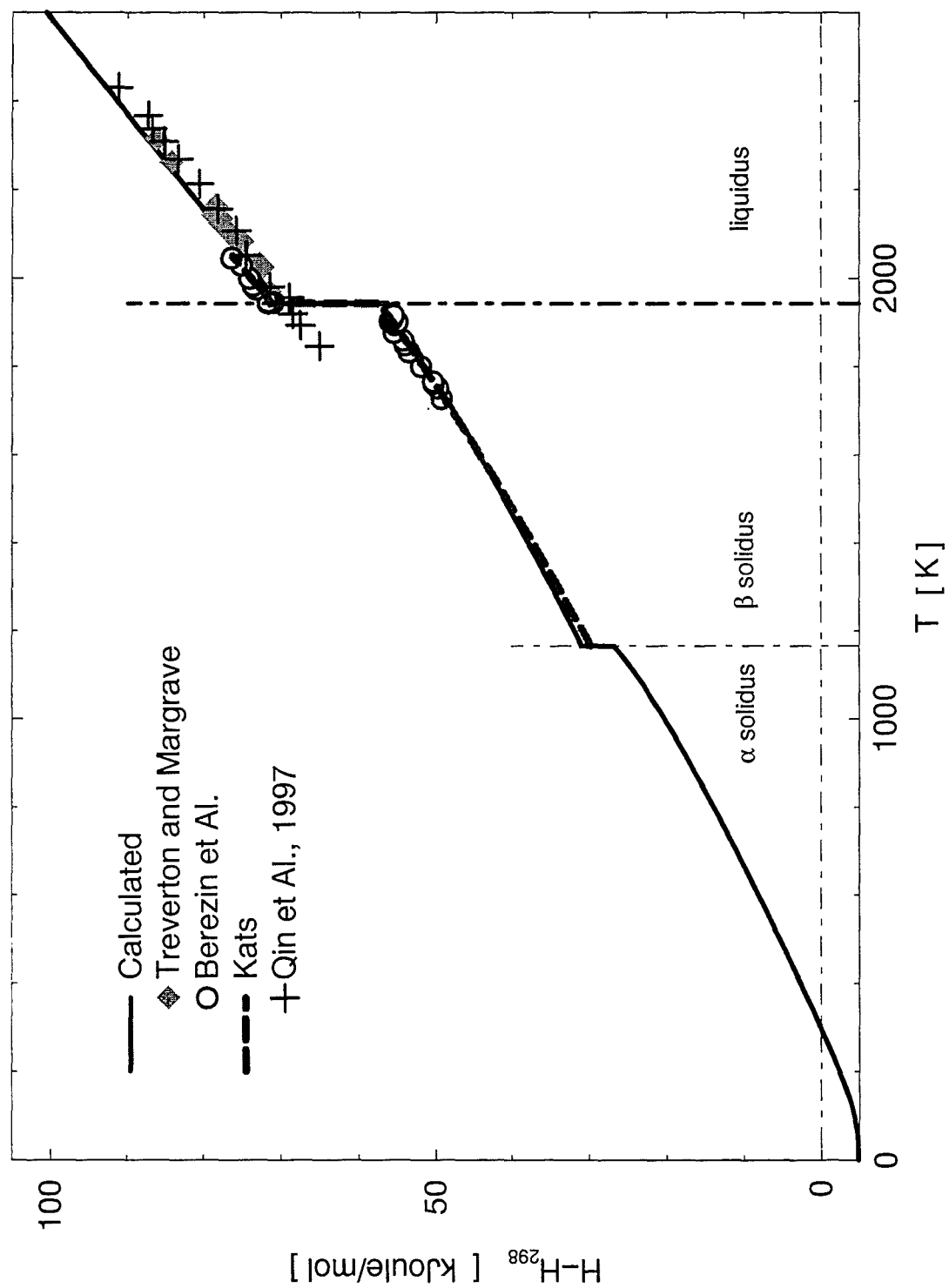


Figure 4.6: Titanium. Enthalpy as a function of the temperature.

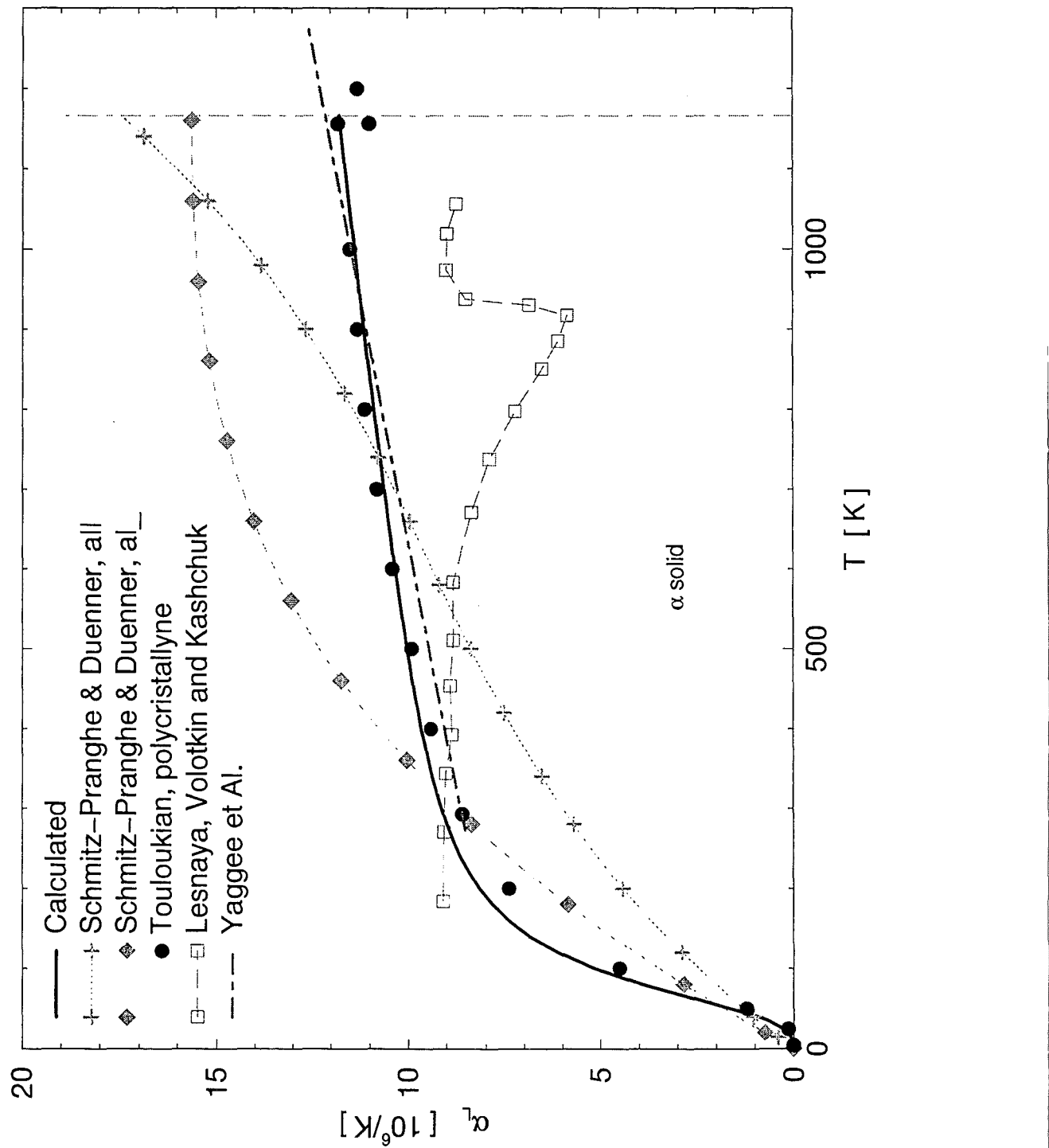


Figure 4.7: Titanium. Coefficient of the linear thermal expansion in the hcp-phase.

Chapter 5

Vanadium

5.1 Phase transitions

Reference		T_M K	ΔH_{fus} kJ/mol
Rudy,	1969, [40], [142]	2202	-
Treverton et al.,	1971, [47]	2175	17.317
Berezin,	1973, [64]	-	23.02
Kenisarin et al.,	1976, [77]	2206	-
Seydel et al.,	1979, [99]	-	27.51
Gathers et al.,	1979, [104]	2190	21.9
Chekhoverkoi et al.,	1981, [116]	2193	23.04
Margrave,	1982, [122], [142]	2194	-
Hiernaut et al.,	1989, [160]	2200	-
Lin and Frohberg,	1991, [174]	-	23.036
Stankus,	1993, [180]	2172	-

Table 5.1: Vanadium. Transform properties

Vanadium is a bright white metal, with a good corrosion resistance. Having a low fission neutron cross-section vanadium is useful as an alloying component in nuclear applications. Its atomic weight is

$$\mu = 50.9415 \frac{g}{mol} \quad . \quad (5.1)$$

The zero-point enthalpy of sublimation is (s. [3]):

$$\Delta H_{sub} = 470.3 \frac{kJ}{mol} \quad . \quad (5.2)$$

Reference		$\rho_{298.15}$ kg/m^3
Hill, Wilcox,	1960, [28]	6117
James, Straumanis,	1961, [28]	6117
Bradford and Carlson,	1962, [11]	6107
Ferrante, Block et Schaller,	1968, [33]	6113
Yaggee, Gilbert, and Styles,	1969, [36]	6089
Ming and Manghnani, buoyancy method	1978, [92]	6102
x-ray diffraction method		6111

Table 5.2: Vanadium. Standard density data

A_0	A_1	A_2	A_3
$T \leq 370 \text{ K}$			
6107.29	0.0193746	$-6.87488 \cdot 10^{-4}$	$8.23105 \cdot 10^{-7}$
$370 \text{ K} < T \leq 2190 \text{ K}$			
6129.73	-0.184435	$9.21438 \cdot 10^{-6}$	$-1.16019 \cdot 10^{-8}$
$2190 \text{ K} < T$			
6425.00	-0.45	0.0	0.0

Table 5.3: Vanadium. Coefficients of the density description

As the critical temperature of vanadium Fortov, Dremin and Leont'ev, [74] assume

$$T_c \sim 12\ 500 \text{ K}$$

The recently measured melting points and heats of fusion of vanadium are collected in the table 5.1 on page 17. As the **melting point** of vanadium I selected

$$T_M = 2190 \text{ K} \quad . \quad (5.3)$$

This value compares well with the data of Gathers et al., Chekhovskoi et al. and with the T_M of Margrave. 2190 K fits also fairly well to the enthalpy data of Lin and Frohberg (s. fig. 5.6 on page 24).

In selecting the **heat of the fusion**

$$\Delta H_{fus} = 23.0 \text{ kJ/mol} \quad (5.4)$$

I followed Berezin, [64], Chekhovskoi and Kats, [116] and Lin & Frohberg [174].

Note to the table 5.1. Treverton and Margrave measured actually not ΔH_{fus} , but the enthalpy of the liquid at T_M and reached their value by subtracting the enthalpy of the melting

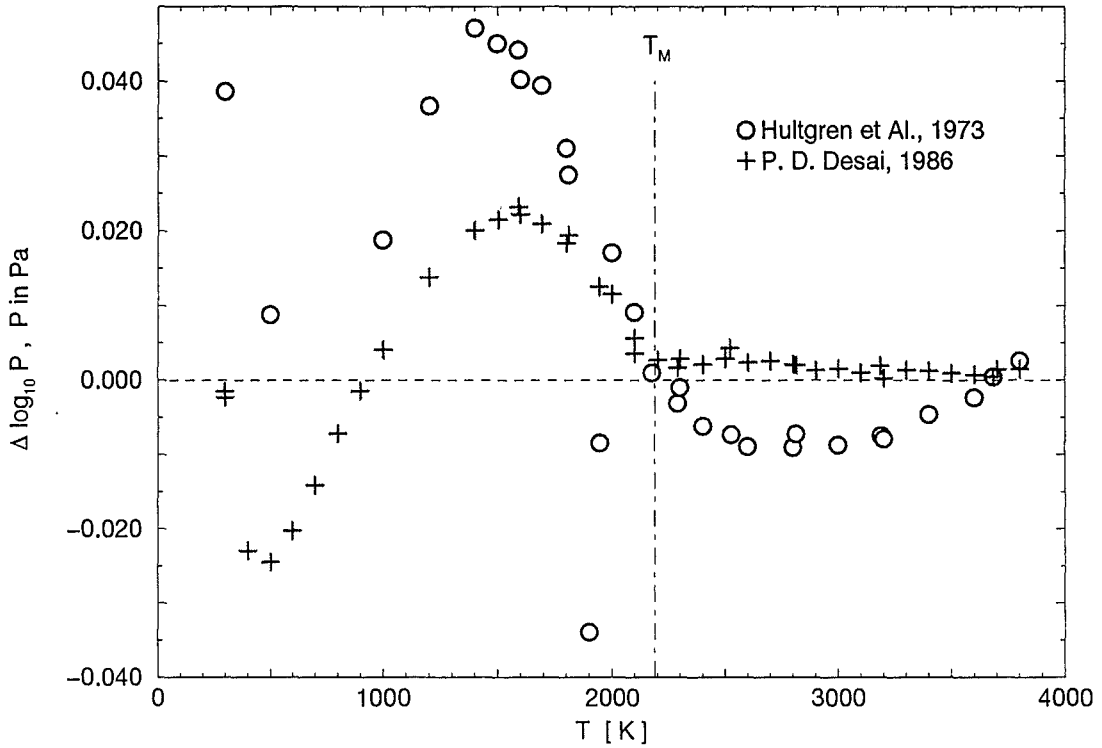


Figure 5.1: Vanadium. Deviations of the vapor pressure data from the Dupré-Rankine description.

solid, as estimated by Hultgren et al., [14]. Taking the enthalpy measured by Berezin in 1973, [64] would give 20.058 kJ/mol , with the solid-enthalpy of Gathers, Shaner, Hixson and Young, [104] one would get 21.274 kJ/mol .

5.2 Vapor pressure

As vapor pressure of vanadium I have taken the critical evaluations of Desai, [142], presented in 1986. The Dupré-Rankine approximation fitted to the Desai points has the following coefficients:

$$\log_{10} p^\circ = 14.9242 - \frac{26979.0}{T} - 0.626353 \cdot \log_{10} T \quad \text{for } T \leq T_M$$

and

(5.5)

$$\log_{10} p^\circ = 21.0956 - \frac{27251.8}{T} - 2.436550 \cdot \log_{10} T \quad \text{for } T \geq T_M .$$

With eq. 5.5 the boiling point of vanadium adds up to

$$T_B = 3682.24 \text{ K} \quad .$$
(5.6)

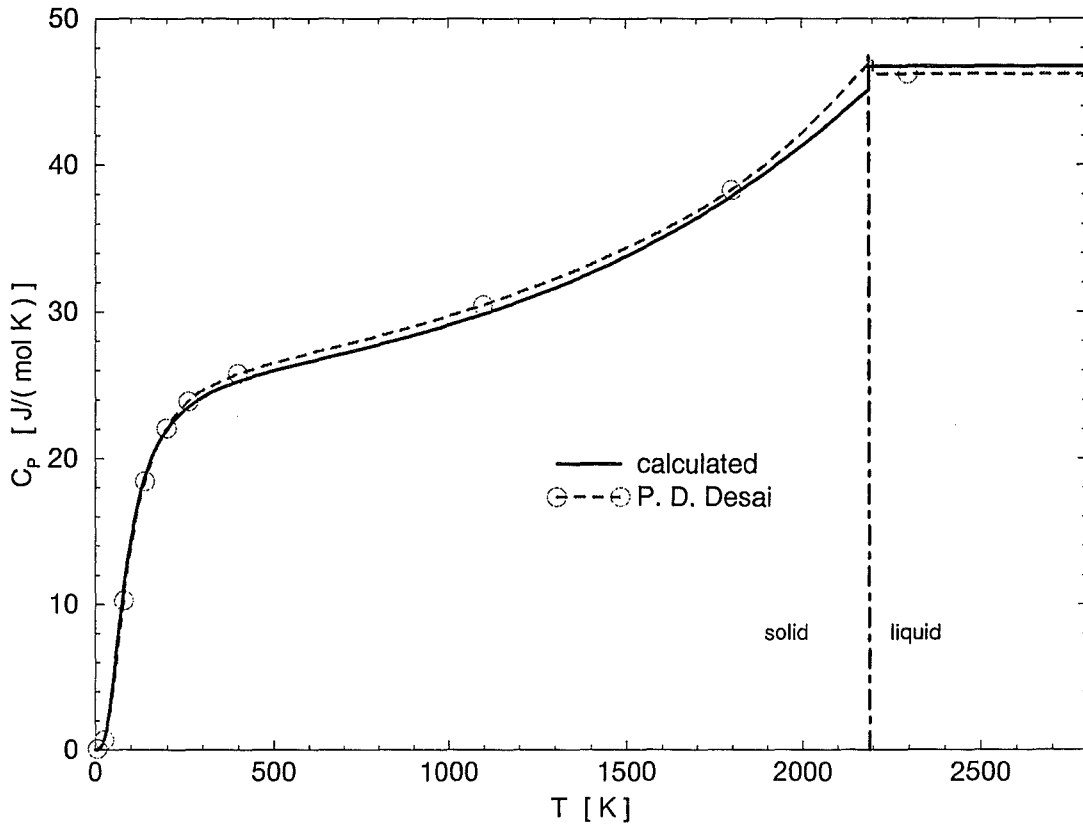


Figure 5.2: Vanadium. Heat capacity C_P as a function of the temperature.

Figure 5.1 on page 19 compares the calculated vapor pressures with the data of Desai. The figure shows also the deviations of the data of Hultgren et al., [56] from the calculated vapor pressures.

5.3 Heat capacity and enthalpy

As base for fitting the heat capacity of solid vanadium I used the data of Berezin 1973, [64], Chekhovskoi and Kalinkina, [61], Berezin and Chekhovskoi, [87], Takahashi, Nakamura and Smith, [124] and of Lin and Frohberg, [174].

To fit the data one needs only the Debye- and the Hoch-functions (eq.s 2.3, 2.5), since no phase transition occurs in solid vanadium:

$$C_{PS} = C_{PD} + C_{PH} \quad \text{for } T \leq T_M . \quad (5.7)$$

The fitting produced the following parameters for C_{PD} and C_{PH} :

$$\Theta_D = 360 \text{ K} , \quad b = 0.003 \frac{\text{J}}{\text{mol K}^2} , \quad d = 1.3 \cdot 10^{-9} \frac{\text{J}}{\text{mol K}^4} . \quad (5.8)$$

As the heat capacity of the liquidus I had taken the C_{PL} value of Lin and Frohberg, [174]:

$$C_{PL} = 46.72 \frac{\text{J}}{\text{mol K}} \quad \text{for } T \geq T_M . \quad (5.9)$$

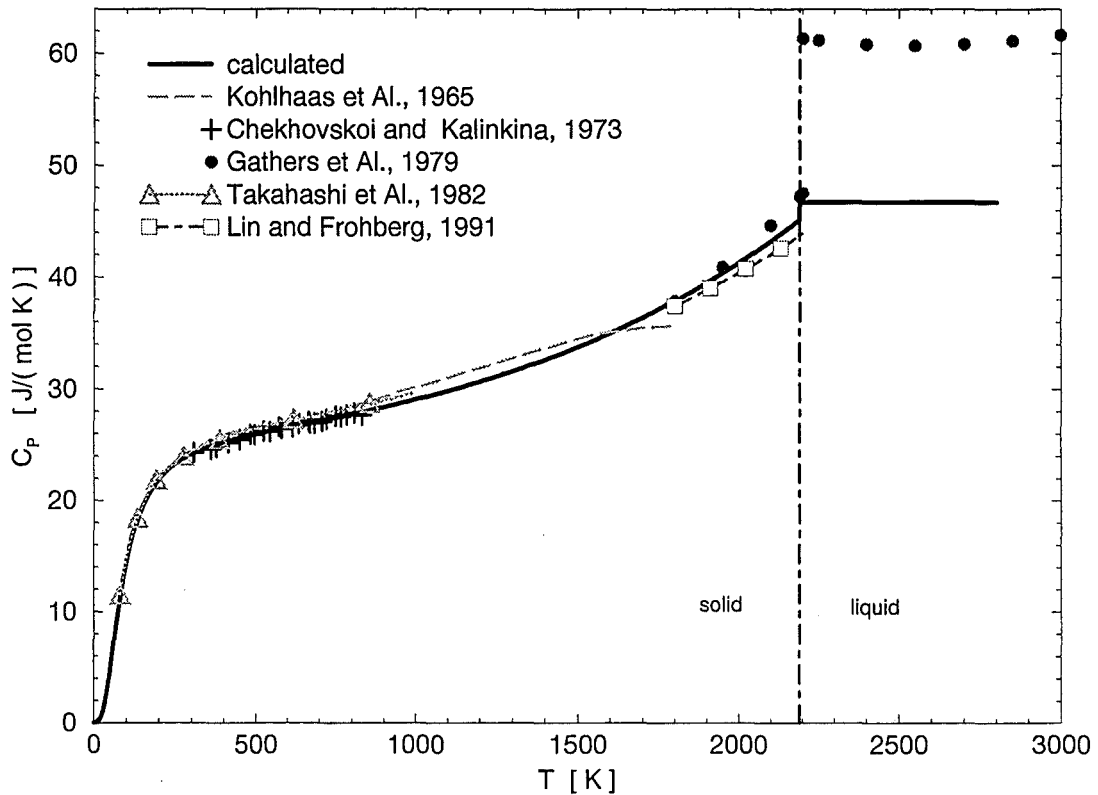


Figure 5.3: Vanadium. Comparison of the measured C_P -s.

Figure 5.2 on page 20 displays the heat capacity calculated by eq.s 5.7 - 5.9. As a comparison the recommended values of P. D. Desai are also shown.

Figure 5.3 compares the calculated heat capacity with the measured C_P -s used in the fitting procedure. 5.3 shows also the C_P -values of Kohlhaas, Braun and Vollmer, [21] and of Gathers, Shaner, Hixson, and Young, [104]. To be able to use the data of Gathers et al. I had to derived the $H(T)$ polynomial given in [104] to get an expression for $C_P(T)$.

Figure 5.6 on page 24 displays the enthalpy of vanadium calculated by eq.s

$$H_S(T) = H_D(T) + H_H(T) \quad \text{for } T \leq T_M \quad \text{and} \quad (5.10)$$

$$H_L(T) = H_S(T_M) + \Delta H_{fus} + C_{PL} \cdot (T - T_M) \quad \text{for } T > T_M$$

with the parameters given in eq. 5.8. The function 5.10 is normalized to 25 grades centigrade (298 K), the zero-point enthalpy beeing $H_0 = -4.73840 \text{ kJ/mol}$. For H_D and H_H see eq.s 2.1 resp. 2.6.

5.4 Thermal expansion and density.

In describing the density and the volumetric thermal expansion of vanadium I depended mainly on the recently measured solid and liquid density data of Stankus, [180].

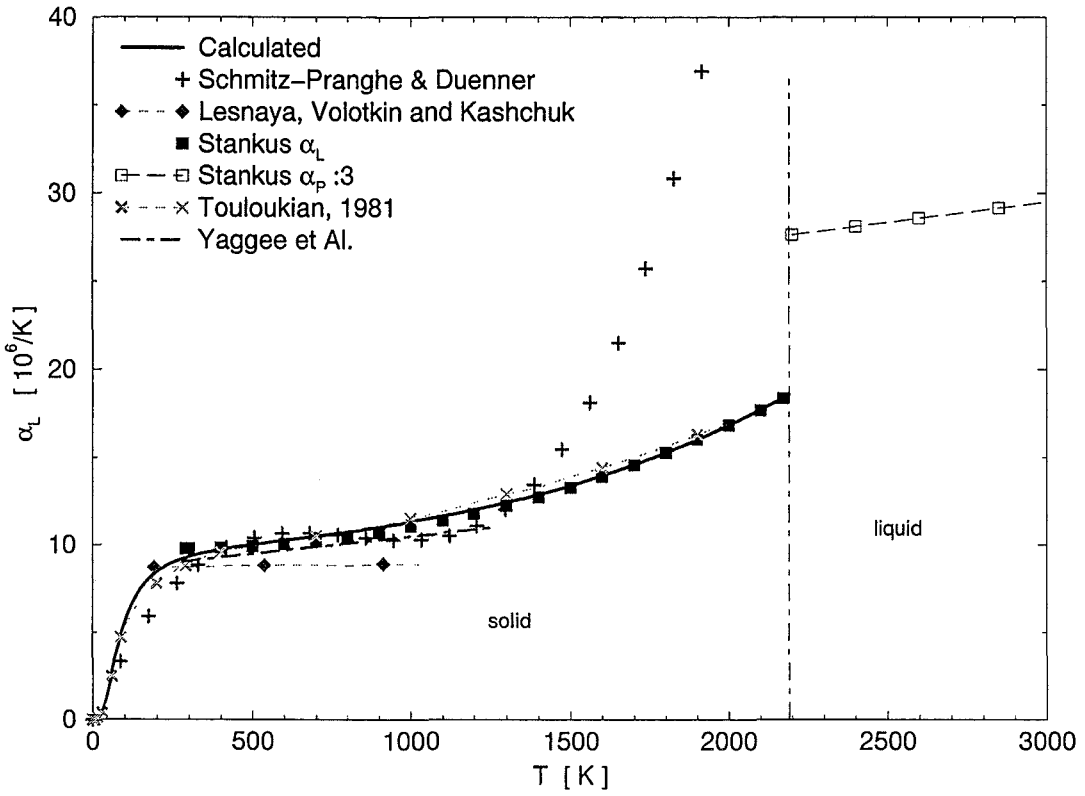


Figure 5.4: Vanadium. Coefficient of the linear thermal expansion.

At first I used the α_L -values of Stankus, to select a well fitting C_P - like description (s. eq. 3.7) for α_L (T) in the solid state:

$$\alpha_L = e \cdot (c_D + c_H) \quad \text{for } T \leq T_M . \quad (5.11)$$

c_D and c_H are Debye-type resp. Hoch-type functions (eq.s 3.4, 3.5) with the parameters

$$\Theta_D = 360 \text{ K} , \quad b = 0.003 \frac{J}{\text{mol K}^2} , \quad d = 1.6 \cdot 10^{-9} \frac{J}{\text{mol K}^4} \quad (5.12)$$

(cf. eq. 5.8). The fitting to the data of Stankus needed a scaling factor of

$$e = 3.85 \cdot 10^{-7} \frac{\text{mol}}{J} . \quad (5.13)$$

Fig. 5.4 displays the calculated property and compares it with measured data of Schmitz-Pranghe and Dünner, [35], Lesnaya, Volotkin, and Kashchuk, [81] and Yaggee et al., [36]. The dataset recommended by Tououloukian in [120] is also shown.

The density-description for vanadium I have constructed as follows:

In the solid state I integrated α_L according to eq. 3.2 to get the volumetric thermal expansion $V(T)$. From this property I calculated the density according to eq. 3.3 using a vanadium standard density of

$$\rho_{298} = 6074 \text{ kg/m}^3 \quad (5.14)$$

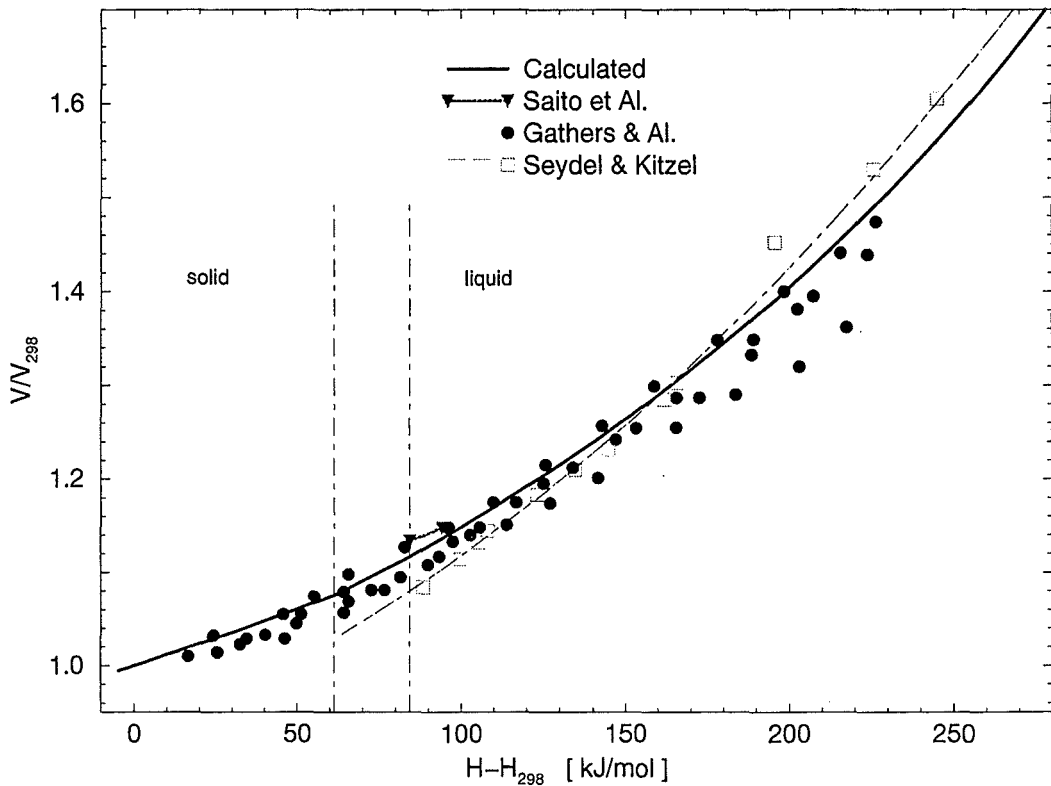


Figure 5.5: Vanadium. Thermal expansion as a function of the enthalpy.

which fitted best to the solid density data of Stankus. (cf. fig. 5.7 on page 25). For a comparison table 5.2 on page 18 displays some recently measured standard densities of different research groups.

In the liquid state I had taken simply the densities, measured by Stankus.

The coefficients of the eq.-3.10-type polynomials, describing vanadium-density in the whole range of the accessible temperatures are collected in the table 5.3 on page 18.

Figure 5.7 on page 25 shows the calculated densities and presents also measured values. The data of Schmitz-Pranghe and Dünner, [35] fit well here at temperatures, not exceeding 1500 K. Saito, Shiraishi, Sakuma, [37] and Eremenko, Ivashchenko and Martsenyuk, [133] measured melting densities somewhat below the value of Stankus. To get the density-temperature points of Gathers et al. I calculated a $V(H)$ function with the approximating polynomials they give in [104], then turned the $V(H)$ relation with the $H(T)$ function 5.10 to a $V(T)$ relation. $\rho(T)$ then was calculated with eq. 3.3 using the standard density of 6074 kg/m^3 . The dataset of Seydel and Kitzel, [99] has been turned into a density - temperature function the same way.

Fig. 5.5 presents the calculated thermal expansion as a function of the enthalpy. The limiting enthalpy-values of the solid resp. the liquid are 61.264 resp. 84.264 kJ/mol .

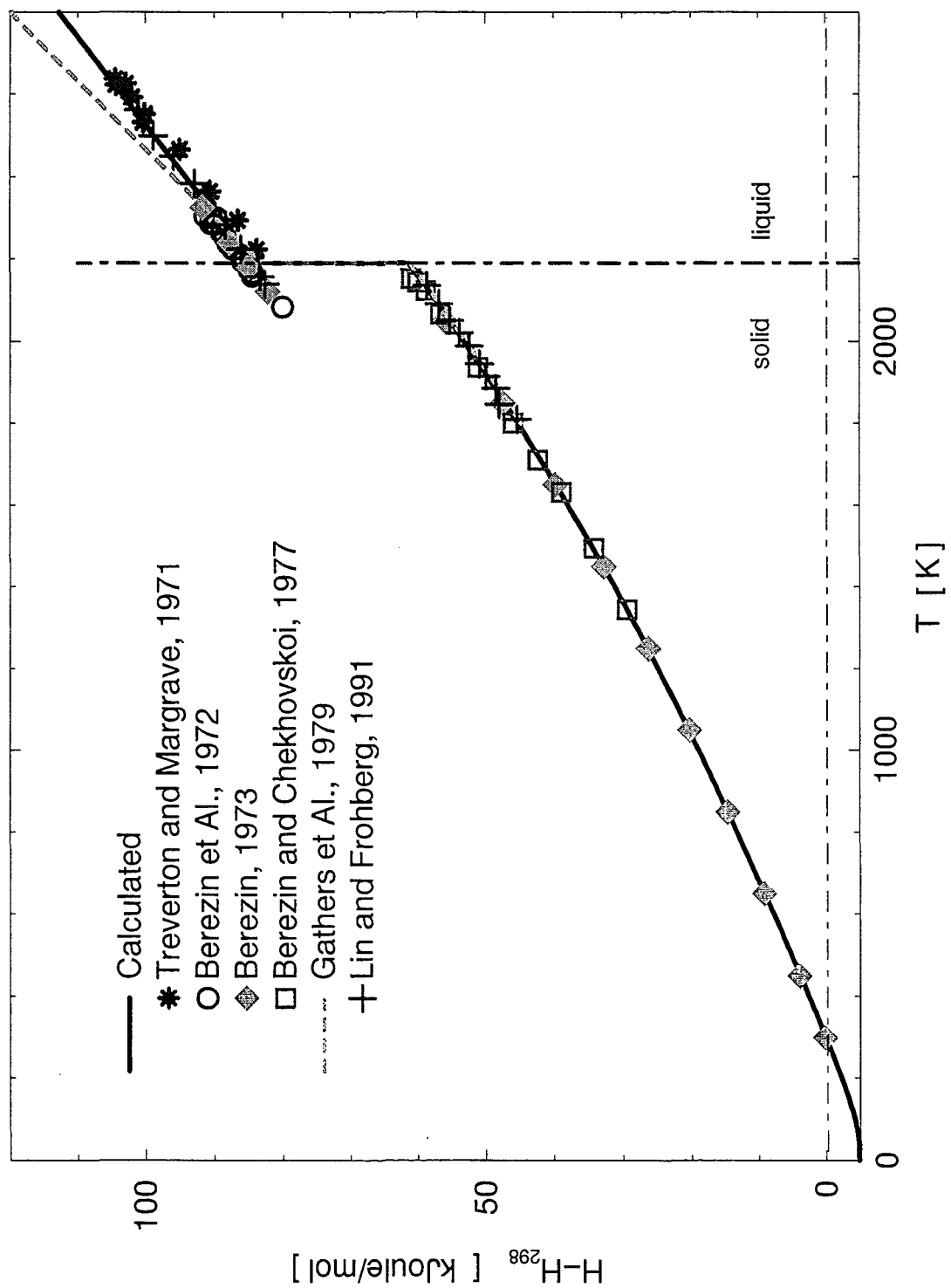


Figure 5.6: Vanadium. Enthalpy as a function of the temperature.

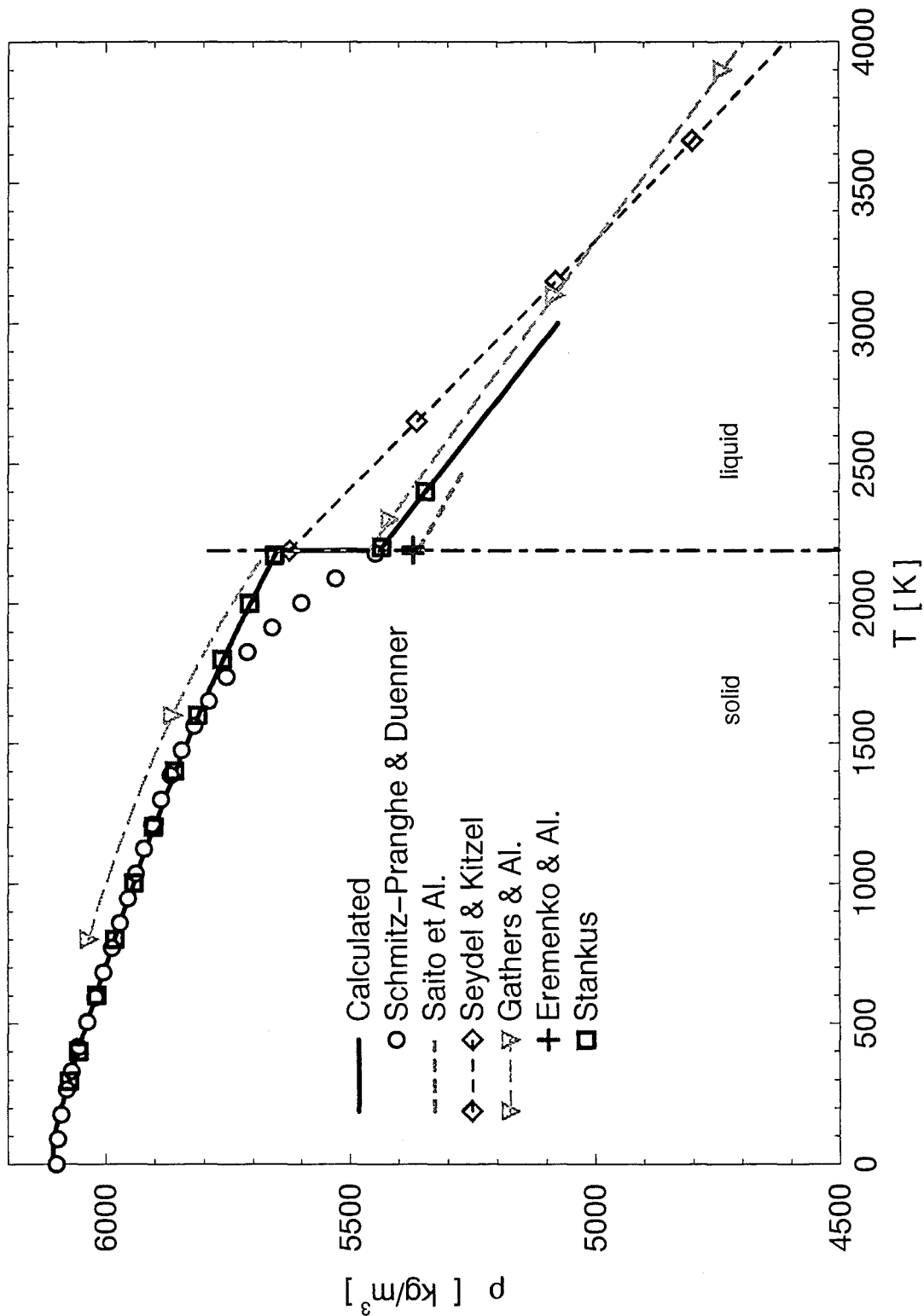


Figure 5.7: Vanadium. Density as a function of the temperature.

Chapter 6

Chromium

6.1 Phase transitions

Chromium is a steel-gray, lustrous, brittle metal. It is often used for creating heat- and corrosion-resistant alloys. Its atomic weight is

$$\mu = 51.996 \frac{g}{mol} \quad (6.1)$$

and the zero-point enthalpy of sublimation is ([3])

$$\Delta H_{sub} = 395.4 \frac{kJ}{mol} \quad . \quad (6.2)$$

Chromium is antiferromagnetic below its Néel temperature, T_N and paramagnetic above this point.

Reference			T_N K	ΔH_N kJ/mol	T_M K	ΔH_{fus} kJ/mol
Hultgren et al.,	1966	[56]	311	0.0067	2130	(16.9)
Williams et al.,	1978	[100]	311.45	0.0014	-	-
Neumann,	1985	-	-	-	2136	-
Lin et al.,	1988	[159]	-	-	-	29.674
Makyeyev et al.,	1991	[175]	-	-	2102	-
Stankus,	1993	[180]	-	-	2131	-

Table 6.1: Chromium. Transform properties

Fortov, Dremin and Leont'ev, [74] estimate

$$T_c \sim 9620 K$$

as the critical temperature of chromium.

Table 6.1 shows the transform temperatures and heats of chromium (after [56] and [100], cited in [159]).

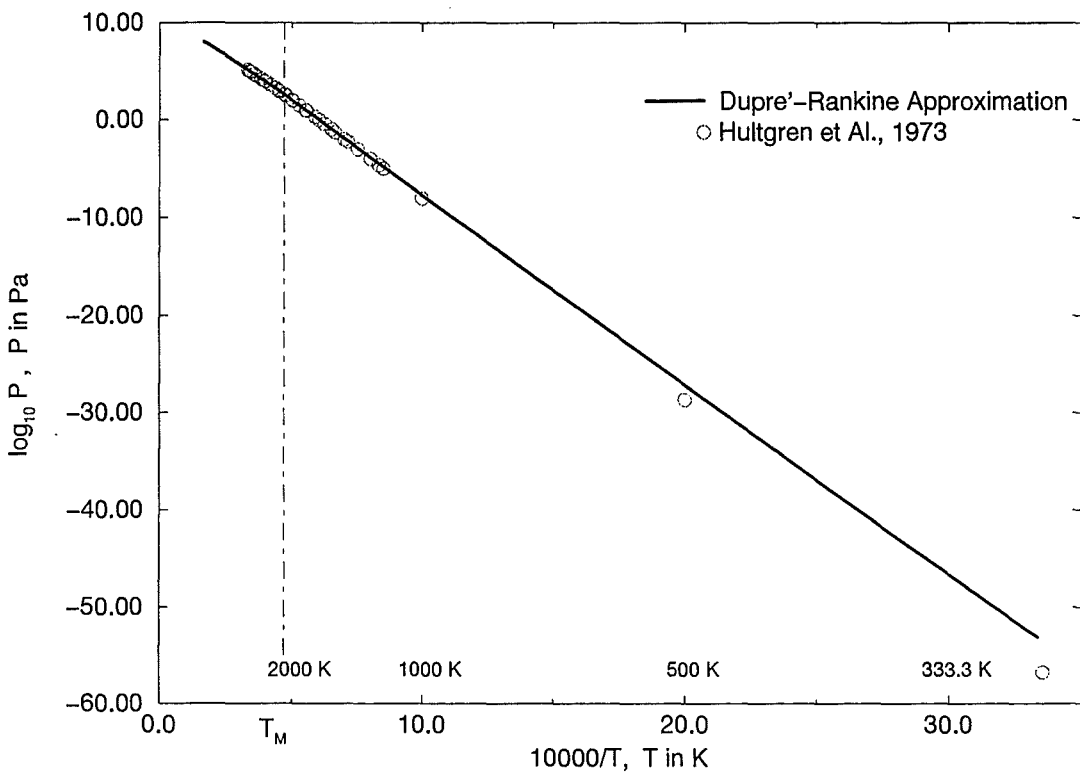


Figure 6.1: Chromium. Vapor pressure - temperature graph

N.B. Neumann's T_M value of 2136 K is given also in Lin and Frohberg as a 'private communication'.

In the case of the **melting point** I follow Hultgren, who recommends

$$T_M = 2130 \text{ K} . \quad (6.3)$$

Waseda and Tamaki, [71] found chromium already in the liquid state at 2173 K (cf. also figure 6.5 on page 33).

Unfortunately there are only few data about the thermal properties of the chromium at near melting and liquid temperatures. I found only four reports concerning this region: the enthalpy measurements of Lin and Frohberg, [159] the density measurements of Saito et al., [37], the density measurements of Makeev and Popel', [175] and the density and thermal expansion measurements of Stankus, [180].

For the **heat of the fusion** I had taken the only existing value from Lin and Frohberg, [159], $\Delta H_{fus} = 29.674 \text{ kJ/mol}$ and corrected it slightly, to fit into the combined enthalpy data of Lin and Frohberg, Chekhovskoi and Zhukova, [105] and of Conway and Hein, [17] (s. figure 6.5 on page 33):

$$\Delta H_{fus} = 28 \text{ kJ/mol} . \quad (6.4)$$

In describing the properties of chromium I have neglected the caloric anomaly at T_N (s. figure 6.3 on page 30).

6.2 Vapor pressure

For the metal chromium there exists quite a lot recently measured vapor pressure data. Lee and Adams, [157] measured the vapor pressure in the temperature-range 1400 - 1625 K. They describe their data as

$$\ln P = A - \frac{\Delta H_{sub}}{R_{gas} \cdot T} \quad (6.5)$$

with $\Delta H_{sub} = 377 \text{ kJ/mol}$ as the enthalpy of sublimation. Murray, Kematick, Myers and Frisch, [167] investigated the vaporization of chromium with different methods of mass spectrometry: they used magnetic (MMS) and quadrupole (QMS) mass detectors. As enthalpies of sublimation they got $\Delta H_{sub} = 379.6$ resp. $\Delta H_{sub} = 379.2 \text{ kJ/mol}$. The most recent data are from Zaitsev, Zemchenko, and Mogutnov, [170]. Zaitsev et al. applied Knudsen technique and mass spectroscopy to get the vapor pressure data. They report a zero-point enthalpy of $\Delta H_{sub} = 393.4 \text{ kJ/mol}$.

To get a Dupré-Rankine equation for the vapor pressure of the chromium I selected:

in the solid state the measurements of Lee & Adams, Murray et al. and some points of the Hultgren vapor pressure table, [56] and

in the liquidus all of the vapor pressure points of Hultgren et al.

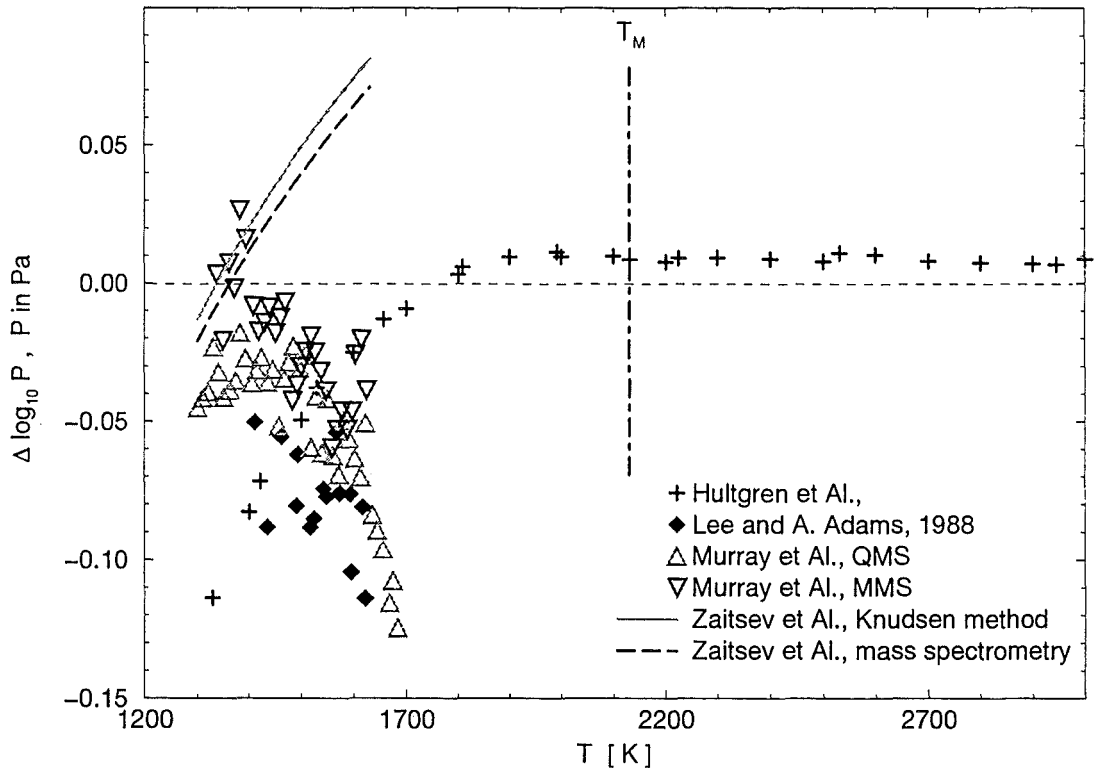


Figure 6.2: Chromium. Deviations of the vapor pressure data from the Dupré-Rankine description.

In the temperature range of the solid I had to drop the two coldest points of [56], they were too low to be included into the fitting (cf. figure 6.1 on page 27).

The fitting gave - reluctantly - the following Dupré-Rankine equation:

$$\log_{10} p^\circ = 11.7662 - \frac{19465.5}{T} \quad \text{for } T \leq T_M$$

and

$$\log_{10} p^\circ = 15.8456 - \frac{19564.7}{T} - 1.21166 \cdot \log_{10} T \quad \text{for } T \geq T_M .$$

As figure 6.2 on page 28 - a display of the deviations of the experimental data from eq. 6.6 - shows, it is not easy to get all the vapor pressure points into one common description.

Eq. 6.6 gives as boiling point

$$T_B = 2948.29 K \quad (6.7)$$

for chromium.

6.3 Heat capacity and enthalpy

For fitting the heat capacity of chromium I selected the low-temperature data ($T \leq 1500 K$) of Touloukian and Ho, [120] and the high temperature points of Lin and Frohberg, [159]. In fitting the the heat capacity data I did not include the very narrow λ - peak at T_N .

N.B. Lin and Frohberg measured actually the excess enthalpy, $H - H_{298}$. They fitted a five-term expression

$$H - H_{298} = a + T (b + T (c + d T^2)) + \frac{e}{T}$$

to these points and derived it, to get the C_P (T) function.

At first I tried to fit to the above set of points a C_P -function consisting only from the Debye- and the Hoch-descriptions (s. eq. 2.3 resp. eq. 2.5):

$$C_{PS} = C_{PD} + C_{PH} \quad \text{for } T \leq T_M . \quad (6.8)$$

The results were not satisfying: the sharp rise of the data of Lin and Frohberg near to the melting point could not be described in this way, the best 6.8 - type function shows only a C_P - shape like the recommended points of Touloukian and Ho (see figure 6.3 on page 30). So in a second try I included a supplementary exponential term, C_{PE} in the description (eq. 2.7):

$$C_{PS} = C_{PD} + C_{PH} + C_{PE} \quad \text{for } T \leq T_M . \quad (6.9)$$

As fig. 6.3 shows, eq. 6.9 with the parameters

$$\Theta_D = 500 K , \quad b = 0.0035 \frac{J}{mol K^2} , \quad d = 3.0 \cdot 10^{-9} \frac{J}{mol K^4}$$

$$g = -2.1 , \quad h = 0.0021 1/K \quad (6.10)$$

is a quite acceptable description of the C_P of solid chromium.

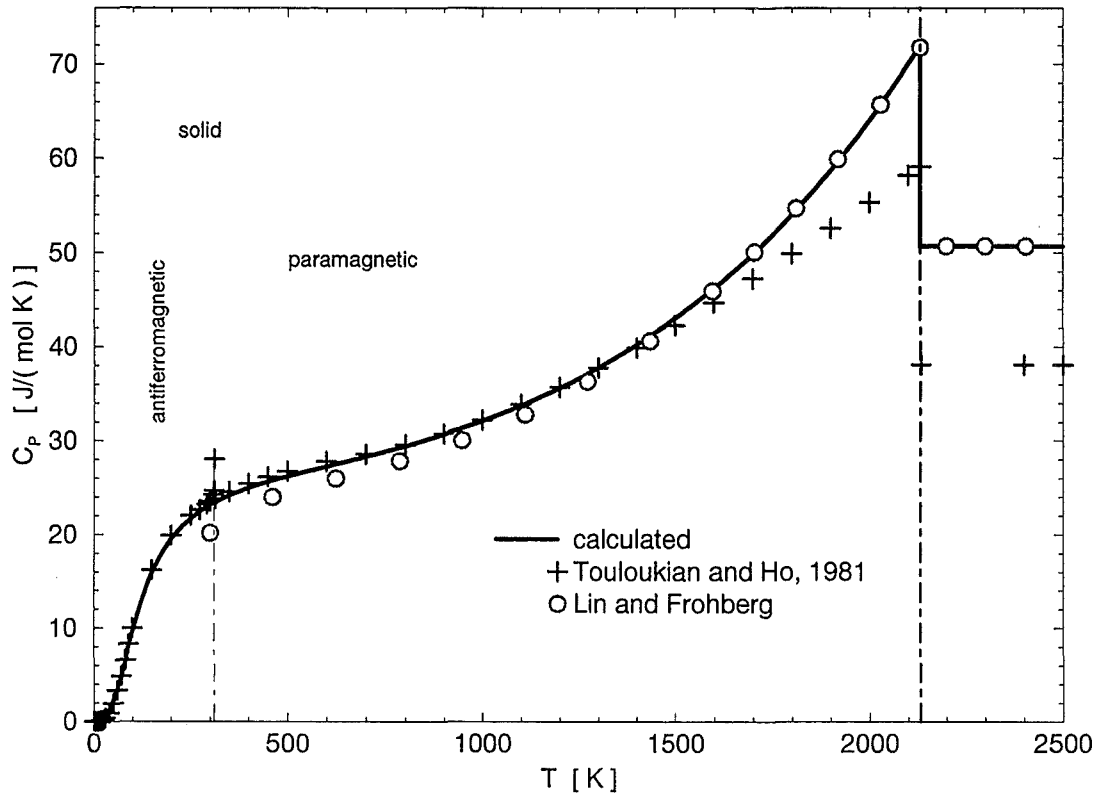


Figure 6.3: Chromium. Heat capacity \$C_P\$ as a function of the temperature.

As the heat capacity of liquid I selected the value of Lin and Frohberg:

$$C_{PL} = 50.71 \frac{\text{J}}{\text{mol K}} \quad \text{for} \quad T_M \leq T . \quad (6.11)$$

The enthalpy description, corresponding to the heat capacity - description 6.9 - 6.11 is

$$H_S(T) = H_D(T) + H_H(T) + H_E(T) \quad \text{for} \quad T \leq T_M \quad \text{and} \quad (6.12)$$

$$H_L(T) = H_S(T_M) + \Delta H_{fus} + C_{PL} \cdot (T - T_M) \quad \text{for} \quad T > T_M .$$

The enthalpy calculated with the above equations shows - as excess enthalpy - figure 6.5 on page 33. The zero-point enthalpy is \$H_0 = -3.98471 \text{ kJ/mol}\$. The figure shows also the data of Conway and Hein, [17], of Chekhovskoi and Zhukova, [105] and of Lin and Frohberg, [159].

6.4 Thermal expansion and density.

The density of solid chromium I developed again by fitting a function to the measured \$\alpha_L\$ - data, then calculating from this function the volumetric thermal expansion and from the volumetric thermal expansion with an appropriate value for the standard density the density in the solid.

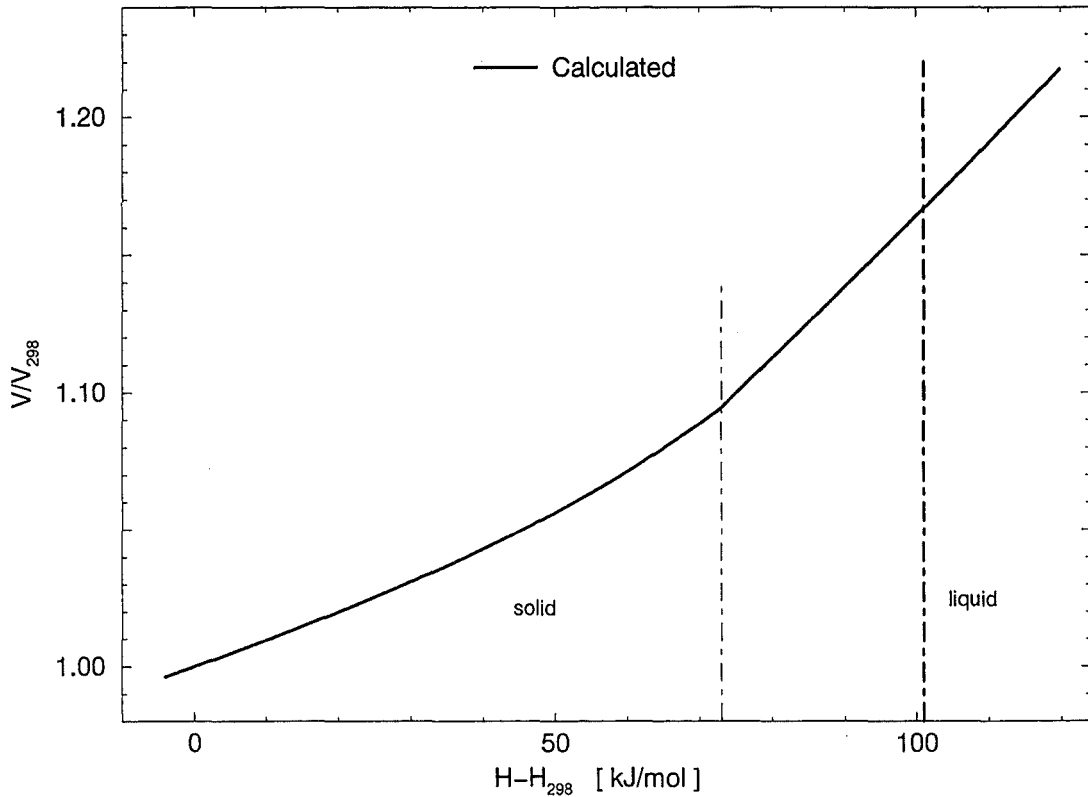


Figure 6.4: Chromium. Thermal expansion as a function of the enthalpy.

For fitting α_L I used the compilation of Tolulokian and Ho, [120] and the most recent measurements of Stankus, [180]. The anomaly at the Néel temperature was ignored again. Likely as in the case of the heat capacity, it was impossible to get a satisfying description of the high temperature part of α_L without a third, exponential term, since the α_L - data of Stankus rise even steeper at pre-melting temperatures, as the C_P points of Lin and Frohberg. To calculate a well-fitted function a complete set of α_L - descriptors were needed:

$$\alpha_L = e \cdot (c_D + c_H + c_E) \quad \text{for } T \leq T_M \quad . \quad (6.13)$$

Figure 6.6 on page 34 compares the resulting "calculated" α_L with the raw data used in the construction. 6.6 shows also the α_L -function of Yaggee et Al., [36]. Actually the authors measured $\Delta L/L$ and then fitted to their data a temperature-polynomial of 3rd degree

$$\{ 1 , 5.68 \cdot 10^{-6} , 8.03 \cdot 10^{-9} , -4.22 \cdot 10^{-12} \} \quad . \quad (6.14)$$

$\alpha_L (T)$ they calculated via eq.s 3.9 and 3.3 using the polynomial above. Since the last coefficient is negative, polynomial 6.14 cannot describe α_L at higher temperatures correctly - namely increasing with increasing T. By fitting a temperature-polynomial of 4th degree

$$\{ 1 , 5.26180 \cdot 10^{-6} , 1.23831 \cdot 10^{-8} , -1.47395 \cdot 10^{-11} , 6.70175 \cdot 10^{-15} \} \quad . \quad (6.15)$$

to the $\Delta L/L$ diagram given in [36] the correct high-temperature behaviour could be achieved.

The scaling factor in eq. 6.13 is

$$e = 3.0 \cdot 10^{-7} \frac{\text{mol}}{\text{J}} . \quad (6.16)$$

The fitting functions - c_D , c_H resp. c_E (eq.s 3.4, 3.5) - have the parameters:

$$\Theta_D = 500 \text{ K} , \quad b = 0.007 \frac{\text{J}}{\text{mol K}^2} , \quad d = 4.7 \cdot 10^{-9} \frac{\text{J}}{\text{mol K}^4} ,$$

$$g = -4 , \quad h = 0.0038 \frac{1}{\text{K}} . \quad (6.17)$$

(cf. eq. 6.10).

The density of the solid I calculated from α_L via eq. 3.3. The ρ (T) function, best describing the data of Stankus I got with a standard density of

$$\rho_{298} = 7200 \text{ kg/m}^3 \quad (6.18)$$

(s. fig. 6.7 on page 35). Ming and Manghnani, [92] report a chromium standard density of $\rho_{298} = 7190 \text{ kg/m}^3$, Yaggee measured $\rho_{298} = 7166 \text{ kg/m}^3$.

As liquid density I used the density data of Stankus, [180].

Table 6.2 collects the coefficients of the density description for chromium in the whole range of temperatures.

A_0	A_1	A_2	A_3
$T \leq 450 \text{ K}$			
7226.46	0.0268548	$-5.36197 \cdot 10^{-4}$	$4.94664 \cdot 10^{-7}$
$450 \text{ K} < T \leq 1500 \text{ K}$			
7256.67	-0.188396	$3.24179 \cdot 10^{-5}$	$-3.76091 \cdot 10^{-8}$
$1500 \text{ K} < T \leq 2130 \text{ K}$			
8328.53	-2.21125	$1.31440 \cdot 10^{-3}$	$-3.10814 \cdot 10^{-7}$
$2130 \text{ K} < T$			
7647.46	-0.693334	0.0	0.0

Table 6.2: Chromium. Coefficients of the density description

Figure 6.7 on page 35 compares the calculated density with measured ones.

Figure 6.4 on page 31 presents the calculated thermal expansion as a function of the enthalpy. The limiting enthalpy-values of the solid resp. the liquid are 73.042 resp. 101.043 kJ/mol . Chromium crosses the antiferromagnetic / paramagnetic border at the enthalpy-value 0.2979 kJ/mol .

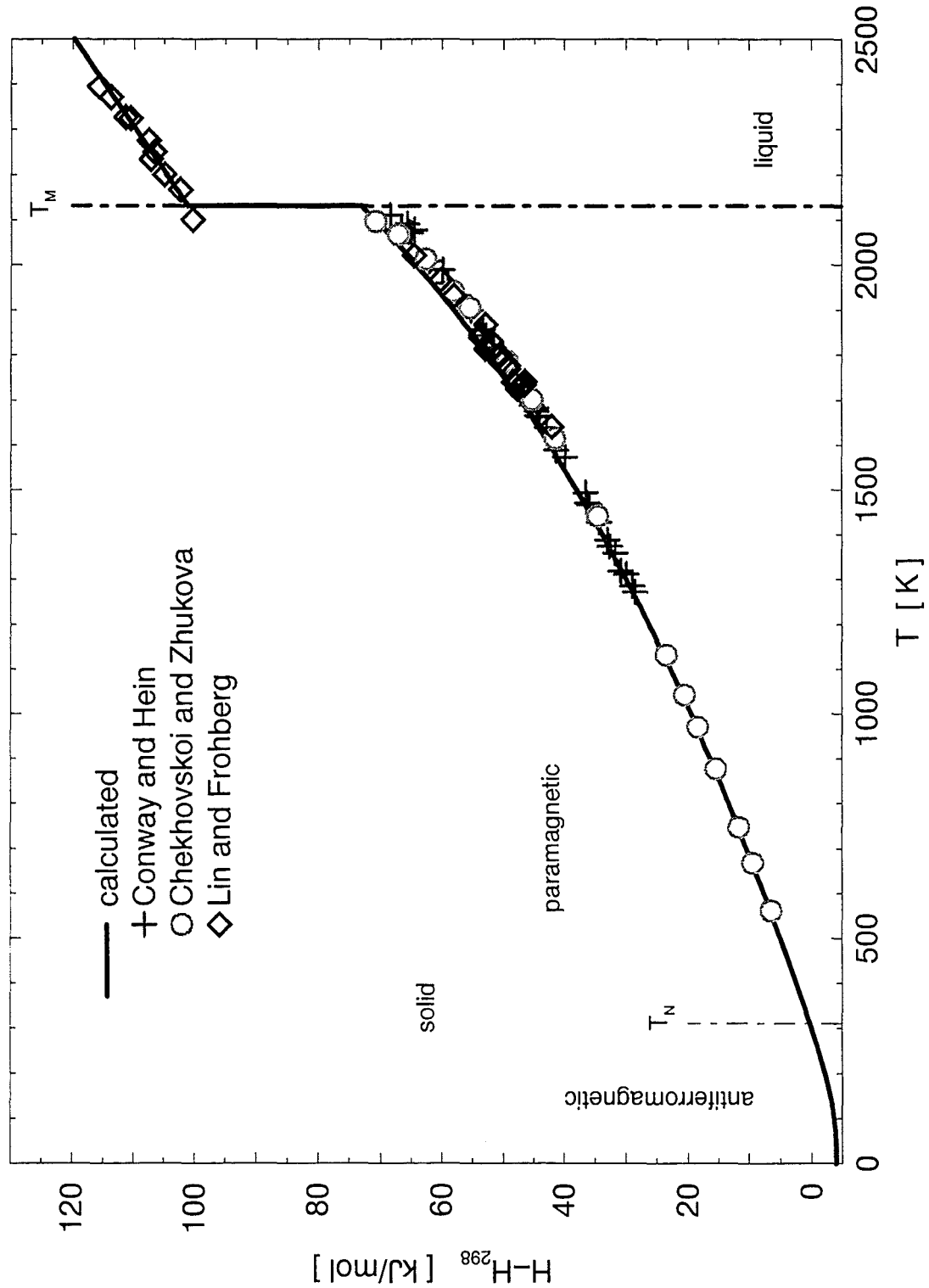


Figure 6.5: Chromium. Enthalpy as a function of the temperature.

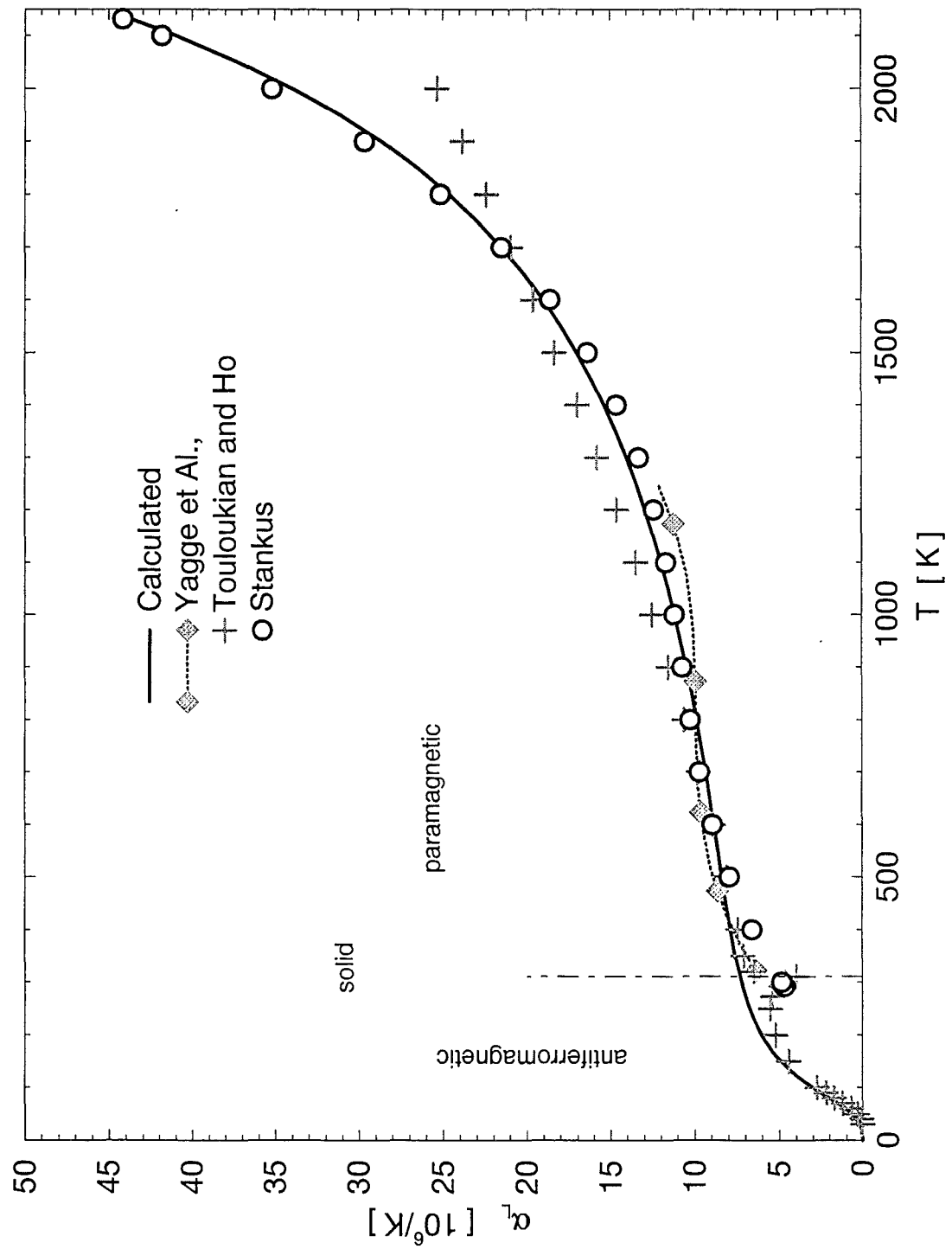


Figure 6.6: Chromium. Coefficient of the linear thermal expansion.

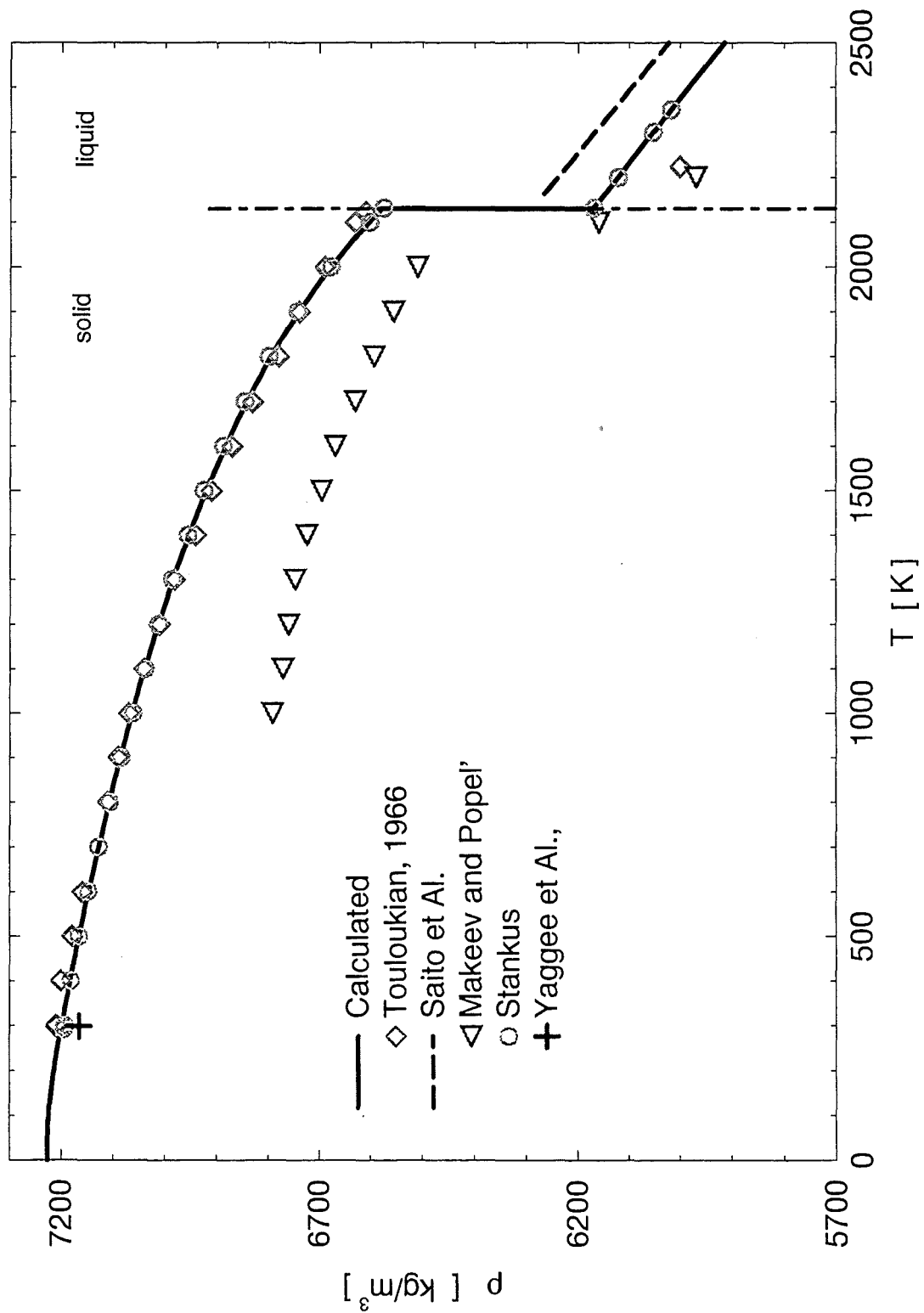


Figure 6.7: Chromium. Density as a function of the temperature.

Chapter 7

Manganese

7.1 Phase transitions

	Naylor 1945 [24]	Rapoport et al. 1966 [34]	Braun et al. 1968 [56]	Hultgren et al. 1973 [102]	Sato et al. 1979 [149]	Desai 1986 [163]
T_N K	-	-	-	95	-	98
T_1 K	1000	1000	1004	980	-	980
ΔH_1 kJ/mol	2.24	2.24	2.17	2.23	-	2.225
T_2 K	1374	1368	1365	1360	-	1360
ΔH_2 kJ/mol	2.28	2.28	2.215	2.12	-	2.120
T_3 K	1410	1407	1404	1410	-	1411
ΔH_3 kJ/mol	1.80	1.80	1.90	1.88	-	1.88
T_M K	-	1517	1514	1517	-	1519
ΔH_{fus} kJ/mol	-	14.65	14.10	(12.1)	11.0	11.0

Table 7.1: Manganese. Transform properties

Manganese is gray-white, very brittle metal. In contrast to most other members of the 3d-group it is chemically reactive. As a steel component it improves strength and hardenability. The atomic weight of the manganese is

$$\mu = 54.938 \frac{g}{mol} . \quad (7.1)$$

Manganese has an extraordinary low zero-point enthalpy of sublimation (s. [3]):

$$\Delta H_{sub} = 282.1 \frac{kJ}{mol} . \quad (7.2)$$

Manganese is antiferromagnetic below its Néel temperature and paramagnetic in the remaining solid states.

As the critical temperature of manganese Fortov, Dremin and Leont'ev, [74] estimate

$$T_c \sim 5940 \text{ K} . \quad (7.3)$$

The most recent data about the phase transitions of manganese are collected in the table 7.1 on page 36.

Note. In the recommendations of Hultgren et al. neither the paper of Rapoport et al. nor the one of Braun et al. has been taken in account.

Regarding the **melting point** I had taken the value recommended by Desai:

$$T_M = 1519 \text{ K} . \quad (7.4)$$

This comparatively low melting temperature corresponds to the low zero-point enthalpy of sublimation of manganese.

My **heat of fusion** is the mean value of the ΔH_{fus} -s of Rapoport, Braun and Sato:

$$\Delta H_{fus} = 13.25 \text{ kJ/mol} . \quad (7.5)$$

Unfortunately there are no measured enthalpy data from the liquid state of manganese to be compared with this estimated value.

Range , T < K	Structure	Transform heat kJ/mol
98	α - Mn , bcc , antiferromagnetic	?
1002	α - Mn , bcc , paramagnetic	2.20
1366	β - Mn , c	2.24
1406	γ - Mn , fcc	1.85
1519	δ - Mn , bcc	13.25

Table 7.2: Manganese. Phases and structures in the solid state

The remaining transform temperatures, $T_1 - T_3$ and the corresponding transform heats $\Delta H_1 - \Delta H_3$ I selected according to the data given by Rapoport et al. and by Braun et al.. Table 7.2 summarizes the transform data of manganese.

7.2 Vapor pressure

As vapor pressure of manganese I use the data given in the critical evaluations of P. D. Desai, [149]. The best-fit Dupré-Rankine approximation to these data has the following coefficients:

$$\log_{10} p^\circ = 18.2019 - \frac{15065.9}{T} - 1.92156 \cdot \log_{10} T \quad \text{for } T \leq T_M$$

and

(7.6)

$$\log_{10} p^\circ = 21.3609 - \frac{14832.3}{T} - 2.96280 \cdot \log_{10} T \quad \text{for } T \geq T_M .$$

The deviations of this approximation from the data of Desai can be seen on figure 7.1. The figure shows also - as pressure-differences - the recommended vapor pressures of Hultgren et al., [56] and the most recent measurements of Zaitsev et al., [170].

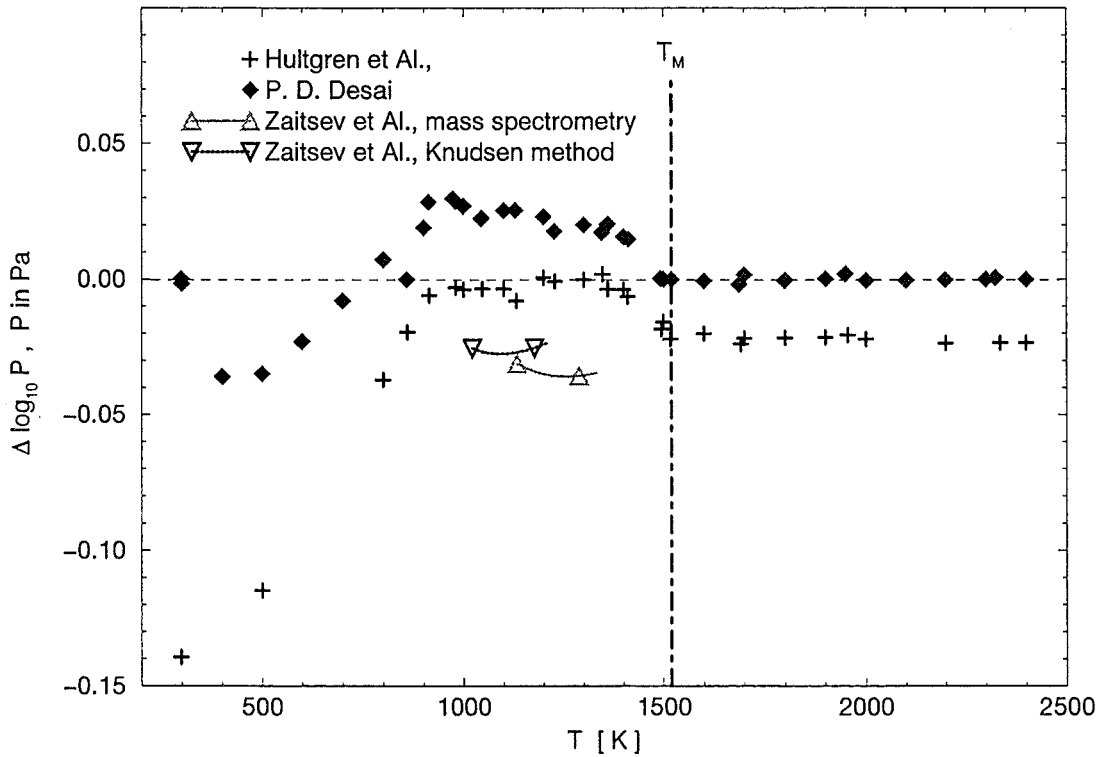


Figure 7.1: Manganese. Deviations of the vapor pressure data from the Dupré-Rankine description.

To the vapor pressure equation 7.6 corresponds a boiling point of

$$T_B = 2324.24 \text{ K} .$$
(7.7)

7.3 Heat capacity and enthalpy

For fitting the heat capacity of manganese I selected the low-temperature data ($T \leq 300 \text{ K}$) of Desai and all the points of Braun, Kohlhaas and Vollmer, [34].

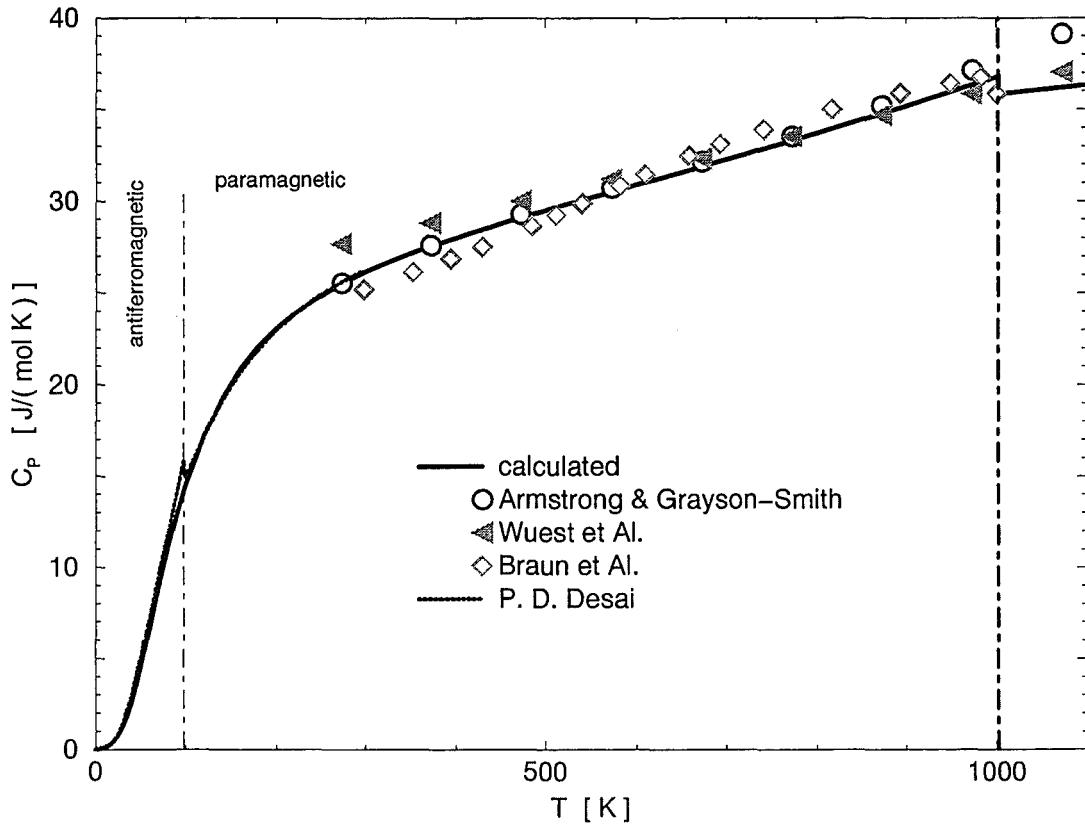


Figure 7.2: Manganese. Heat capacity in the bcc-phase.

In the α - Mn one needs for the C_P -description only the Debye- and the Hoch- function (eq.s 2.1, 2.5). The small caloric anomaly at the Nèel temperature was not taken into account.

$$C_{P\alpha} = C_{PD} + C_{PH} \quad \text{for} \quad T \leq T_1 \quad (7.8)$$

The best fitting parameters for C_{PD} and C_{PH} were

$$\Theta_D = 375 \text{ K} , \quad b = 0.01 \frac{\text{J}}{\text{mol K}^2} , \quad d = 2 \cdot 10^{-9} \frac{\text{J}}{\text{mol K}^4} . \quad (7.9)$$

Figure 7.2 compares the heat capacity of the α -manganese calculated by eq. 7.8 with the data of Armstrong, H. Grayson-Smith, [8], with the data of Wuest, [5] and with the data of Braun et al., [34].

In the remaining solid phases I describe the heat capacity of manganese with polynomials fitted to the data of Braun et al., [34]:

$$C_{P\beta} [\text{J}/(\text{mol K})] = 30.8946 + T \cdot 4.94519 \cdot 10^{-3} \frac{\text{J}}{\text{mol K}} \quad \text{for} \quad T_1 < T \leq T_2 , \quad (7.10)$$

$$C_{P\gamma} [\text{J}/(\text{mol K})] = 44.1611 \quad \text{for} \quad T_2 < T \leq T_3 \quad \text{and} \quad (7.11)$$

$$C_{P\delta} [\text{J}/(\text{mol K})] = 43.308 + T \cdot 2.45354 \cdot 10^{-3} \quad \text{for} \quad T_3 < T \leq T_M . \quad (7.12)$$

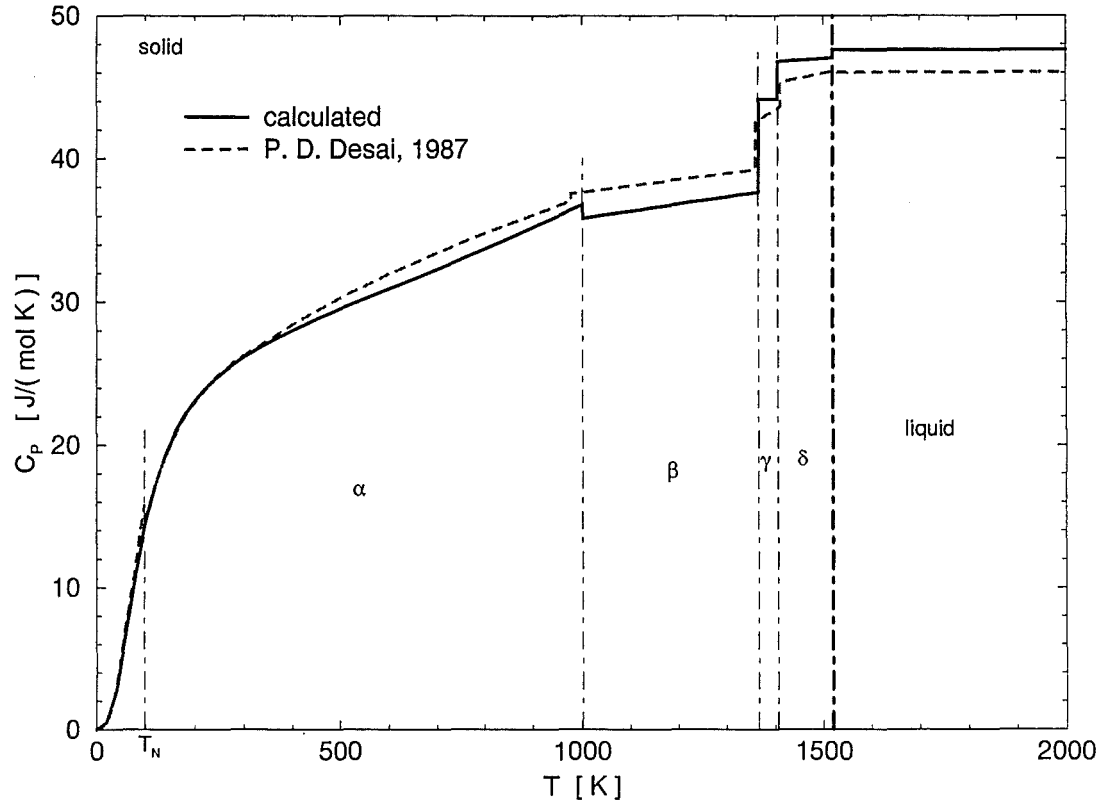


Figure 7.3: Manganese. Heat capacity C_P as a function of the temperature.

In liquid manganese I use

$$C_{PL} [J/(mol K)] = 47.60 \quad (7.13)$$

as heat capacity, to be in accord with Braun et al.. The $C_{PL} = 46.0 \text{ J}/(\text{mol K})$ value of Desai stems from Hultgren et al., Hultgren describes it as an estimation made by Kelley in 1960.

Figure 7.3 displays the heat capacity calculated by eq.s 7.8 - 7.13. As a comparison the recommended values of P. D. Desai are also shown.

The enthalpy of manganese can be expressed as

$$\begin{aligned}
 H_\alpha(T) &= H_D(T) + H_H(T) && \text{for } T \leq T_1 \\
 H_\beta(T) &= H_\alpha(T_1) + \Delta H_1 + \int_{T_1}^T dt C_{P\beta}(t) && \text{for } T_1 < T \leq T_2 \\
 H_\gamma(T) &= H_\beta(T_1) + \Delta H_2 + C_{P\gamma} \cdot (T - T_2) && \text{for } T_2 < T \leq T_3 \\
 H_\delta(T) &= H_\gamma(T_3) + \Delta H_3 + \int_{T_3}^T dt C_{P\delta}(t) && \text{for } T_3 < T \leq T_M \\
 H_L(T) &= H_\beta(T_M) + \Delta H_{fus} + C_{PL} \cdot (T - T_M) && \text{for } T_M < T .
 \end{aligned} \quad (7.14)$$

The enthalpy calculated according to eq. 7.13 can be seen on fig. 7.5 on page 43. The zero-point enthalpy of the normalized function is $H_0 = -4.95512 \text{ kJ/mol}$. The figure shows also the solely existing enthalpy data of B. F. Naylor, [7] from the year 1945.

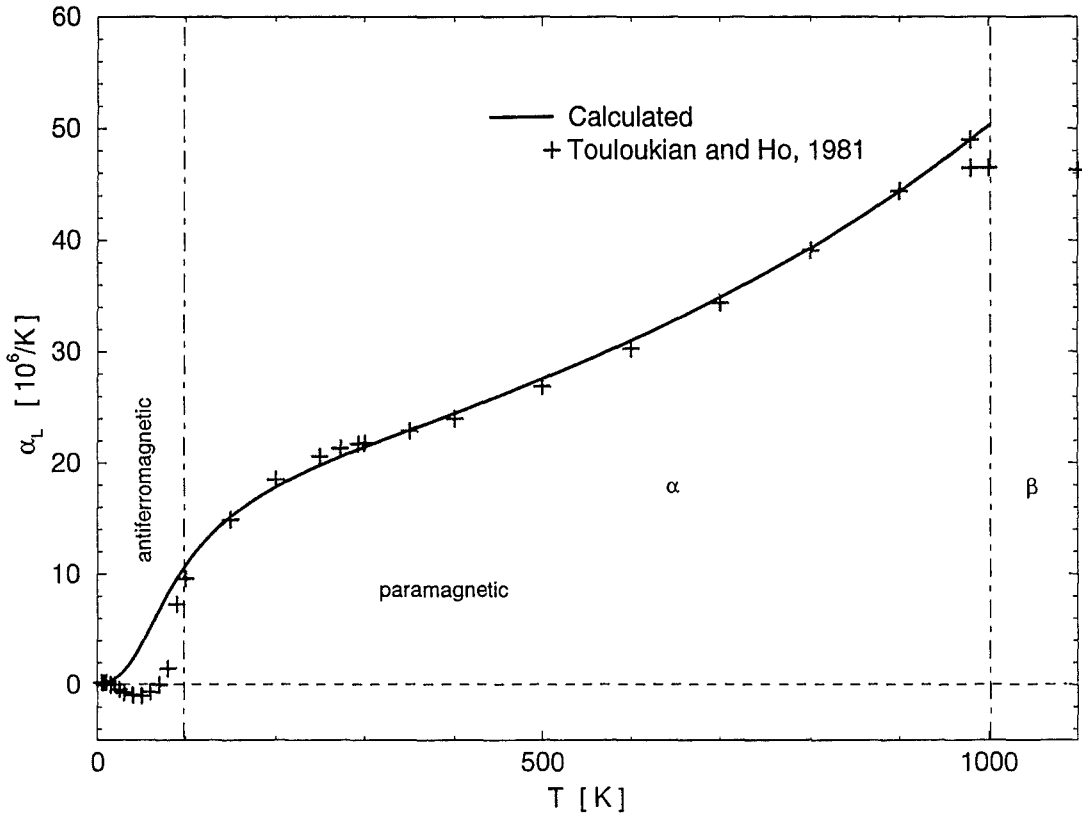


Figure 7.4: Manganese. Coefficient of the linear thermal expansion in the bcc-phase.

7.4 Thermal expansion and density

For solid manganese I developed at first the volumetric thermal expansion, depending on the tabulated data of Tolulokian and Ho, [120]. In describing the data the anomalous behaviour of the α -manganese below the Néel temperature was ignored.

In the α - Mn it was the α_L dataset of [120], to which I fitted a heat capacity-like function

$$\alpha_L = e \cdot (c_D + c_H) \quad \text{for } T \leq T_1 \quad . \quad (7.15)$$

As scaling factor in the above eq. I needed

$$e = 6.5 \cdot 10^{-7} \frac{\text{mol}}{J} \quad , \quad (7.16)$$

and the c_D , c_H parameters

$$\Theta_D = 375 \text{ K} \quad , \quad b = 0.031 \frac{J}{\text{mol K}^2} \quad , \quad d = 2.15 \cdot 10^{-8} \frac{J}{\text{mol K}^4} \quad (7.17)$$

(cf. eq. 7.9). V/V_{298} then I calculated from the α_L using eq. 3.2. Figure 7.4 on page 41 compares the fitting and fitted values.

In the remaining β , γ and δ -phases of the solid I fitted linear functions to the $\Delta L/L$ - data of Touloukian and Ho, and converted these functions via eq. 3.9 into the volumetric thermal expansions.

To calculate the densities from the volumetric thermal expansions (eq. 3.3) one needs the standard density, ρ_{298} too. The only density value I found in the solid state is $\rho_{293} = 7430 \text{ kg/m}^3$, reported in Touloukian and Ho, [120]. $\rho_{293} = 7438 \text{ kg/m}^3$ corresponds to a standard density of

$$\rho_{298} = 7428 \text{ kg/m}^3 . \quad (7.18)$$

In the liquid manganese there exist only one density measurement, made by Saito, Shiraishi, Sakuma, [37]. As density of liquid manganese I use their ρ (T) function directly.

Figure 7.6 on page 44 shows the density calculated from the volumetric thermal expansion and from the standard density given above (eq. 3.3). The figure displays also the densities, corresponding to the lattice data of Schmitz-Pranghe and Dünner, [35].

A_0	A_1	A_2	A_3
$T \leq 220 \text{ K}$			
7513.92	0.0639726	$-1.79144 \cdot 10^{-3}$	$2.01484 \cdot 10^{-6}$
$220 \text{ K} < T \leq 1002 \text{ K}$			
7550.04	-0.350643	$-1.64361 \cdot 10^{-4}$	$-1.17880 \cdot 10^{-7}$
$1002 \text{ K} < T \leq 1366 \text{ K}$			
7534.36	-0.886305	0.0	0.0
$1366 \text{ K} < T \leq 1406 \text{ K}$			
7526.10	-0.898348	0.0	0.0
$1406 \text{ K} < T \leq 1519 \text{ K}$			
7276.32	-0.761535	0.0	0.0
$1519 \text{ K} < T$			
7170.00	-0.930000	0.0	0.0

Table 7.3: Manganese. Coefficients of the density description

Table 7.3 shows the coefficients of the sets of polynomials describing the density of manganese in the solid and liquid states.

Figure 7.7 on page 45 presents the volumetric thermal expansion calculated from the density as a function of the enthalpy. The limiting enthalpy-values indicated on the figure are the following ones (in kJ/mol):

22.229, 24.429, 37.806, 40.046, 41.813, 43.663, 48.962, 62.212.

The enthalpy-value at the antiferromagnetic / paramagnetic border is -4.427 kJ/mol .

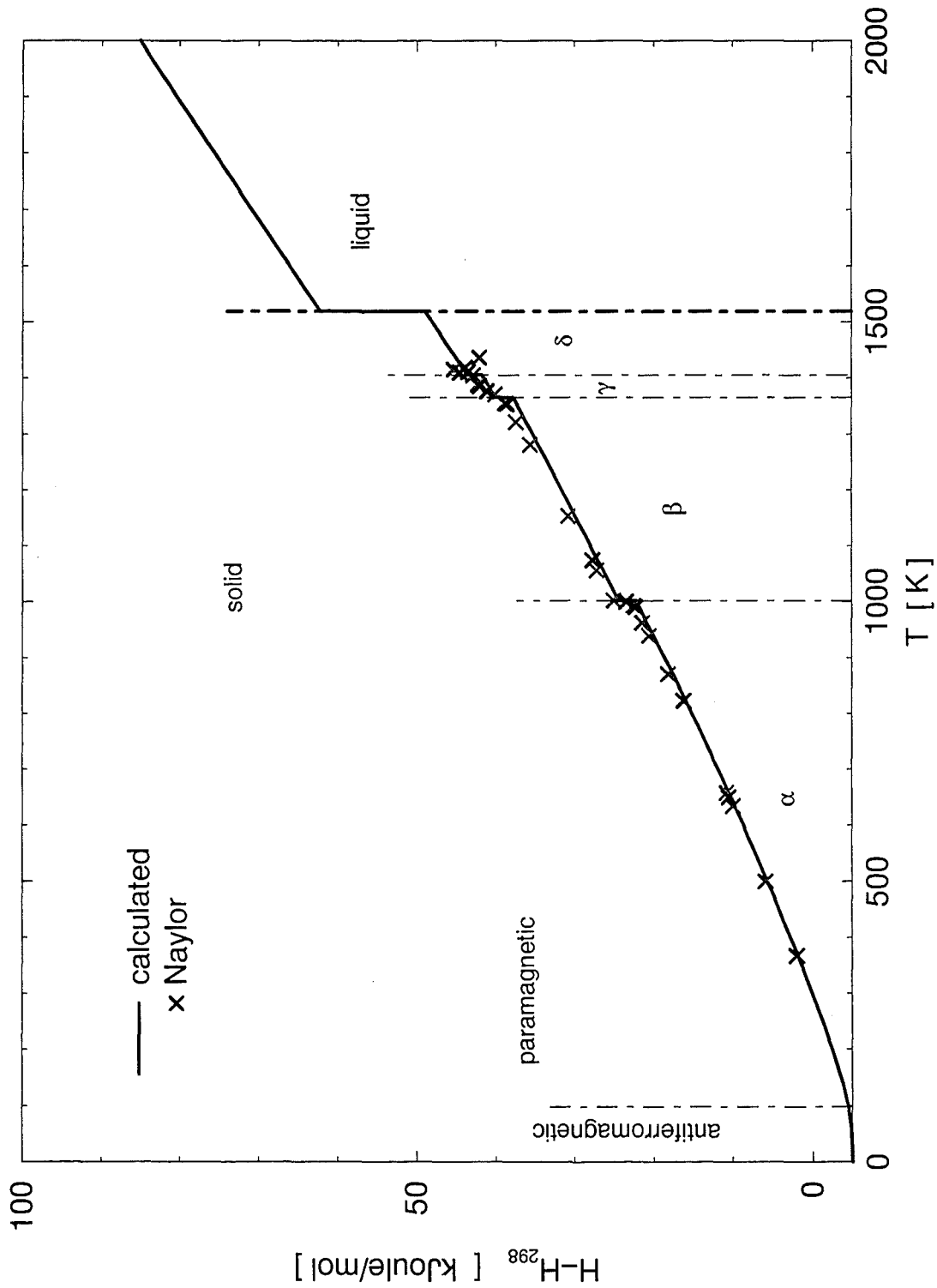


Figure 7.5: Manganese. Enthalpy as a function of the temperature.

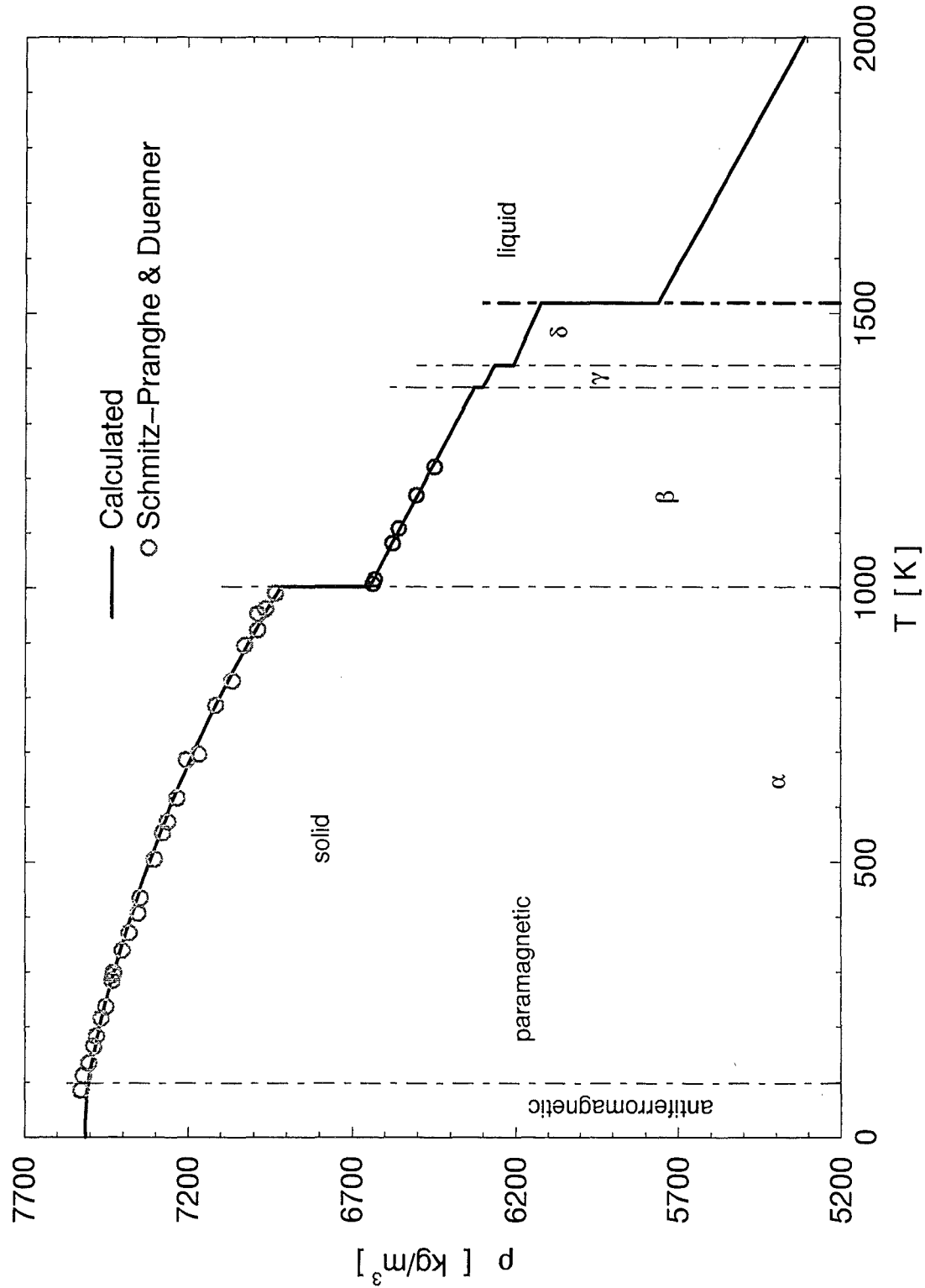


Figure 7.6: Manganese. Density as a function of the temperature.

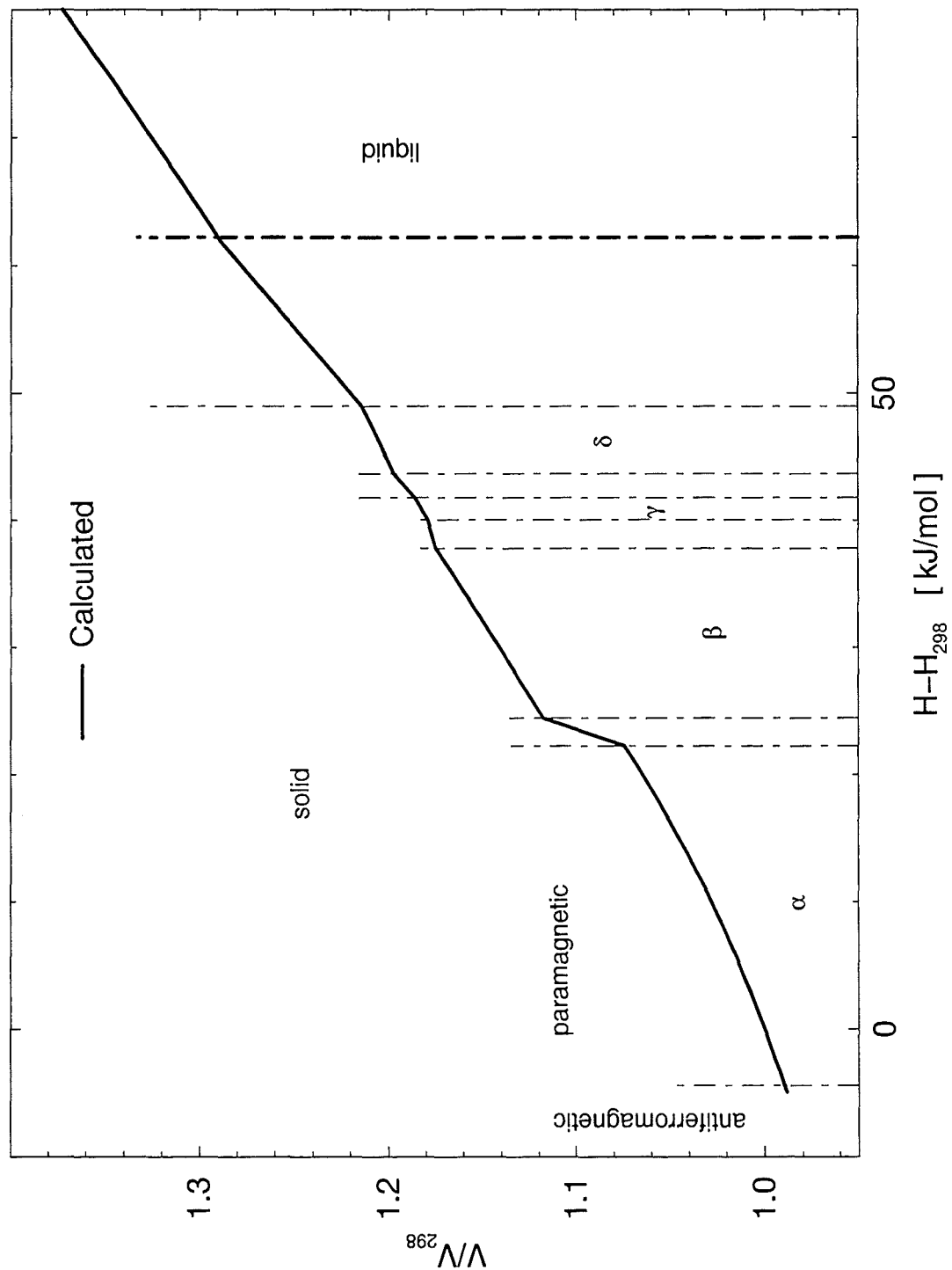


Figure 7.7: Manganese. Thermal expansion as a function of the enthalpy.

Chapter 8

Iron

8.1 Phase transitions

Reference		T_{Cu}	T_1	ΔH_1	T_2	ΔH_2	T_M	ΔH_{fus}
		K	K	$\frac{kJ}{mol}$	K	$\frac{kJ}{mol}$	K	$\frac{kJ}{mol}$
Hultgren	1967 [14]	1042	1184	0.90	1665	0.84	1809	13.816
Braun	1968 [34]	1039	1184	0.91	1664	0.85	1809	14.40
Treverton	1971 [47]	-	-	-	-	-	-	13.85
Cezairliyan	1975 [70]	-	-	-	1663	0.89	1808	-
Seydel	1977 [88]	-	-	-	-	-	-	15.36
Seydel	1979 [103]	-	-	-	-	-	-	15.53
Drotning	1981 [115]	-	-	-	-	-	1811	-
Desai	1985 [145]	1043	1185	0.90	1667	0.85	1811	13.81
Dobro-savljević	1985 [138]	1043	1208	-	1664	-	-	-
Pottlacher	1987 [147]	-	-	-	1664	-	-	15.02

Table 8.1: Iron. Transform properties

Iron is a relatively abundant metal, as well in the universe as in the crust of the earth.

The pure metal is silvery white, soft, ductile and chemically very reactive. Its atomic

weight is

$$\mu = 55.847 \frac{g}{mol} , \quad (8.1)$$

its zero-point enthalpy of sublimation (s. [3])

$$\Delta H_{sub} = 413.0 \frac{kJ}{mol} . \quad (8.2)$$

Iron is ferromagnetic below its Curie point and paramagnetic beyond this temperature.

Range , T < K	Structure	Transform heat kJ/mol
1043	α - Fe , bcc , ferromagnetic	-
1190	α - Fe , bcc , paramagnetic	0.91
1664	γ - Fe , fcc	0.85
1811	δ - Fe , bcc	13.85

Table 8.2: Iron. Phases and structures in the solid state

In choosing the **melting point** of iron I follow Desai, [145], respectively Drotning, [115] by setting

$$T_M = 1811 K . \quad (8.3)$$

For the **heat of the fusion** I have taken

$$\Delta H_{fus} = 13.85 kJ/mol \quad (8.4)$$

as measured by Treverton and Margrave, [47].

The Curie temperature, the transform-temperatures T_1 and T_2 and the corresponding heats I selected comparing the data of the groups Braun, [34] and Dobrosavljević, [138] (cf. tables 8.2 and 8.1).

Table 8.3 on page 48 shows estimated critical temperatures of iron.

8.2 Vapor pressure

As vapor pressure of iron I use the critical evaluations of Desai. The best-fit Dupré-Rankine approximation to these data is

$$\log_{10} p^\circ = 19.3846 - \frac{22142.8}{T} - 2.02528 \cdot \log_{10} T \quad \text{for } T \leq T_M$$

and

$$(8.5)$$

$$\log_{10} p^\circ = 21.0467 - \frac{21748.4}{T} - 2.60229 \cdot \log_{10} T \quad \text{for } T \geq T_M .$$

Figure 8.1 on page 48 compares the above approximation with the vapor pressure data of Desai. 8.1 displays also - as deviations from the above approximation - the vapor pressure

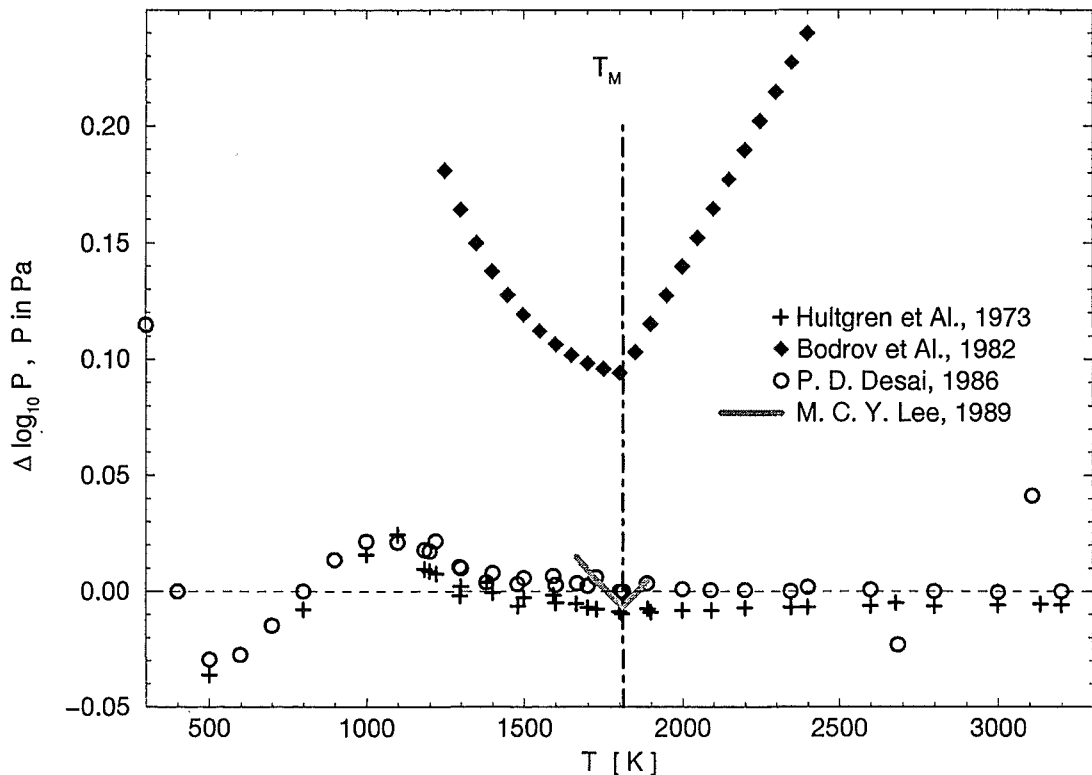


Figure 8.1: Iron. Deviations of the vapor pressure data from the Dupré-Rankine description.

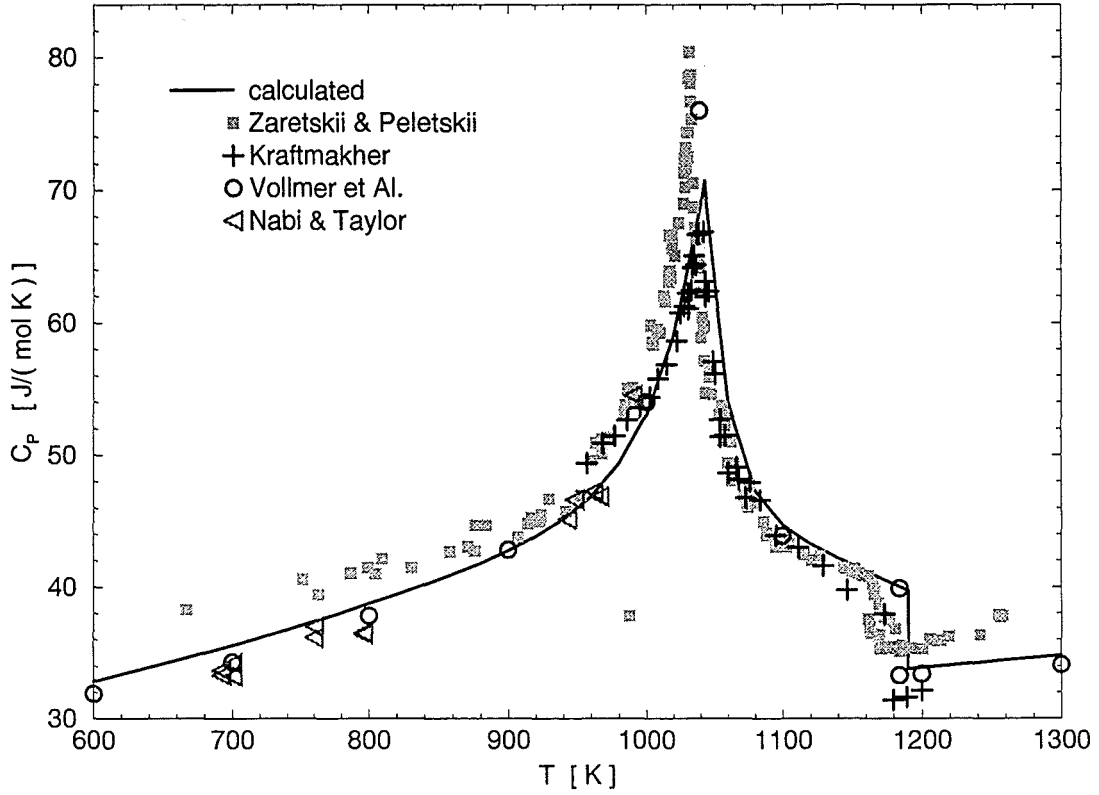
recommendations of the group Hultgren, [56], the experimental points of Bodrov, Nikolaev, and Nemec, [121] and the recently measured data of Lee, [162].

To the vapor pressure equation, eq. 8.5 corresponds a boiling point of

$$T_B = 3132.05 \text{ K} . \quad (8.6)$$

Author		T_c [K]	P_c [bar]
Young and Alder	[183] 1971	9340	10154
Fortov et al.	[74] 1975	9600	-
Drotning	[115] 1981	8300	-
Beutl et al.	[183] 1994	9250	8750

Table 8.3: Iron. Estimated critical temperatures and pressures

Figure 8.2: Iron. C_P change at the Curie-point.

8.3 Heat capacity and enthalpy

For fitting the heat capacity of iron I selected the low-temperature data ($T \leq 300$ K) of Desai, all the points of Kraftmakher, [60], of Peletskii and Zaretskii, [98] and the smoothed data of Dobrosavljević, Maglić and Perović, [138]. The C_P data of Kraftmakher show a T_{Cu} at 1040 K, the three data series of Peletskii and Zaretskii have Curie points at 1031, 1032 resp. 1033 K. To be able to use these data in the fitting I shifted the temperatures to get a common T_{Cu} at 1043 K.

In the first temperature range - for the ferromagnetic α -iron - one needs the Debye-, the Hoch- and the exponential- C_P -descriptions (eq.s 2.3, 2.5, 2.7). Fitting the combined data with

$$C_{P\alpha f} = C_{PD} + C_{PH} + C_{PE} \quad \text{for} \quad T \leq T_{Cu} \quad (8.7)$$

gives the following parameters for C_{PD}, C_{PH}, C_{PE} :

$$\Theta_D = 450 \text{ K} , \quad b = 0.01 \frac{\text{J}}{\text{mol K}^2} , \quad d = 1.2 \cdot 10^{-8} \frac{\text{J}}{\text{mol K}^4} , \\ g = -26.9303 , \quad h = 28.7829 \cdot 10^{-3} \text{ 1/K} . \quad (8.8)$$

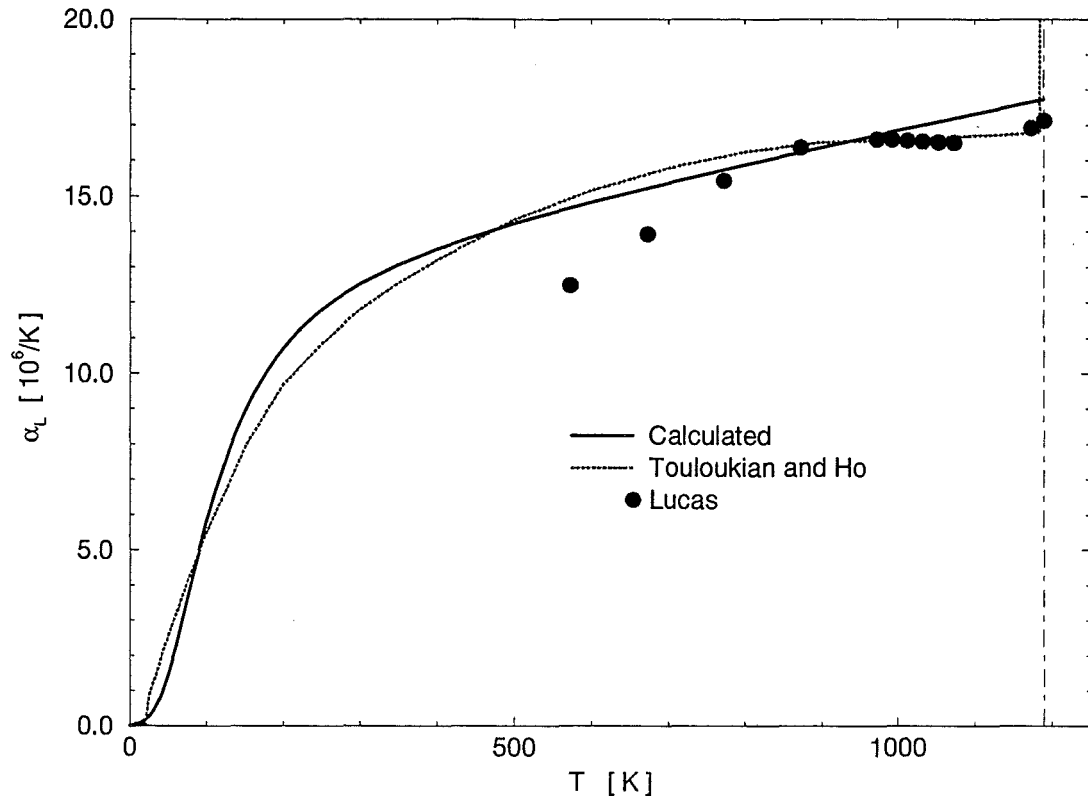


Figure 8.3: Iron. Coefficient of the linear thermal expansion in the bcc-phase.

To describe the heat capacity of the paramagnetic α -iron one needs, besides of a temperature-polynomial also an exponential expression:

$$C_{P\alpha p} [J/(mol K)] = 96.9948 - T \cdot 48.1135 \cdot 10^{-3} + e^{(g + T \cdot h)} \quad (8.9)$$

for $T_{Cu} < T \leq T_1$, with $g = 69.243$, $h = -63.3582 \cdot 10^{-3} 1/K$.

In the remaining solid-phases the heat capacity depends linearly from the temperature:

$$C_{P\gamma} [J/(mol K)] = 22.6632 + T \cdot 9.352 \cdot 10^{-3} \quad \text{for } T_1 < T \leq T_2, \quad (8.10)$$

and

$$C_{P\delta} [J/(mol K)] = -12.8556 + T \cdot 31.9468 \cdot 10^{-3} \quad \text{for } T_2 < T \leq T_M. \quad (8.11)$$

As the heat capacity of liquid I set

$$C_{PL} = 46.083 J/(mol K), \quad \text{for } T_M < T. \quad (8.12)$$

The above C_{PL} was measured recently by Beutl et al., [183] and compares also well with the data of Trevorton and Margrave (s. also fig. 8.7 on page 55).

Figure 8.6 on page 54 displays the heat capacity calculated by eq.s 8.7 - 8.12. The averaged C_P data of Dobrosavljević et al. and the recommended values of Desai are also shown. Figure

8.2 on page 49 compares the calculated heat capacity with the measured C_P -s in the vicinity of the Curie point. The measurements of Vollmer, Kohlhaas and Braun, [25] and the recently published values of Nabi and Taylor, [173] are also shown.

According to eq.s 8.7 - 8.12 the enthalpy of iron can be calculated as

$$H_{\alpha f}(T) = H_D(T) + H_H(T) + H_E(T) \quad \text{for } T \leq T_{Cu} \quad (8.13)$$

$$H_{\alpha p}(T) = H_{\alpha f}(T_{Cu}) + \int_{T_{Cu}}^T dt C_{P\alpha p}(t) \quad \text{for } T_{Cu} < T \leq T_1$$

$$H_{\gamma}(T) = H_{\alpha p}(T_1) + \Delta H_1 + \int_{T_1}^T dt C_{P\gamma}(t) \quad \text{for } T_1 < T \leq T_2$$

$$H_{\delta}(T) = H_{\gamma}(T_2) + \Delta H_2 + \int_{T_2}^T dt C_{P\delta}(t) \quad \text{for } T_2 < T \leq T_M$$

$$H_L(T) = H_{\delta}(T_M) + \Delta H_{fus} + C_{PL} \cdot (T - T_M) \quad \text{for } T_M < T$$

The enthalpy, described by the above eq. is shown on figure 8.7 on page 55. The enthalpy is normalized to 298.15 K, with a zero-point value of $H_0 = -4.52088 \text{ kJ/mol}$.

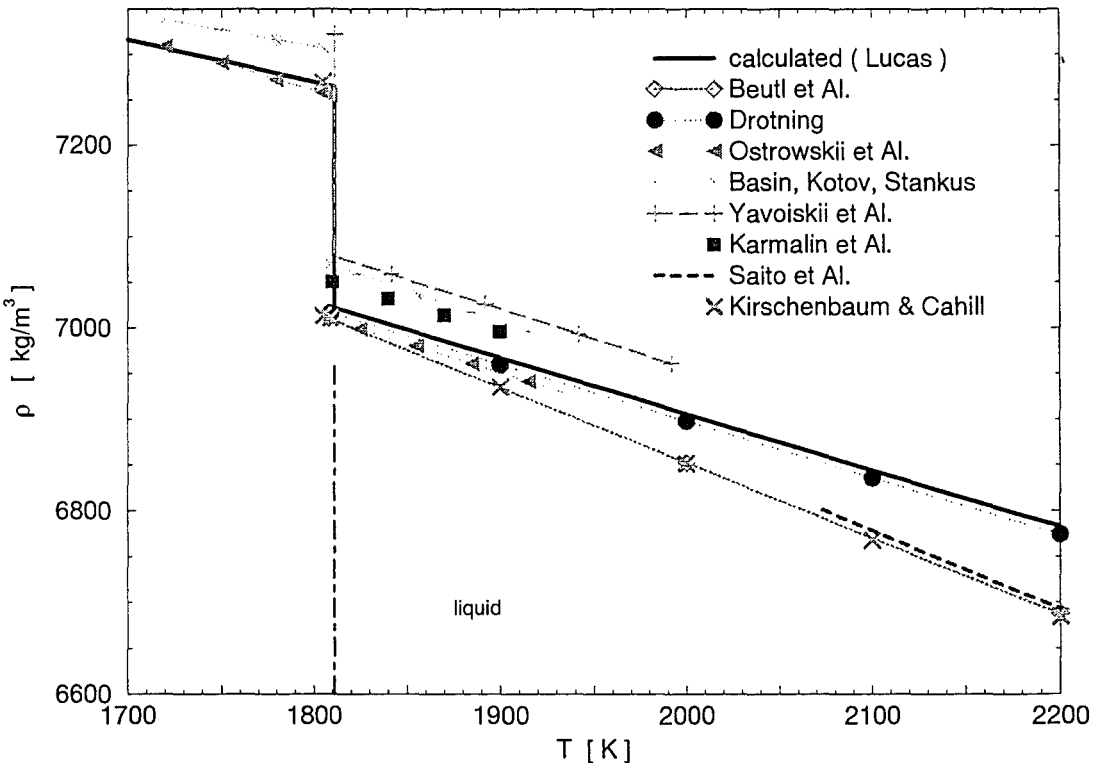


Figure 8.4: Iron. Density in the liquid state.

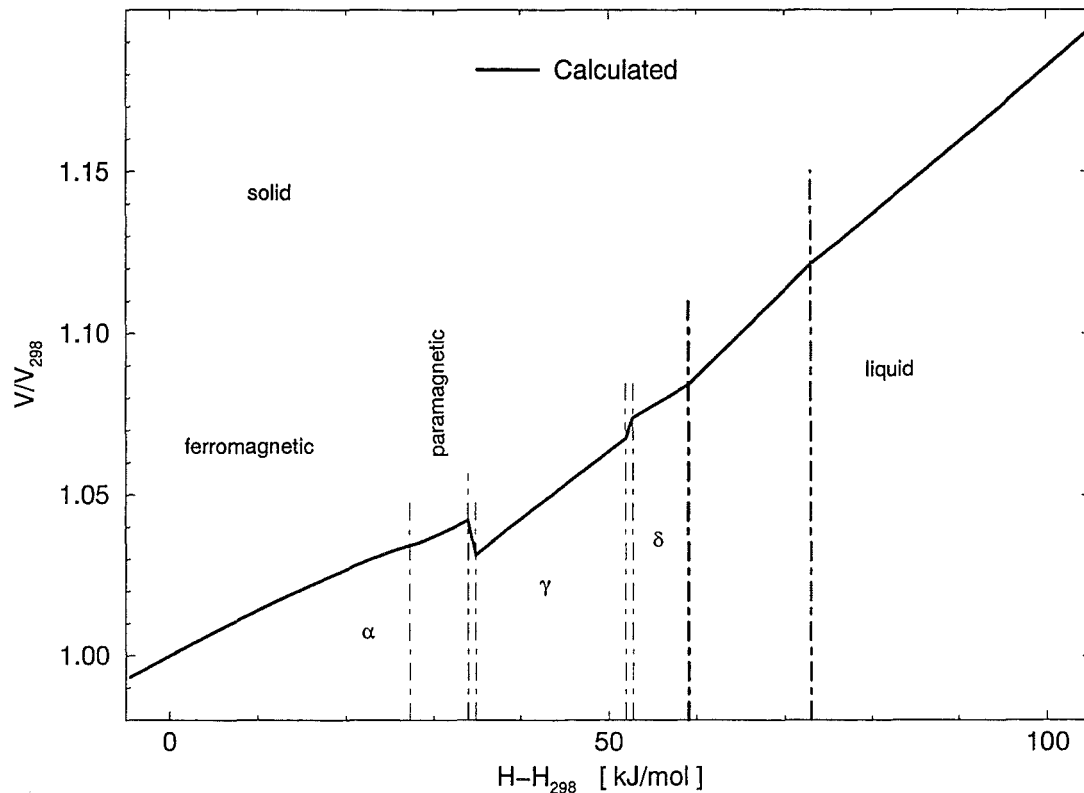


Figure 8.5: Iron. Thermal expansion as a function of the enthalpy.

8.4 Thermal expansion and density

In developing a density description for iron I selected the recommended α_L data of Tolulokian and Ho, [120] for the bcc (α) - phase of the solid and the measurements of Lucas, [50] in the remaining domains.

Figure 8.3 on page 50 displays the coefficient of the thermal expansion of the α -iron. The function, fitted to the tabulated data of Tolulokian and Ho

$$\alpha_L = e \cdot (c_D + c_H) \quad \text{for } T \leq T_1 \quad (8.14)$$

has the scaling factor of

$$e = 5 \cdot 10^{-7} \frac{\text{mol}}{\text{J}} , \quad (8.15)$$

and the parameters

$$\Theta_D = 450 \text{ K} , \quad b = 0.009 \frac{\text{J}}{\text{mol K}^2} . \quad (8.16)$$

The α_L - data of Lucas, shown in the figure are calculated from the tabulated V/V_{298} - values. To this end a polynomial of 5th grade

$0.957834 \quad 2.77082 \cdot 10^{-4} \quad -6.68390 \cdot 10^{-7} \quad 8.76136 \cdot 10^{-10} \quad -5.37173 \cdot 10^{-13} \quad 1.26264 \cdot 10^{-16}$
was adjusted to the points to be able to calculate α_L by eq. 3.1.

Density of the α -iron To get the density in the bcc - iron the volumetric thermal expansion was calculated from the α_L function 8.14 (eq. 3.2). Now this property was compared with the density points of Lucas via eq. 3.3. Best fitting resulted at a standard density of

$$\rho_{298} = 7875 \text{ kg/m}^3 \quad (8.17)$$

(cf. figure 8.8 on page 56). Touloukian and Ho, [120] recommend as standard density $\rho_{298} = 7867 \text{ kg/m}^3$.

In the γ - and δ - solid I have taken the densities of Lucas.

Density of liquid iron Figure 8.4 on page 51 shows densities of liquid iron, measured by Beutl, Pottlacher, and Jäger, [183], by Drotning, [115], by Ostrowskii, Ermachenkov, Popov, Grigoryan and Kogan, [109] by Basin, Kolotov and Stankus, [101], by Yavoiskii, Ezhov, Kravchenko, Uckov, Nebosov, Chernov and Dorofeev, [66], by Karmalin, [82], by Lucas,[50] by Saito, Shiraishi and Sakuma, [37] and by Kirshenbaum and Cahill, [12].

As the figure shows, the densities of Drotning, of Ostrowskii et al. and those of Lucas are very close to each-other, so for liquid iron I have selected the data of Lucas.

Note. Drotning and the russian group used the γ -attenuation technique, Lucas applied the Archimedean method.

The whole density - temperature relation for iron can be seen on the figure 8.8 on page 56. The coefficients of the density polynomials for iron are collected in the table 8.4.

A_0	A_1	A_2	A_3
$T \leq 210 \text{ K}$			
7927.62	0.034817	$-8.84347 \cdot 10^{-4}$	$3.62674 \cdot 10^{-7}$
$210 \text{ K} < T \leq 1190 \text{ K}$			
7954.13	-0.233256	$-1.18840 \cdot 10^{-4}$	$2.82515 \cdot 10^{-8}$
$1190 \text{ K} < T \leq 1664 \text{ K}$			
8284.36	-0.545729	0.0	0.0
$1664 \text{ K} < T \leq 1811 \text{ K}$			
8106.47	-0.464781	0.0	0.0
$1811 \text{ K} < T$			
8136.09	-0.615060	0.0	0.0

Table 8.4: Iron. Coefficients of the density description

Figure, 8.5 on page 52 displays the volumetric thermal expansion as a function of the normalized enthalpy.

The enthalpy values, separating the different iron phases, are:

27.281, 34.015, 34.925, 51.993, 52.843, 59.113 and 72.963 kJ/mol .

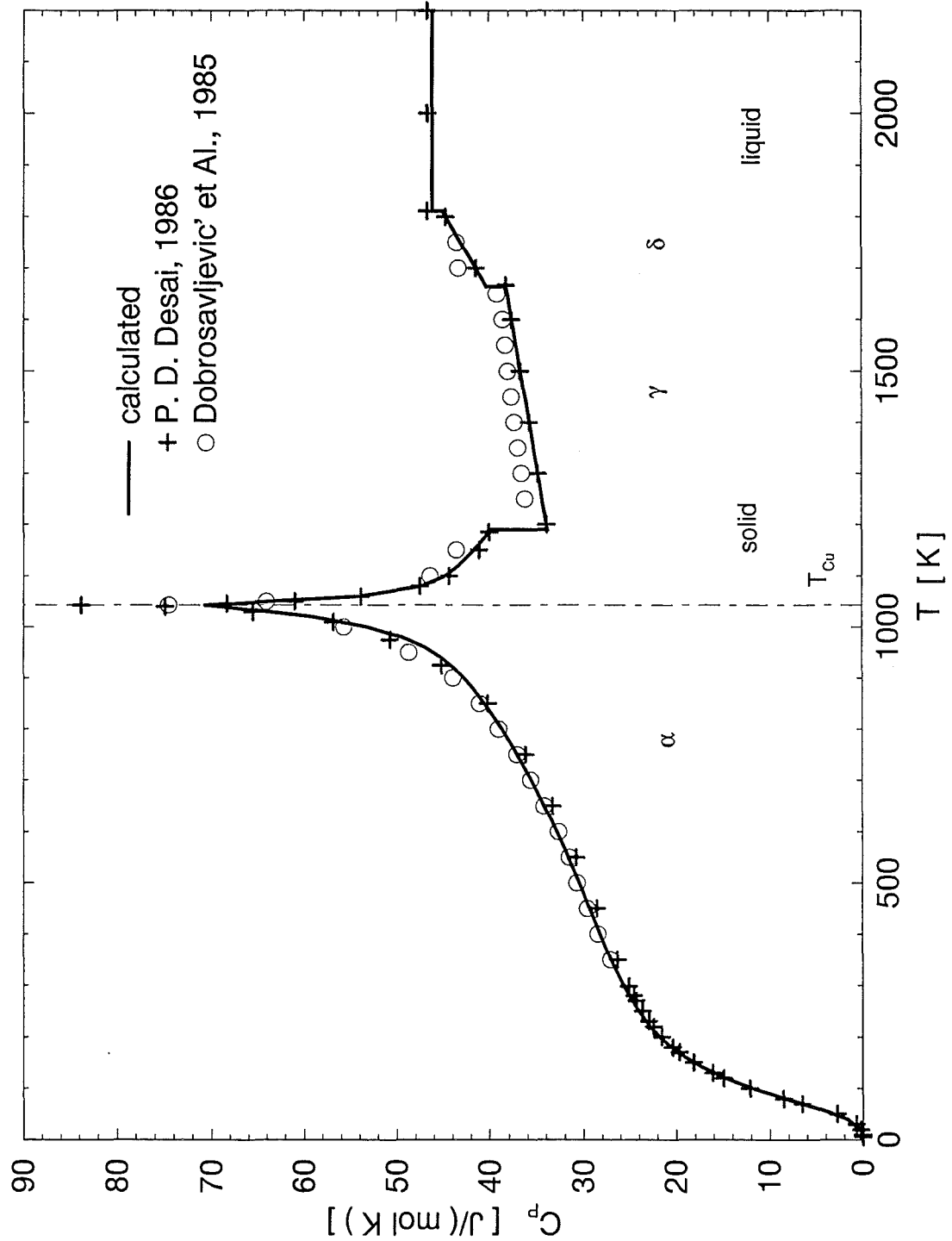


Figure 8.6: Iron. Heat capacity C_P as a function of the temperature.

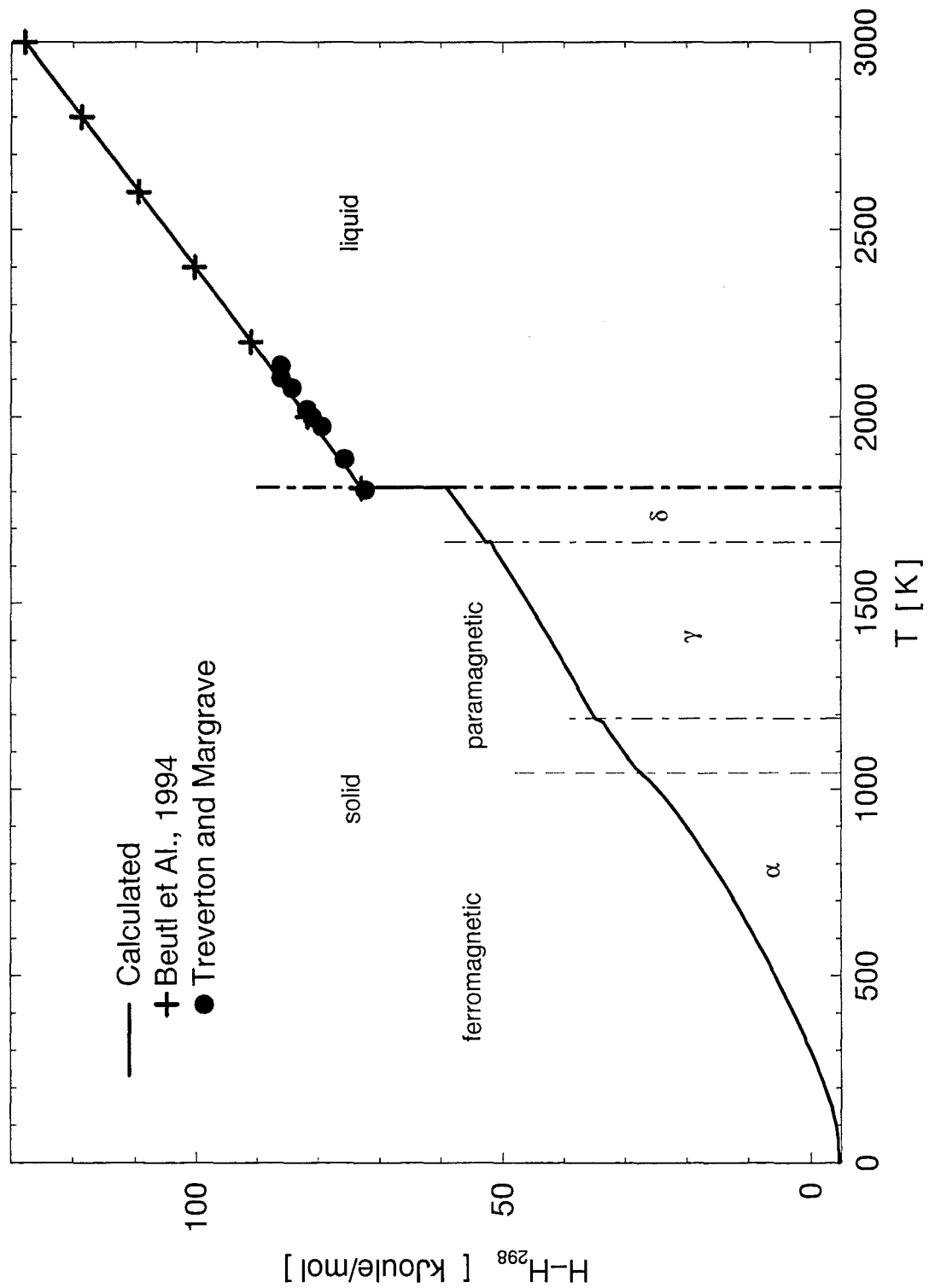


Figure 8.7: Iron. Enthalpy as a function of the temperature

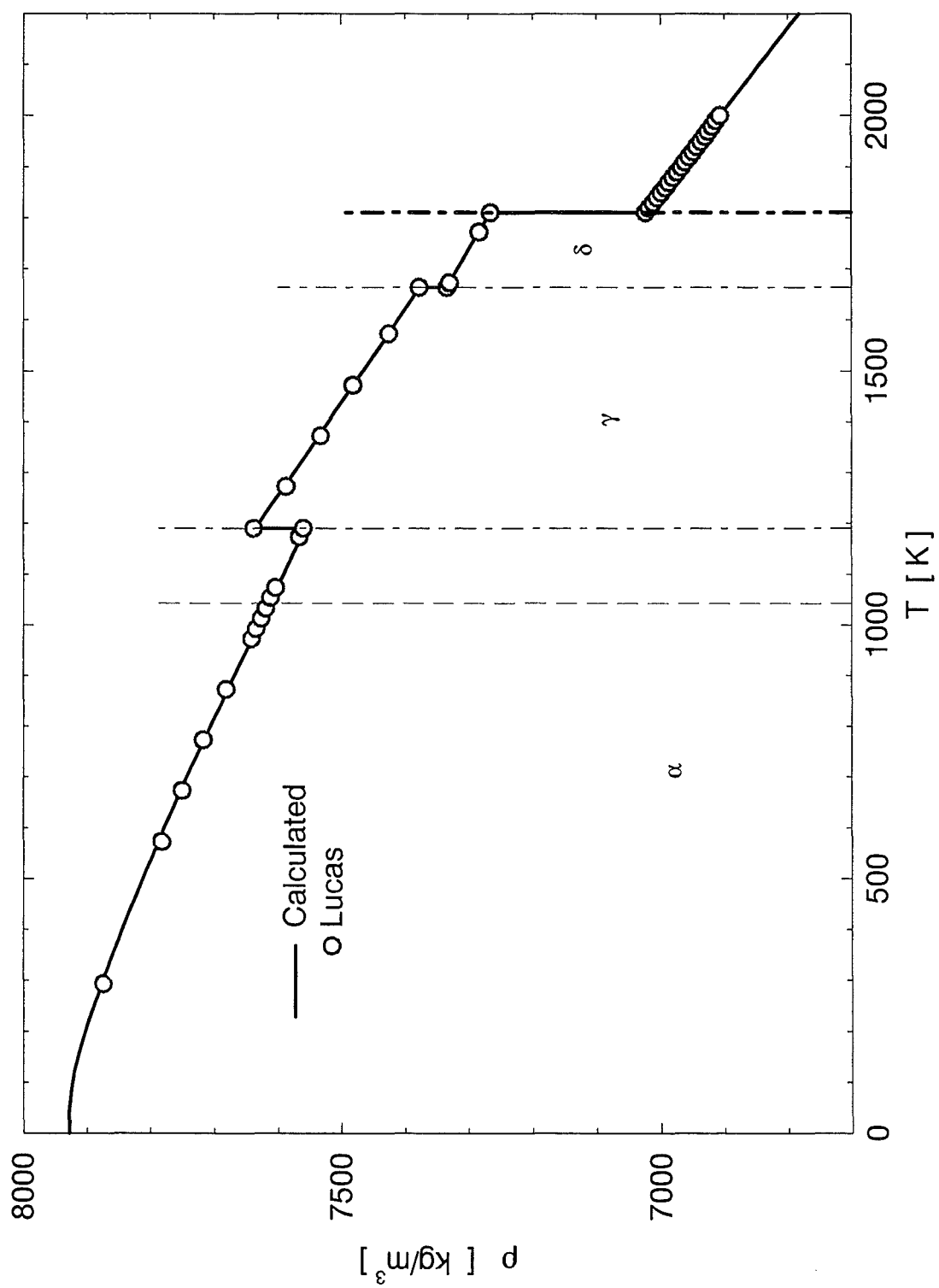


Figure 8.8: Iron. Density as a function of the temperature.

Chapter 9

Cobalt

9.1 Phase transitions

Cobalt is a bluish, hard and brittle metal. It has an atomic weight of

$$\mu = 58.933 \frac{g}{mol} , \quad (9.1)$$

its zero-point enthalpy of sublimation is (s. [3])

$$\Delta H_{sub} = 423.1 \frac{kJ}{mol} . \quad (9.2)$$

Range , T < K	Structure	Transform heat kJ/mol
718	α - Co , hcp , ferromagnetic	0.4551
1380	β - Co , fcc , ferromagnetic	-
1767	β - Co , fcc , paramagnetic	16.20

Table 9.1: Cobalt. Phases and structures in the solid state

Solid cobalt changes from the hcp- to the fcc-phase at $\sim 700 K$. The heat of this transformation I had taken from Adams and Alstetter, [32], the temperature from Dobrosavljević, Maglić and Perović, [164].

Cobalt is ferromagnetic below its Curie point, and paramagnetic above it.

$$T_{Cu} = 1380 K , \quad (9.3)$$

the Curie point of cobalt I had taken equally from [164].

As the melting point of cobalt I use the value of Drotning [115]:

$$T_M = 1767 K . \quad (9.4)$$

In selecting the heat of the fusion I follow Braun, Kohlhaas und Vollmer, [34]:

$$\Delta H_{fus} = 16.2 kJ/mol . \quad (9.5)$$

Reference		T_{Cu}	T_1	ΔH_1	T_M	ΔH_{fus}
		K	K	$\frac{kJ}{mol}$	K	$\frac{kJ}{mol}$
Hultgren	1966 [56]	1394	700	0.452	1768	16.20
Braun	1968 [34]	1377	703	0.45	1767	16.20
Adams et al.,	1968 [32]	-	695	0.4551	-	-
Seydel	1977 [88]	-	-	-	-	17.72
Seydel	1979 [103]	-	-	-	-	17.80
Touloukian and Ho	1981 [120]	1395	715	0.452	1767	16.148
Drotning	1981 [115]	-	-	-	1767	-
Dobrosavljević et al.,	1989 [164]	1380	718	-	-	-

Table 9.2: Cobalt. Transform properties

Table 9.2 presents phase transition data of cobalt.

As the critical temperature of cobalt Fortov, Dremin and Leont'ev, [74] estimate

$$T_c \sim 9620K . \quad (9.6)$$

9.2 Vapor pressure

As vapor pressure of cobalt I use the data recommended by Hultgren et al., [56]. In adjusting a Dupré-Rankine equation to the tabulated values I dropped the first of them, for it didn't fit to the other points (s. figure 9.1 on page 59).

The best-fit Dupré-Rankine approximation to the remaining points is

$$\log_{10} p^\circ = 17.5569 - \frac{22750.5}{T} - 1.48534 \cdot \log_{10} T \quad \text{for } T \leq T_M$$

and

$$(9.7)$$

$$\log_{10} p^\circ = 17.3628 - \frac{21903.6}{T} - 1.57314 \cdot \log_{10} T \quad \text{for } T \geq T_M .$$

To the above vapor pressure equation corresponds a boiling point of

$$T_B = 3200.98 K . \quad (9.8)$$

9.3 Heat capacity and enthalpy

For fitting the heat capacity of cobalt I selected the low-temperature data ($T \leq 300 K$) of Touloukian and Ho, [120], all the points of Vollmer et al., [25], of Kraftmakher, [60], of Peletskii

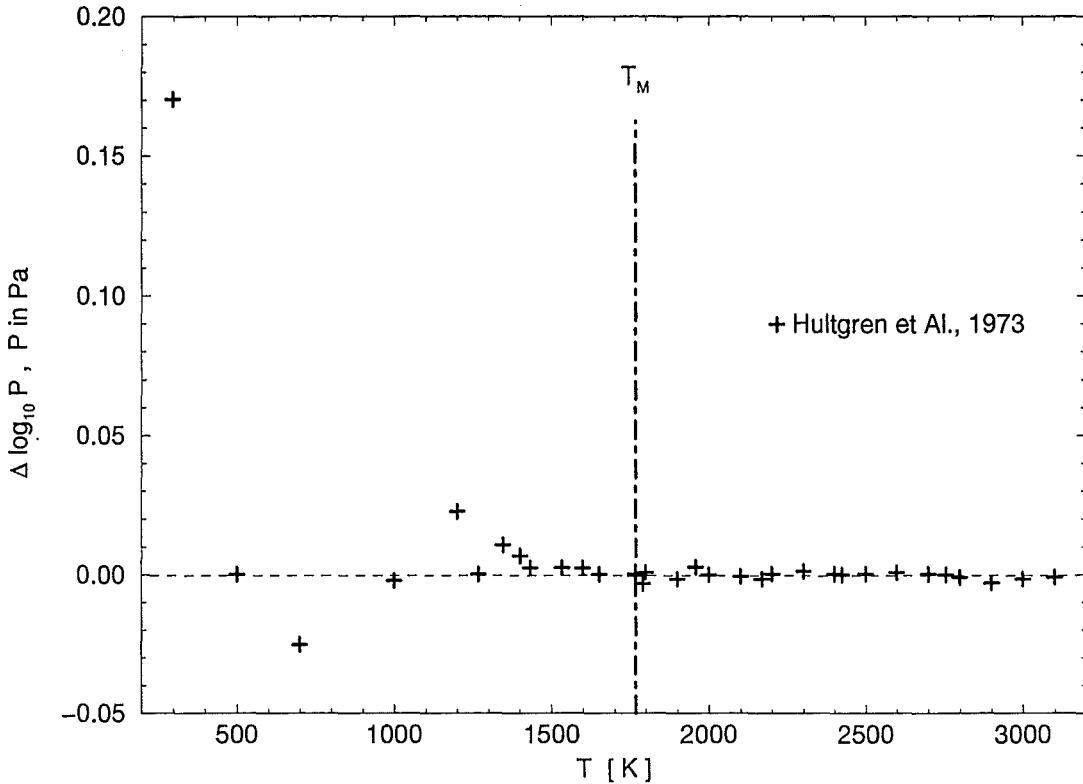


Figure 9.1: Cobalt. Deviations of the vapor pressure data of Hultgren from the Dupré-Rankine description.

and Zaretskii, [98] and the smoothed data of Dobrosavljević et al., [164].

To describe the heat capacity of the ferromagnetic α cobalt one needs all the three fitting functions: the Debye-, the Hoch- and the exponential- descriptions (s. eq.s 2.3, 2.5, 2.7):

$$C_{P\alpha f} = C_{PD} + C_{PH} + C_{PE} \quad \text{for} \quad T \leq T_1 \quad (9.9)$$

The parameters of the best fitted description have the following values:

$$\begin{aligned} \Theta_D &= 390 \text{ K} , \quad b = 0.006 \frac{\text{J}}{\text{mol K}^2} , \quad d = 8.0 \cdot 10^{-9} \frac{\text{J}}{\text{mol K}^4} , \\ g &= -153.856 , \quad h = 0.218408 \text{ 1/K} . \end{aligned} \quad (9.10)$$

In the ferromagnetic β cobalt one needs again, as in the case of the iron, a supplementary exponential expression besides of a temperature-polynomial:

$$C_{P\beta f} [\text{J/(mol K)}] = 17.5 - T \cdot 0.019 + e^{(g + T \cdot h)} \quad (9.11)$$

$$\text{for} \quad T_1 < T \leq T_{Cu} , \quad \text{with} \quad g = -9.38386 , \quad h = 0.0087 \text{ 1/K} .$$

In the paramagnetic β cobalt the heat capacity decreases exponentially until it reaches a constant value:

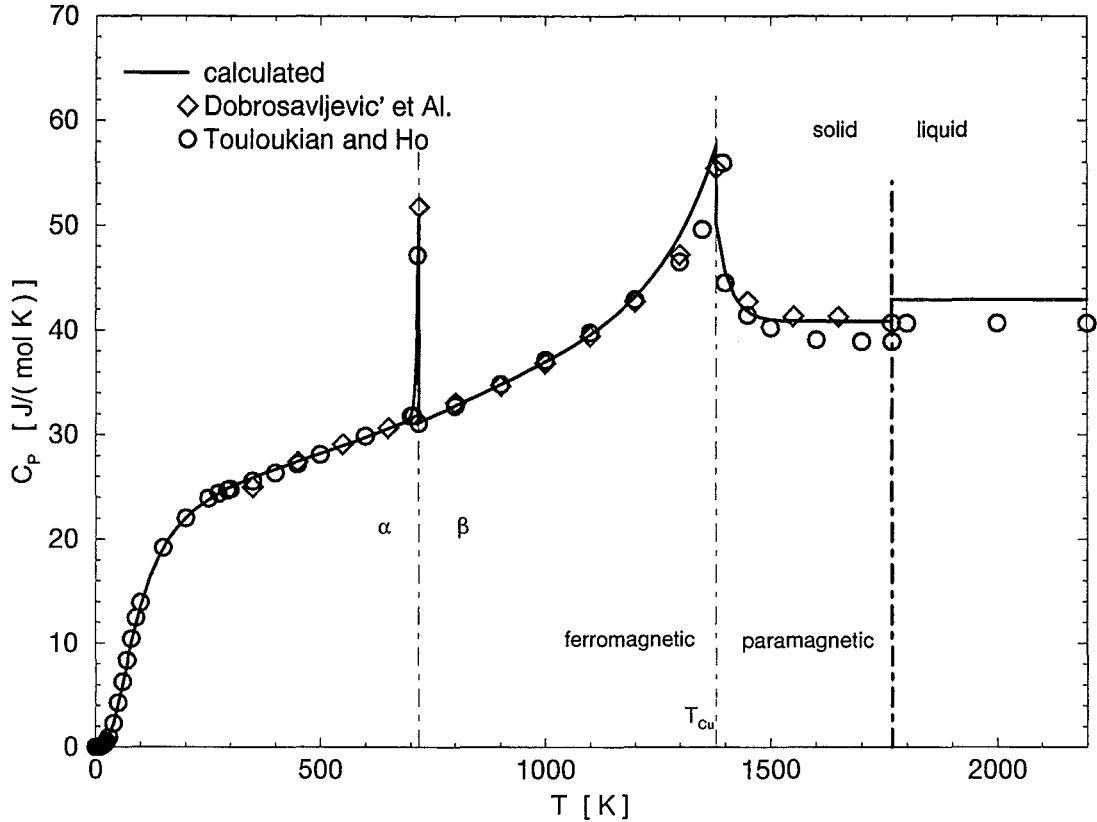


Figure 9.2: Cobalt. Heat capacity C_P as a function of the temperature.

$$C_{P\beta p} [\text{J}/(\text{mol K})] = 40.85 + e^{(g + T \cdot h)} \quad (9.12)$$

for $T_{Cu} < T \leq T_M$, with $g = 47.604$, $h = -0.0328803 \text{ J/K}$.

For liquid cobalt I selected a heat capacity, which describes the enthalpy increase measured in the liquid by Wüst, Meuthen and Durrer, [5] (s. figure 9.7 on page 65):

$$C_{PL} = 42.89 \text{ J}/(\text{mol K}) , \text{ for } T_M < T . \quad (9.13)$$

The enthalpy of cobalt can be calculated according to:

$$H_{\alpha f}(T) = H_D(T) + H_H(T) + H_E(T) \quad \text{for } T \leq T_1 \quad (9.14)$$

$$H_{\beta f}(T) = H_{\alpha f}(T_1) + \Delta H_1 + \int_{T_1}^T dt C_{P\beta f}(t) \quad \text{for } T_1 < T \leq T_{Cu}$$

$$H_{\beta p}(T) = H_{\beta f}(T_{Cu}) + \int_{T_{Cu}}^T dt C_{P\beta p}(t) \quad \text{for } T_{Cu} < T \leq T_M$$

$$H_L(T) = H_{\beta p}(T_M) + \Delta H_{fus} + C_{PL} \cdot (T - T_M) \quad \text{for } T_M < T .$$

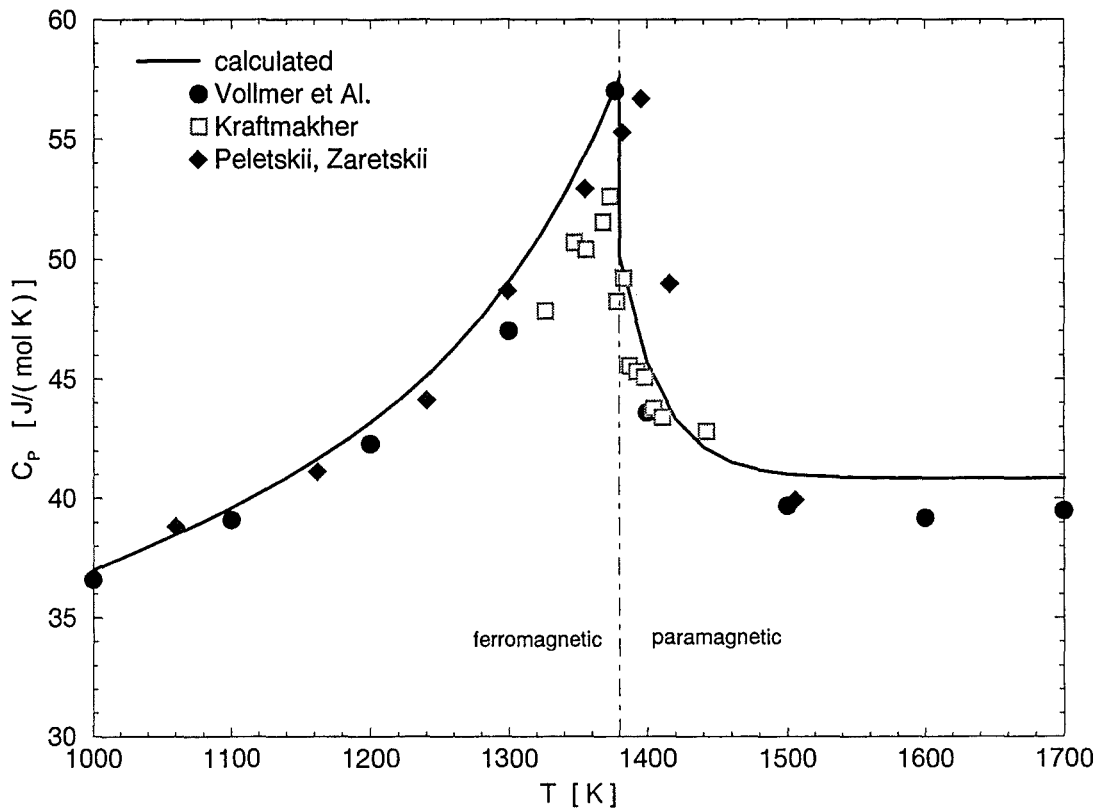
Figure 9.3: Cobalt. C_P change at the Curie-point.

Figure 9.2 on page 60 shows the heat capacity calculated by eq.s 9.9 - 9.13. Figure 9.3 compares calculated and measured C_P -s in the vicinity of the Curie point.

Figure 9.7 on page 65 shows the corresponding enthalpy - temperature relation. The enthalpy is normalized to 25 centigrades and has a zero-point value $H_0 = -4.69508 \text{ kJ/mol}$. 9.7 displays also the measurements of Wuest et al. and of S. Umino, [6]. Both datasets I have taken from the cobalt-report of Guillermet, [151].

9.4 Thermal expansion and density

In developing the density function of cobalt I use, as in the case of the iron, the recommended data of Tolulokian & Ho, [120] and the measurements of Lucas, [50].

In the hcp-phase the α_L -values from [120] can be easily fitted with an

$$\alpha_L = e \cdot (c_D + c_H) \quad \text{for } T \leq T_1 \quad (9.15)$$

type equation. The hcp - cobalt has the same scaling factor as the bcc-iron, namely

$$e = 5 \cdot 10^{-7} \frac{\text{mol}}{\text{J}} \quad . \quad (9.16)$$

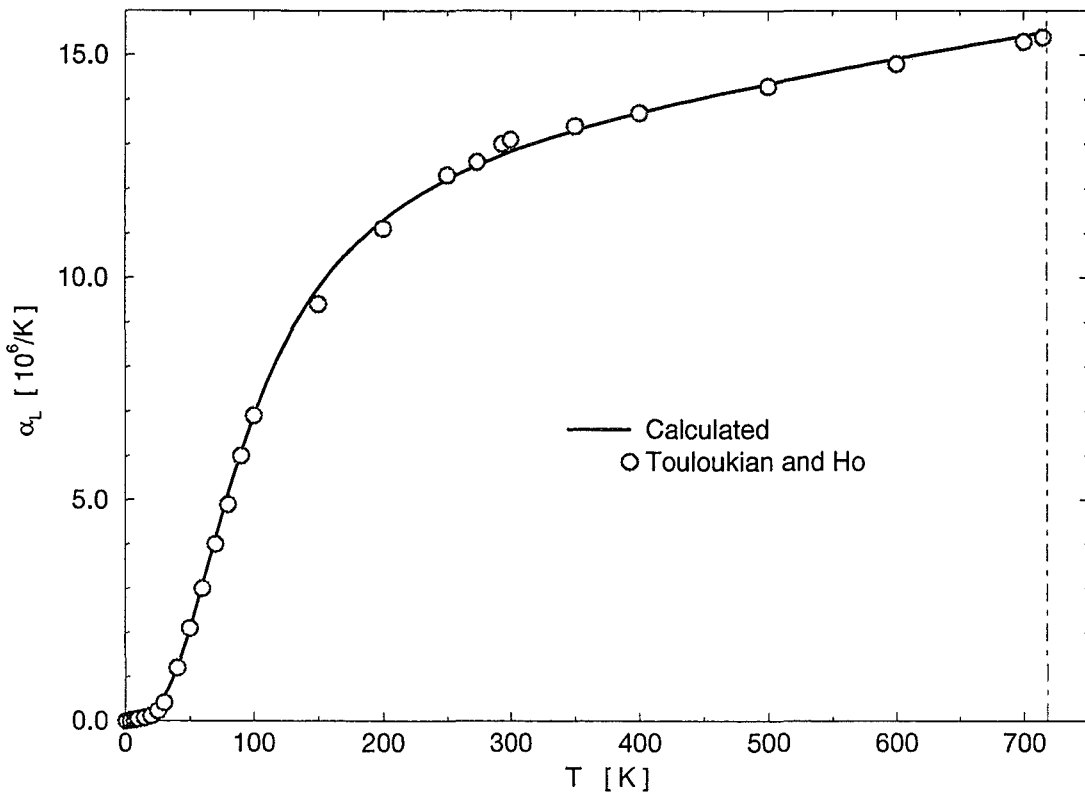


Figure 9.4: Cobalt. Coefficient of the linear thermal expansion in the hcp-phase.

The remaining parameters are

$$\Theta_D = 390 \text{ K} , \quad b = 0.009 \frac{\text{J}}{\text{mol K}^2} . \quad (9.17)$$

Figure 9.4 compares α_L data of the hcp-phase with values, calculated by eq. 9.15.

In calculating the density of the hcp - cobalt from the α_L function via eq. 3.3. I use

$$\rho_{298} = 8830 \text{ kg/m}^3 \quad (9.18)$$

as standard density. Laubitz and Matsumura report in [62] a cobalt density of

$$\rho(293\text{K}) = 8831 \text{ kg/m}^3 ,$$

leading to the above value at the standard-temperature 298.15 K.

Note. Touloukian and Ho recommend $\rho_{298} = 8831 \text{ kg/m}^3$.

In the fcc-phase (β - cobalt) I have taken the $\Delta L/L$ data from [120], calculated from them the $V(T)/V_{298}$ -function (eq. 3.9) and turned V/V_{298} with the standard density into the density - temperature function (eq. 3.3).

The liquid state. Figure 9.5 on page 63 displays a number of recently measured density - temperature functions for liquid cobalt. The data of Drotning, [115] of Ostrovskii et al., [109]

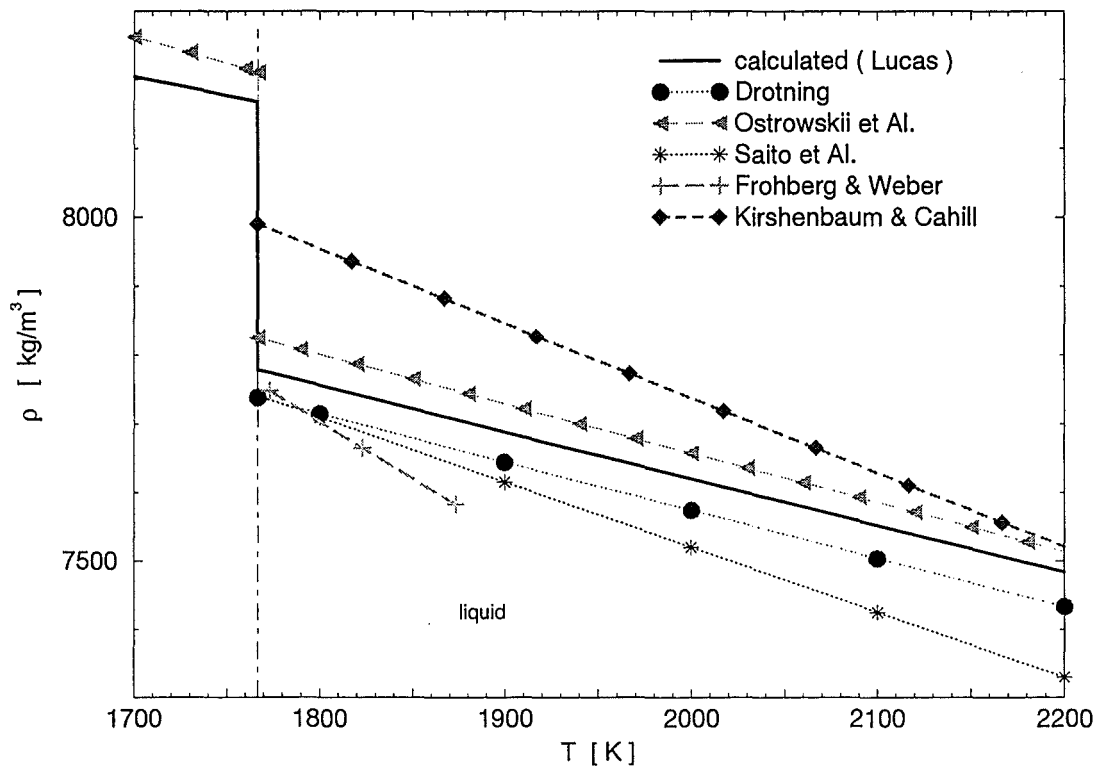


Figure 9.5: Cobalt. Density in the liquid state.

and of Lucas compare well with each other, as it was also the case in liquid iron. So I have taken again the description of Lucas, [50] for the density in liquid state:

$$\rho(T) = \frac{1000}{0.107273 + T \cdot 1.1997 \cdot 10^{-5}}, \quad (9.19)$$

and fitted a linear $\rho(T)$ function to it.

Table 9.3 on page 64 shows the coefficients of the density description of cobalt for the whole temperature region. Figure 9.8 on page 66 displays the $\rho(T)$ function described by these coefficients.

Figure 9.6 on page 64 shows the corresponding volumetric thermal expansion as a function of the enthalpy. The enthalpy values, separating in the figure the different cobalt phases, are:

11.996, 12.451, 38.808, 54.899 and 71.099 kJ/mol.

A_0	A_1	A_2	A_3
$T \leq 210 \text{ K}$			
8893.89	0.0261404	$-8.26870 \cdot 10^{-4}$	$-1.11014 \cdot 10^{-6}$
$150 \text{ K} < T \leq 718 \text{ K}$			
8914.61	-0.222135	$-2.40621 \cdot 10^{-4}$	$1.11430 \cdot 10^{-7}$
$718 \text{ K} < T \leq 1767 \text{ K}$			
8854.38	-0.222111	$-9.41919 \cdot 10^{-5}$	0.0
$1767 \text{ K} < T$			
8981.88	-0.680856	0.0	0.0

Table 9.3: Cobalt. Coefficients of the density description

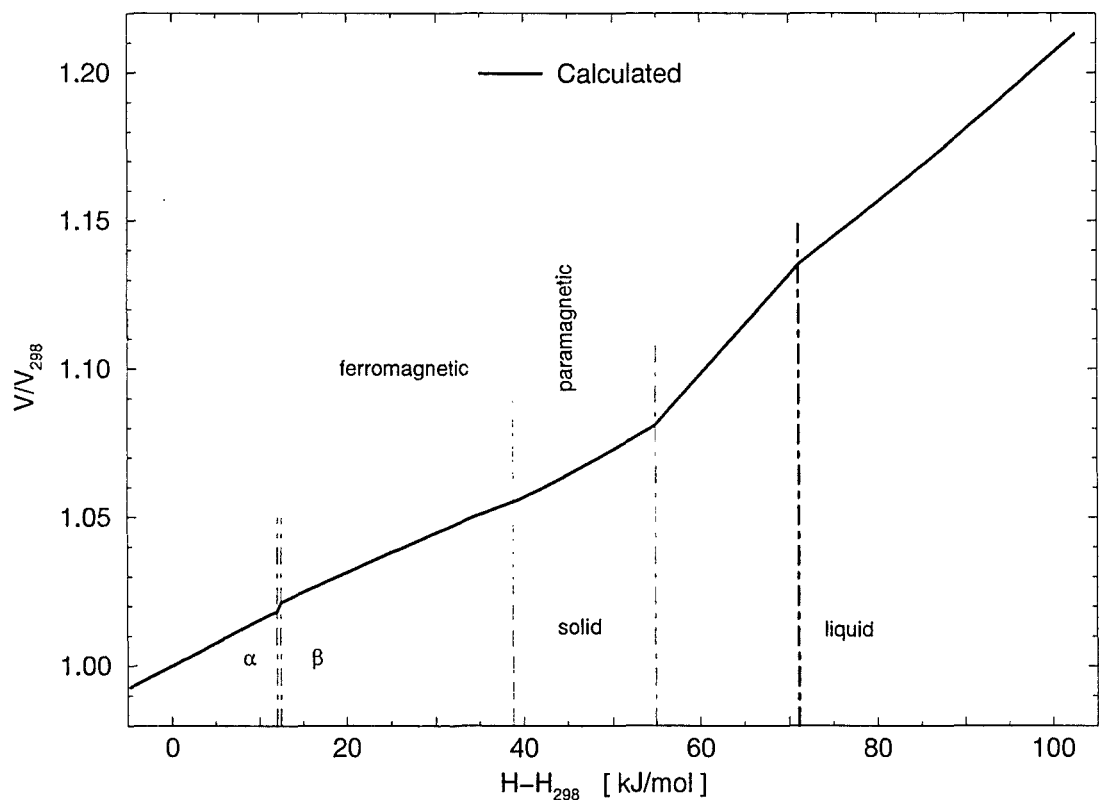


Figure 9.6: Cobalt. Thermal expansion as a function of the enthalpy.

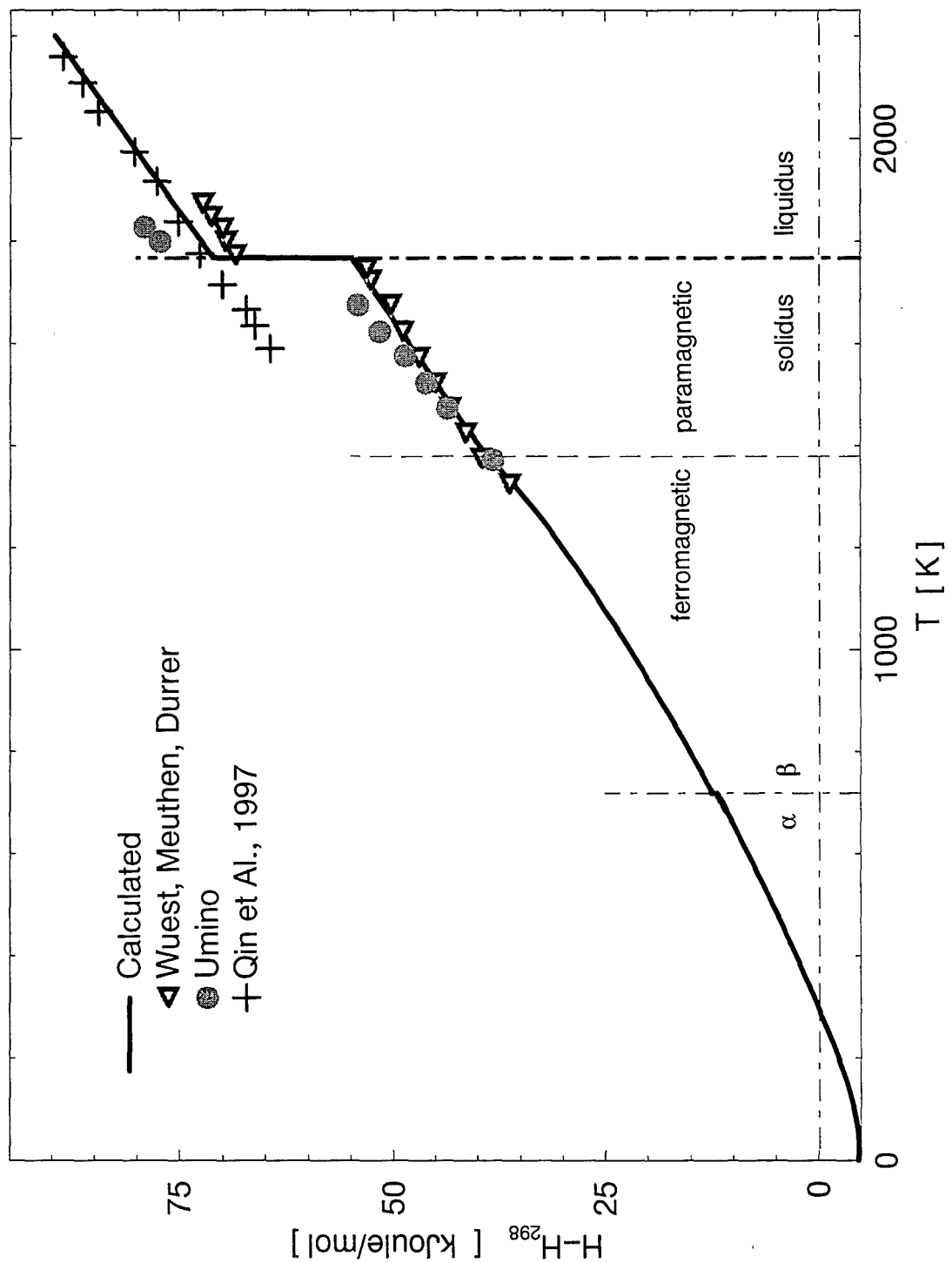


Figure 9.7: Cobalt. Enthalpy as a function of the temperature

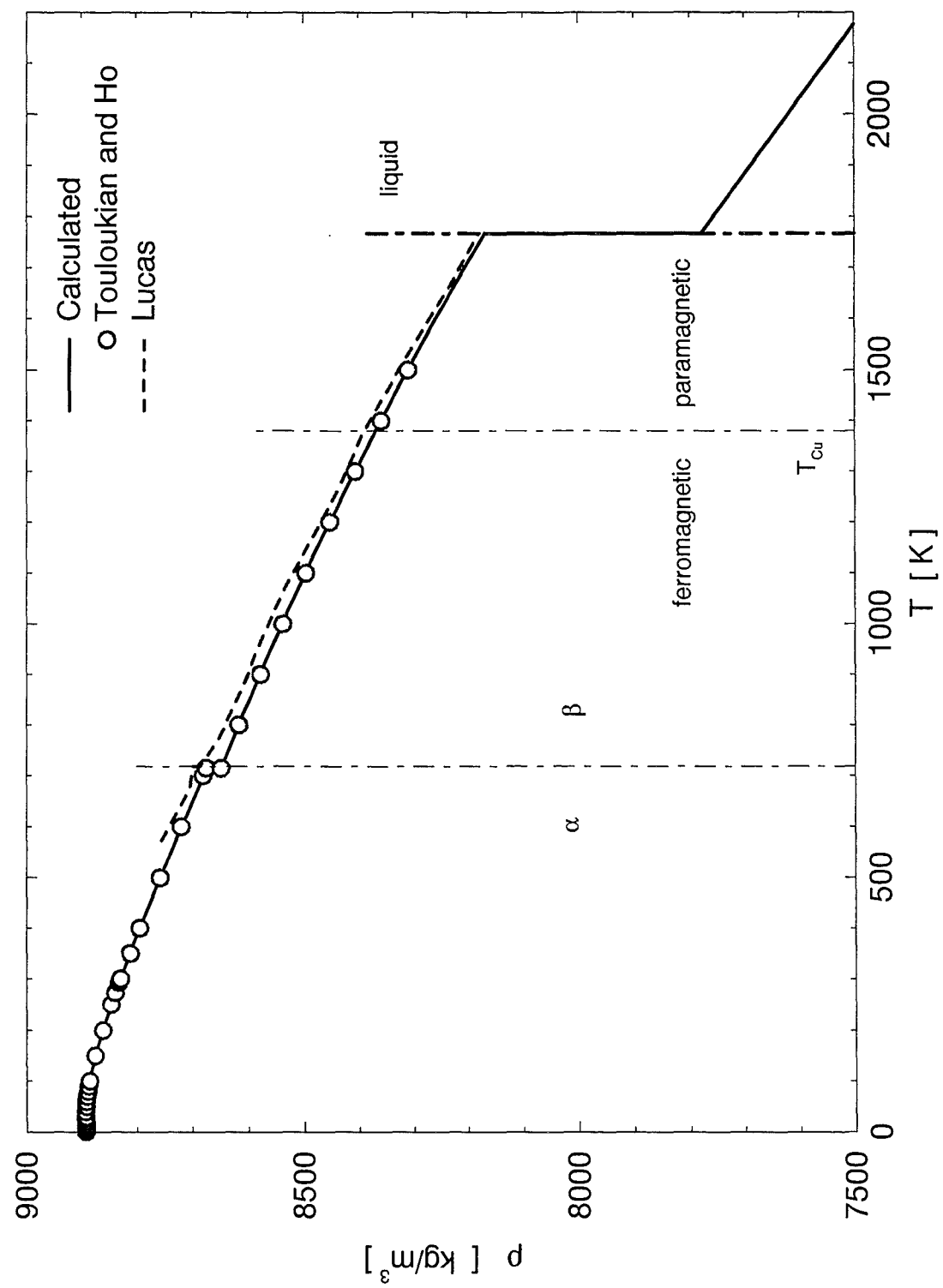


Figure 9.8: Cobalt. Density as a function of the temperature.

Chapter 10

Nickel

10.1 Phase transitions

Nickel is a silvery white, hard, yet ductile metal. It is often used for creating workable and corrosion-resistant alloys. The atomic weight of nickel is

$$\mu = 58.69 \frac{g}{mol} , \quad (10.1)$$

and its zero-point enthalpy of sublimation (s. [3])

$$\Delta H_{sub} = 428. \frac{kJ}{mol} . \quad (10.2)$$

Nickel is ferromagnetic below its Curie point and paramagnetic above this temperature.

Range , T < K	Structure	Transform heat kJ/mol
629	α - Ni , fcc , ferromagnetic	-
1728	α - Ni , fcc , paramagnetic	17.1

Table 10.1: Nickel. Phases and structures in the solid state

The most recent phase transition data of nickel are collected in the table 10.2 on page 68. Taking into account the data of the table 10.2 I selected as the Curie point

$$T_{Cu} = 629. K . \quad (10.3)$$

As the **melting point** of nickel is

$$T_M = 1728 K \quad (10.4)$$

commonly accepted. As the **heat of the fusion** I had taken (see [25], [147], [172] and [184])

$$\Delta H_{fus} = 17.1 \text{ kJ/mol} . \quad (10.5)$$

Reference		T_{Cu}	T_M	ΔH_{fus} $\frac{kJ}{mol}$
		K	K	
Hultgren	1966 [56]	631	1726	17.48
Braun	1966 [25]	631	1725	16.90
Seydel	1977 [88]	-	-	18.90
Seydel	1979 [103]	-	-	17.96
Drotning	1979 [96]	-	1728	-
Novikov et al.,	1981 [119]	630	-	-
Cezairliyan et al.	1983 [128]	-	1729	-
Yousuf et al.,	1986 [143]	629	-	-
Pottlacher et al.,	1987 [147]	-	-	17.14
P. D. Desai,	1987 [153]	625	1728	17.47
Maglič et al.,	1987 [146]	630	-	-
Korobenko and Savvatimskii	1990 [172]	-	-	17.14
Kaschnitz et al.,	1994 [184]	-	-	17.03

Table 10.2: Nickel. Transform properties

As the critical temperature of nickel Fortov, Dremin and Leont'ev, [74] estimate

$$T_c \sim 10300 \text{ K} . \quad (10.6)$$

Drotning, [115] receives - from the derivative of the liquid density

$$T_c \sim 8300 \text{ K} . \quad (10.7)$$

10.2 Vapor pressure

To fit a vapor pressure equation I use the data given in the critical evaluations of P. D. Desai, [153]. The best Dupré-Rankine description of these has the coefficients

$$\log_{10} p^\circ = 15.6948 - \frac{22497.2}{T} - 0.91577 \cdot \log_{10} T \quad \text{for } T \leq T_M$$

and

$$(10.8)$$

$$\log_{10} p^\circ = 20.7219 - \frac{22633.0}{T} - 2.44423 \cdot \log_{10} T \quad \text{for } T \geq T_M .$$

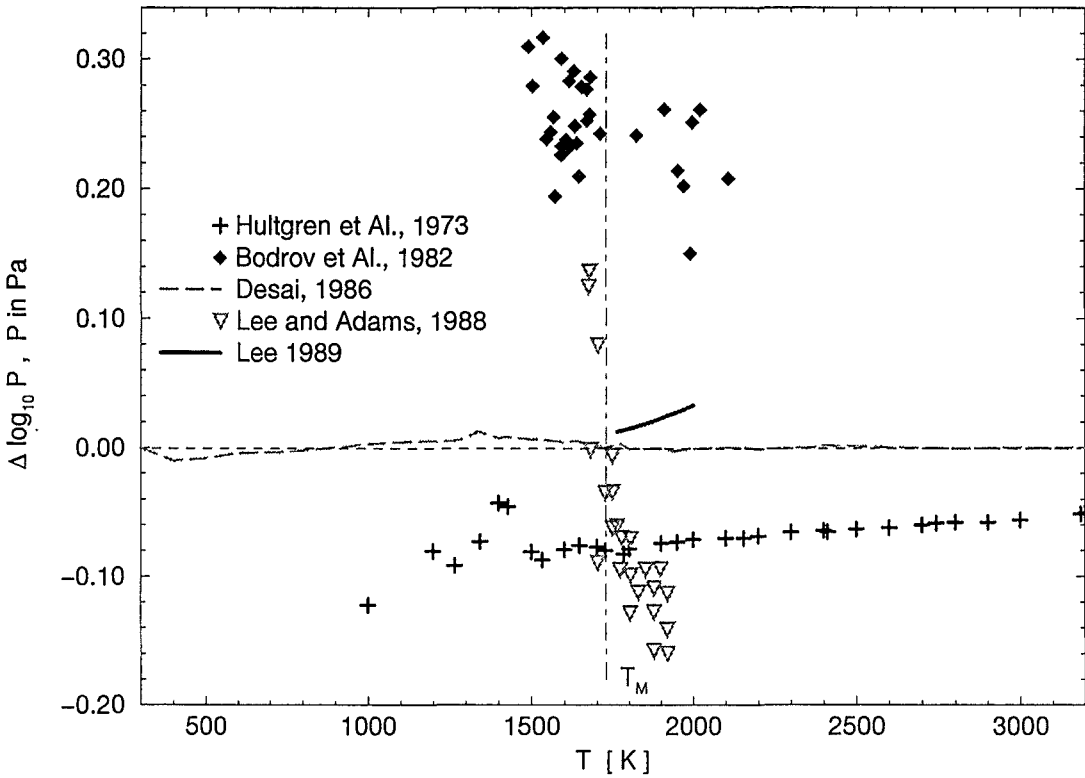


Figure 10.1: Nickel. Deviations of the vapor pressure data from the Dupré-Rankine description.

Figure 10.1 shows the vapor pressure data of the Hultgren-Group, [56], of Bodrov et al. [123], of Desai, [153], of Lee and Adams, [157] and of Lee, [162] as deviations from the Dupré-Rankine eq. 10.8.

To the vapor pressure equation, given above corresponds a boiling temperature of

$$T_B = 3160.10 \text{ K} \quad . \quad (10.9)$$

10.3 Heat capacity and enthalpy

For fitting the heat capacity of nickel I selected the low-temperature data ($T \leq 300 \text{ K}$) of Desai, [153], the data of Vollmer, Kohlhaas, und Braun, [25], the data of Cezairliyan and Miiller, [128] and the smoothed data of Maglić, Dobrosavljević and Perović, [146] (s. figure 10.2 on page 70). To describe the heat capacity in the vicinity of the Curie point I used also the data of Kraftmakher, [60] and of Novikov, Roshchupkin, Mozgovoi and Semashko, [119] (s. figure 10.3 on page 71).

The heat capacity of the ferromagnetic nickel can be well described with a combination of Debye-, Hoch- and the exponential- functions:

$$C_{Pfm} = C_{PD} + C_{PH} + C_{PE} \quad \text{for} \quad T \leq T_{Cu} \quad . \quad (10.10)$$

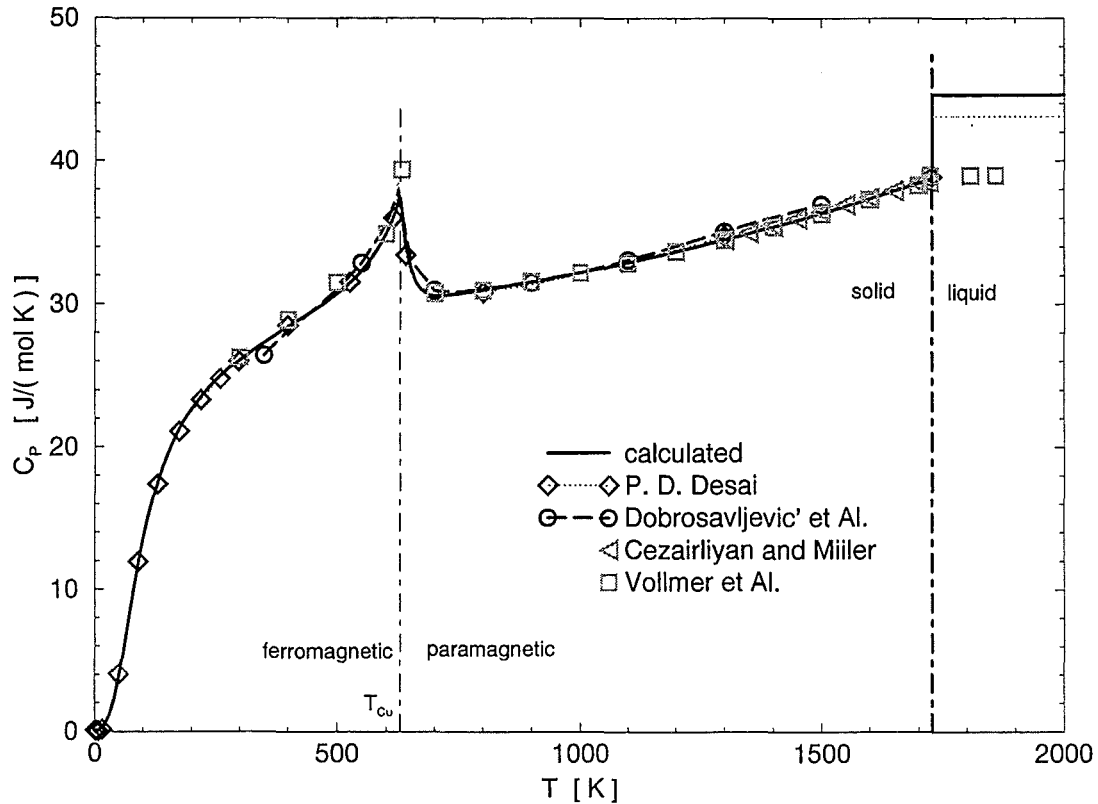


Figure 10.2: Nickel. Heat capacity C_P as a function of the temperature.

The parameters, needed in the above eq.s are:

$$\Theta_D = 400 \text{ K} , \quad b = 0.01 \frac{J}{\text{mol K}^2} , \quad d = 1.0 \cdot 10^{-8} \frac{J}{\text{mol K}^4} , \\ g = -11. , \quad h = 0.0198 \text{ 1/K} . \quad (10.11)$$

In the paramagnetic nickel one needs a temperature - polynomial and an exponential expression to describe the heat capacity correctly:

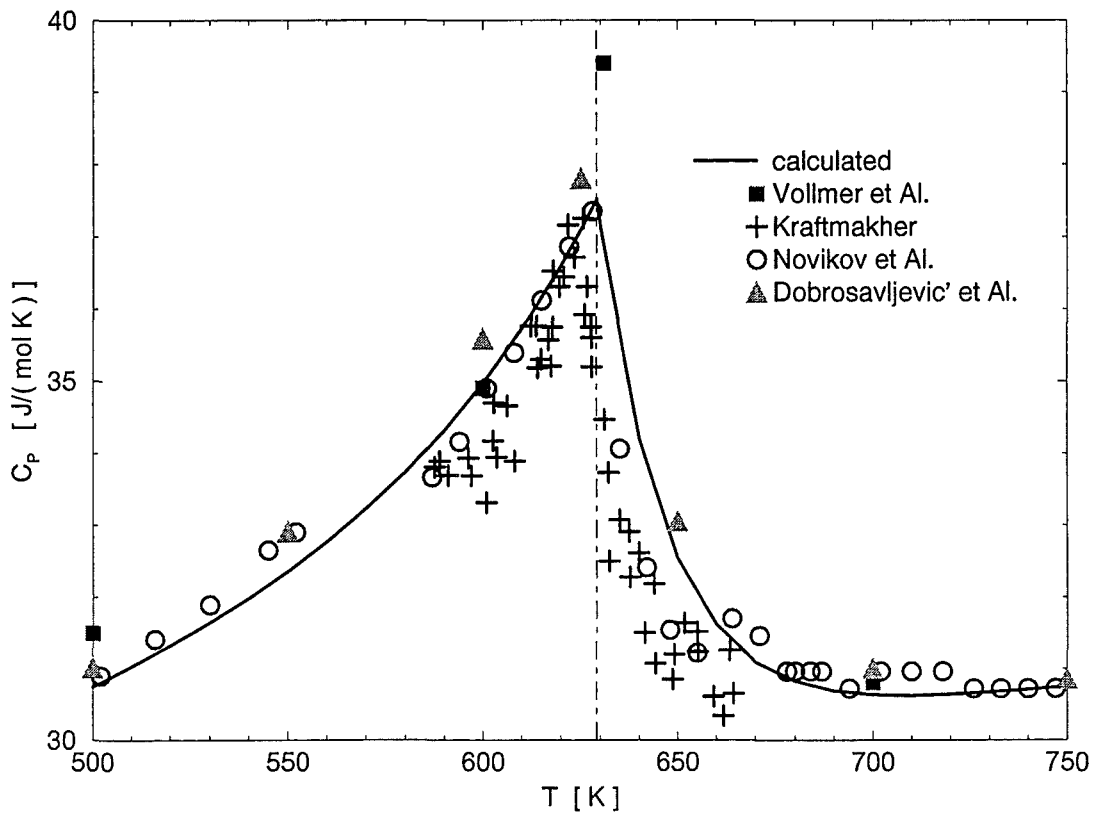
$$C_{Ppm} [\text{J}/(\text{mol K})] = 28.7 + T \cdot 3.5 \cdot 10^{-4} + T^2 \cdot 3.17 \cdot 10^{-6} + e^{(g + T \cdot h)} \quad (10.12)$$

$$\text{for } T_{Cu} < T \leq T_M , \quad \text{with } g = 37.22 , \quad h = -0.056 \text{ 1/K} .$$

As the heat capacity of liquid I use a $\partial H / \partial T$ value, which corresponds as well to the enthalpy data of Obendrauf, Kaschnitz, Pottlacher and Jäger, [181] as to the data of Korobenko & Savvatimskii [172] (s. figure 10.5 on page 74):

$$C_{PL} = 44.6 \text{ J}/(\text{mol K}) , \quad \text{for } T_M < T . \quad (10.13)$$

Figure 10.2 displays the heat capacity calculated by eq.s 10.10 - 10.13. Figure 10.3 on page 71 shows the heat capacity transition at the Curie point.

Figure 10.3: Nickel. C_P change at the Curie-point.

To the C_P equations 10.10 - 10.13 corresponds the following nickel - enthalpy - equation:

$$H_{fm}(T) = H_D(T) + H_H(T) + H_E(T) \quad \text{for } T \leq T_{Cu} \quad (10.14)$$

$$H_{pm}(T) = H_{fm}(T_{Cu}) + \int_{T_{Cu}}^T dt C_{Ppm}(t) \quad \text{for } T_{Cu} < T \leq T_M$$

$$H_L(T) = H_{pm}(T_M) + \Delta H_{fus} + C_{PL} \cdot (T - T_M) \quad \text{for } T_M < T .$$

Figure 10.5 on page 74 shows the enthalpy - temperature relation of nickel calculated according to eq. 10.14. Some recently measured enthalpy data are also displayed. The enthalpy of the nickel at 0 K is $H_0 = -4.81532 \text{ kJ/mol}$.

10.4 Thermal expansion and density.

In constructing the density description of nickel I use the α_L data of Kollie, [89] in the solid and the $\rho(T)$ results of Ostrovskii, Ermachenkov, Popov, and Grigoryan, [109] in the liquid.

A_0	A_1	A_2	A_3
$T \leq 450 \text{ K}$			
8969.62	0.0273214	$-1.12865 \cdot 10^{-3}$	$1.07638 \cdot 10^{-6}$
$450 \text{ K} < T \leq 1728 \text{ K}$			
9032.01	-0.401631	$9.93220 \cdot 10^{-6}$	$-3.21561 \cdot 10^{-8}$
$1728 \text{ K} < T$			
9020.85	-0.678154	0.0	0.0

Table 10.3: Nickel. Coefficients of the density description

In the ferromagnetic solid one needs, to describe the the α_L data of Kollie the Debye-, the Hoch- and the exponential- functions (eq.s 2.3, 2.5, 2.7):

$$\alpha_{Lfm} = e \cdot (c_D + c_H + c_E) \quad \text{for } T \leq T_{Cu} \quad . \quad (10.15)$$

The scaling factor is again

$$e = 5 \cdot 10^{-7} \frac{\text{mol}}{J} \quad (10.16)$$

and the remaining parameters are

$$\Theta_D = 400 \text{ K} , \quad b = 0.008 \frac{J}{\text{mol K}^2} , \quad d = 2.0 \cdot 10^{-8} \frac{J}{\text{mol K}^4} , \\ g = -47.09 , \quad h = 0.0762 \text{ 1/K} . \quad (10.17)$$

In the paramagnetic solid the description of $\alpha_L(T)$ corresponds also to the paramagnetic $C_P(T)$ description (cf. 10.12):

$$\alpha_{Lpm} [1/K] = 25.2697 + T \cdot 6.26832 \cdot 10^{-3} + T^2 \cdot 5.48223 \cdot 10^{-6} + e^{(g + T \cdot h)} \quad (10.18)$$

$$\text{for } T_{Cu} < T \leq T_M , \quad \text{with} \quad g = 33.51 , \quad h = -0.051 \text{ 1/K} .$$

To convert α_L into the density function $\alpha_L(T)$ was integrated and normalized into the property $V(T)/V_{298}$ (eq. 3.2). The reduced volume-expansion, V/V_{298} together with the standard density, ρ_{298} allows to calculate the density of solid nickel via eq. 3.3.

The standard density

$$\rho_{298} = 8906 \text{ kg/m}^3 \quad (10.19)$$

I got by extrapolating the density - ρ (293 K) = 8908 kg/m³ - measured by Laubitz and Matsumura, [76] for nickel at 293 K.

In the liquid state of nickel I use simply the density equation of Ostrovskii et al., [109] to describe the property.

Figure 10.7 on page 76 displays the density - temperature function of nickel. The density is again described by a set of polynomials with the coefficients given in table 10.3.

Figure 10.7 shows also recently measured liquid nickel densities (for Kirshenbaum and Cahill see [13]). The measurements of Lucas, [50] - concerning the solid state of nickel - are in

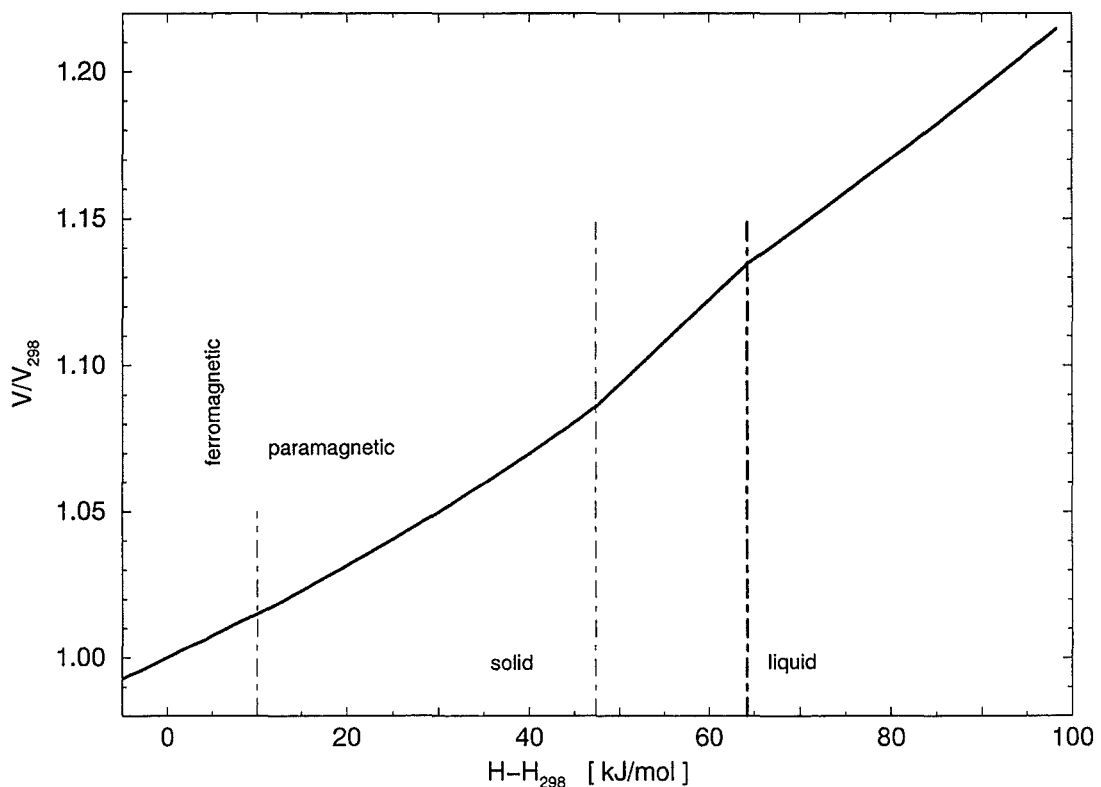


Figure 10.4: Nickel. Thermal expansion as a function of the enthalpy.

good agreement with the calculated data. In the liquid state of nickel the data of Drotnig, of Ostrovskii et al. and of Lucas compare even better with each other as it was the case in liquid cobalt.

Figure 10.4 displays the thermal expansion as a function of the enthalpy. The border values of the enthalpy - indicated in the figure - are 10.034, 47.349 and 64.449 kJ/mol .

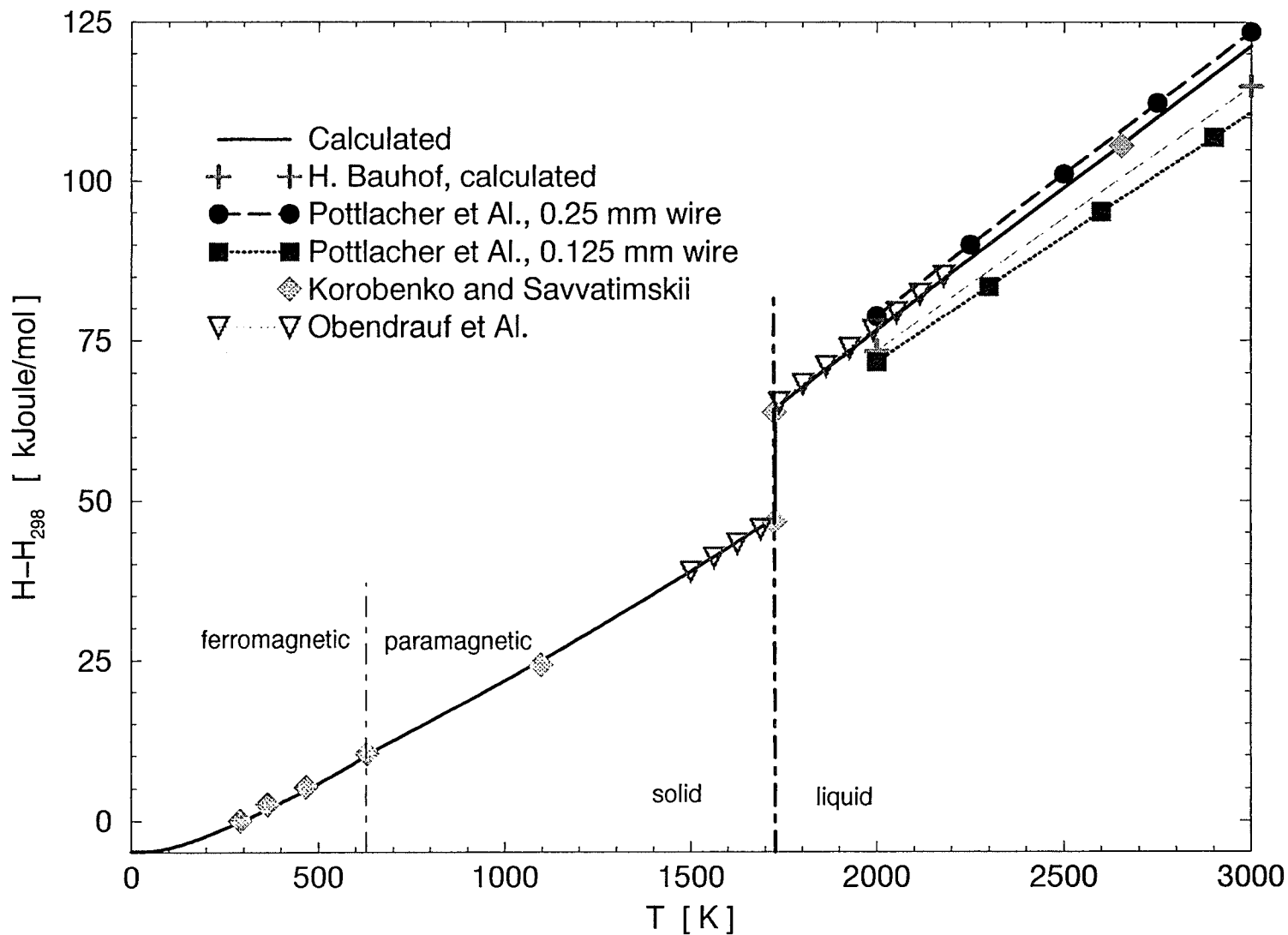


Figure 10.5: Nickel. Enthalpy as a function of the temperature

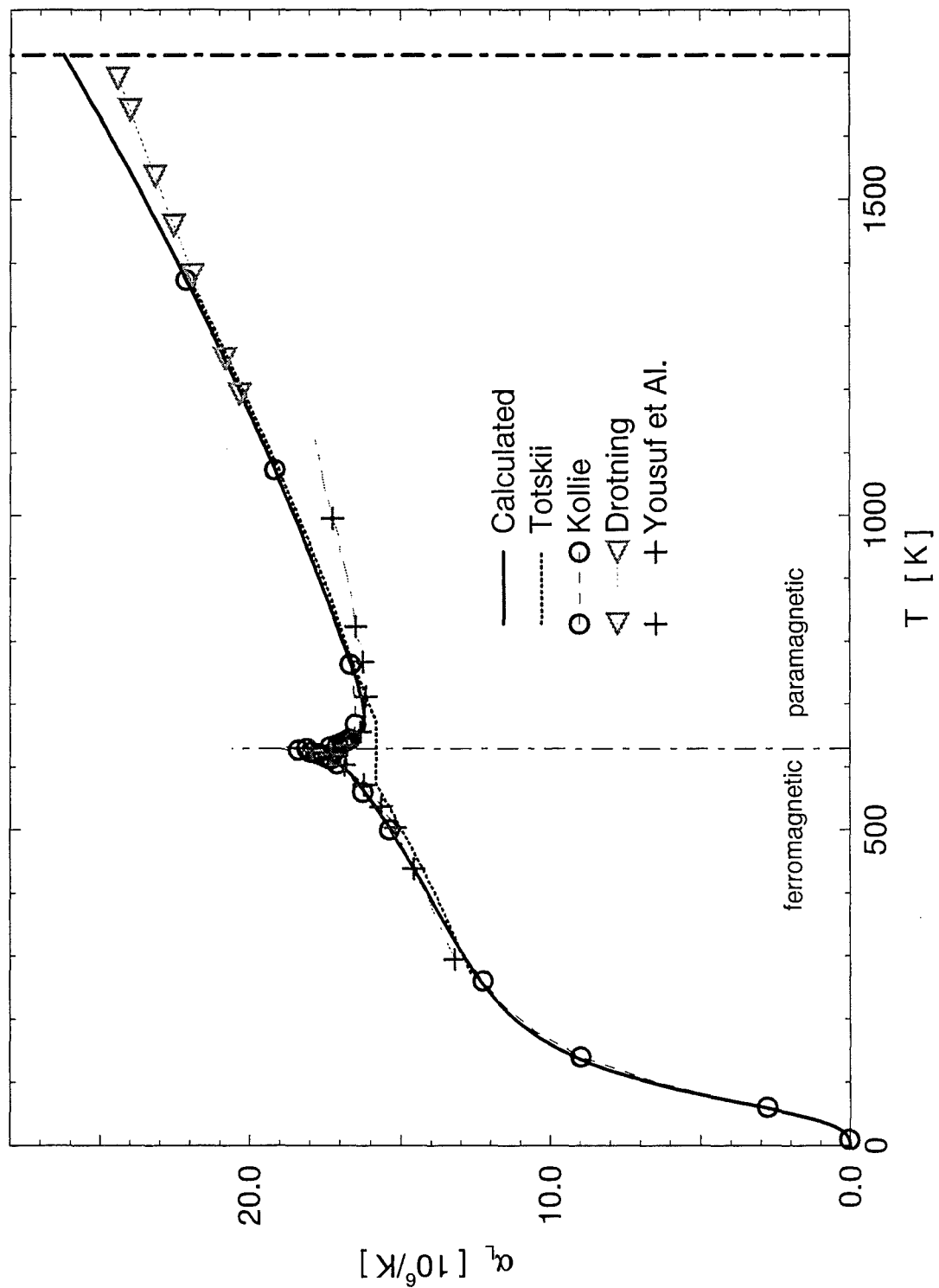


Figure 10.6: Nickel. Coefficient of the linear thermal expansion in the solid state.

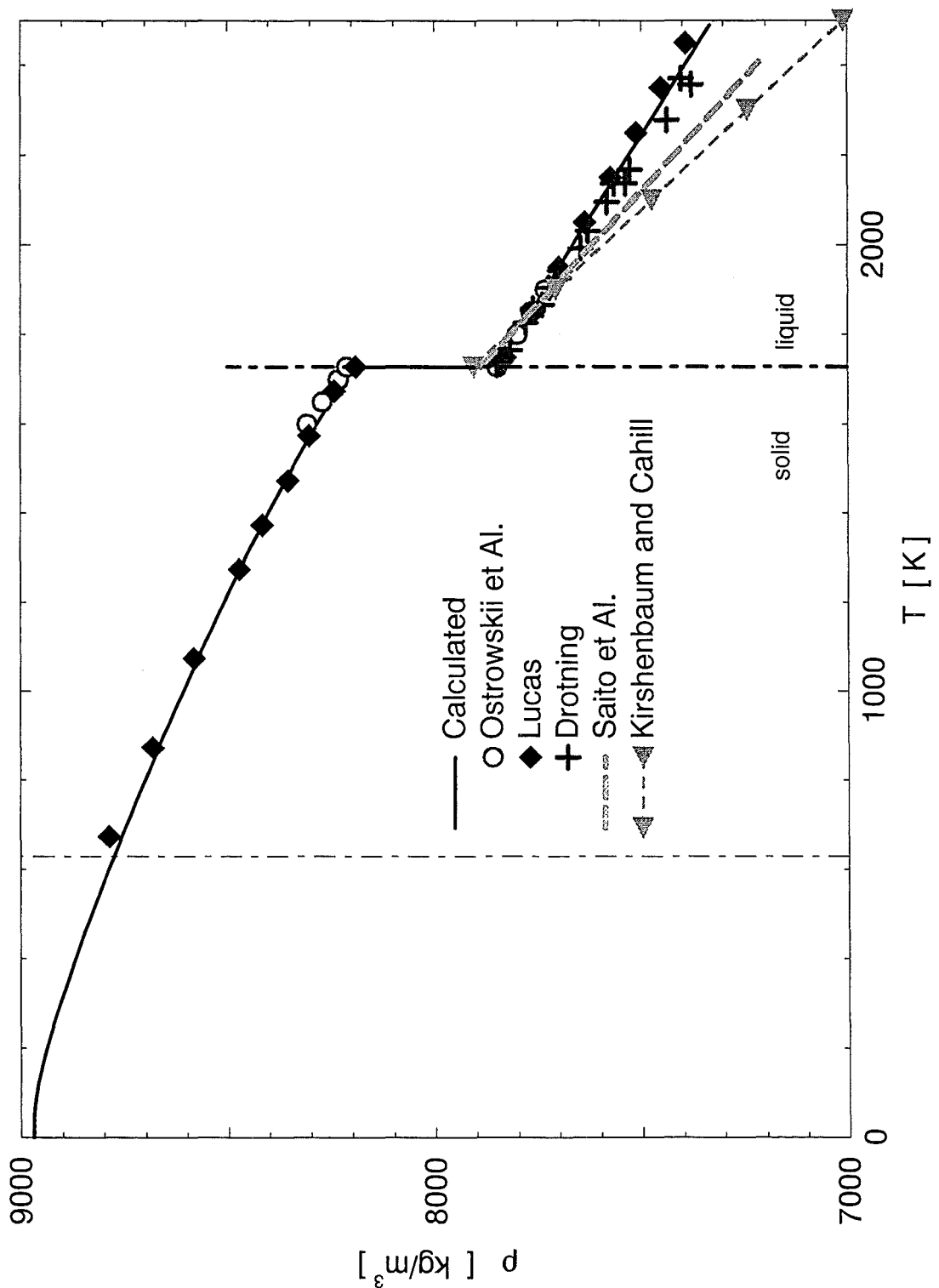


Figure 10.7: Nickel. Density as a function of the temperature.

Chapter 11

Niobium

11.1 Phase transitions

Niobium is a shiny, white, soft and ductile metal. It starts to oxidize in the air at 200 C. Since niobium has a low capture cross-section for thermal neutrons it is often used as an alloying agent in the structure material of thermal reactors.

Reference	T_M K	year
Schofield	2745	1957
Pemsler	2744	1961
Hausner	2752	1965
Rudy and Progulski	2752	1967
Cezairliyan	2750	1967
Berezin, Kenisarin, Chekhovskoi	2742	1972

Table 11.1: Niobium. Measured melting points

The atomic weight of niobium is

$$\mu = 92.9064 \frac{g}{mol} , \quad (11.1)$$

and its zero-point enthalpy of sublimation (s. [3])

$$\Delta H_{sub} = 730. \frac{kJ}{mol} . \quad (11.2)$$

As the critical temperature of niobium Fortov, Dremin and Leont'ev, [74] estimate

$$T_c \sim 19\,000 K.$$

Melting point: Kenisarin, Berezin and Chekhovskoi, [77] recommend

$$T_M = 2748 \text{ K} \quad (11.3)$$

as the melting point of niobium. This value results as the mean temperature from a table of T_M -values, reported by Chekhovskoi, Berezin and Kenisarin, in [65]. Their table (table 11.1 on page 77) can now be completed with two new values: Chekhovskoi and Kats, [116] measured in 1980 $T_M = 2742 \text{ K}$, Hiernaut, Sakuma and Ronchi, [160] in 1988 $T_M = 2752 \text{ K}$. Since these new data don't alter the mean T_M significantly, I use - as melting point - the recommended 2748 K.

Reference		ΔH_{fus} $\frac{\text{kJ}}{\text{mol}}$
Margrave	1970 [43]	33.1
Sheindlin et al.	1972 [53]	27.6
Savvatimskii	1973 [63]	27.6
Martynyuk et al.	1975 [75]	33.0
Shaner et al.	1977 [83]	27.9
Cezairliyan and Miiler	1980 [107]	31.5
Betz and Frohberg	1980 [108]	30.5
Chekhovskoi and Kats	1981 [116]	27.5
Gallo et al.	1985 [134]	28.7
Cezairliyan and McClure	1987 [152]	31.1

Table 11.2: Niobium. Measured heats of fusion

Heat of Fusion: Table 11.2 shows recently measured values of ΔH_{fus} . In 11.2 I had taken from the report of Cezairliyan and McClure [152] and completed it with the ΔH_{fus} value of Chekhovskoi and Kats.

As the heat of the fusion I selected the value of Betz and Frohberg, [108]:

$$\Delta H_{fus} = 30.5 \text{ kJ/mol} , \quad (11.4)$$

since only this value fits correctly to the measured enthalpy data around the melting point (cf. figure 11.4 on page 82).

11.2 Vapor pressure

For the vapor pressure of niobium the most recent data are given in the critical evaluations of Hultgren et al., [56]. In approximating the data with a Dupré-Rankine equation I dropped

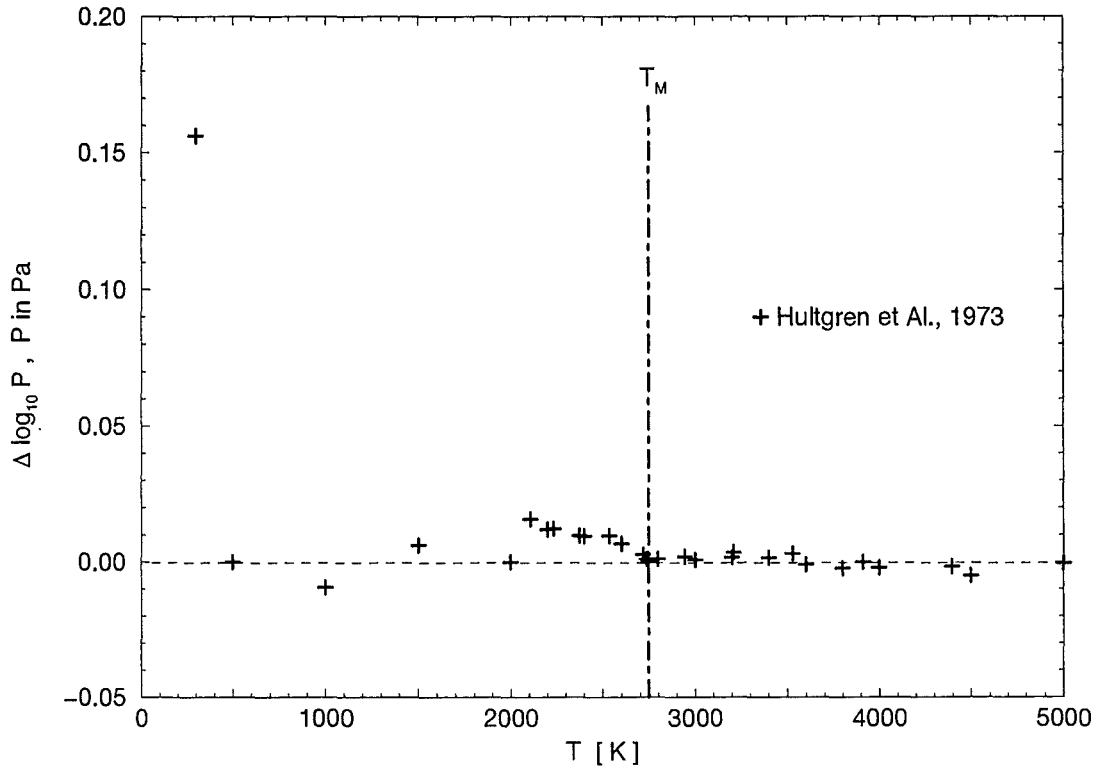


Figure 11.1: Niobium. Deviations of the vapor pressure data of Hultgren from the Dupré-Rankine description.

the first vapor pressure point, for it didn't fit to the others (s. figure 11.1). Adjusting Dupré-Rankine approximations to the remaining points resulted in

$$\log_{10} p^\circ = 14.5888 - \frac{37893.9}{T} - 0.483088 \cdot \log_{10} T \quad \text{for } T \leq T_M$$

and

(11.5)

$$\log_{10} p^\circ = 13.0763 - \frac{36040.3}{T} - 0.239442 \cdot \log_{10} T \quad \text{for } T \geq T_M .$$

Figure 11.1 displays the deviation of the data of Hultgren from the formula 11.5.

To the vapor pressure equation given above corresponds a boiling point of

$$T_B = 5016.36 \text{ K} .$$
(11.6)

11.3 Heat capacity and enthalpy

For fitting the heat capacity of niobium I selected the data of Kirillin, Sheindlin, Chekhovskoi and Zhukova, [18], of Sheindlin, Berezin and Chekhovskoi, [53], of Novikov, Roshchupkin,

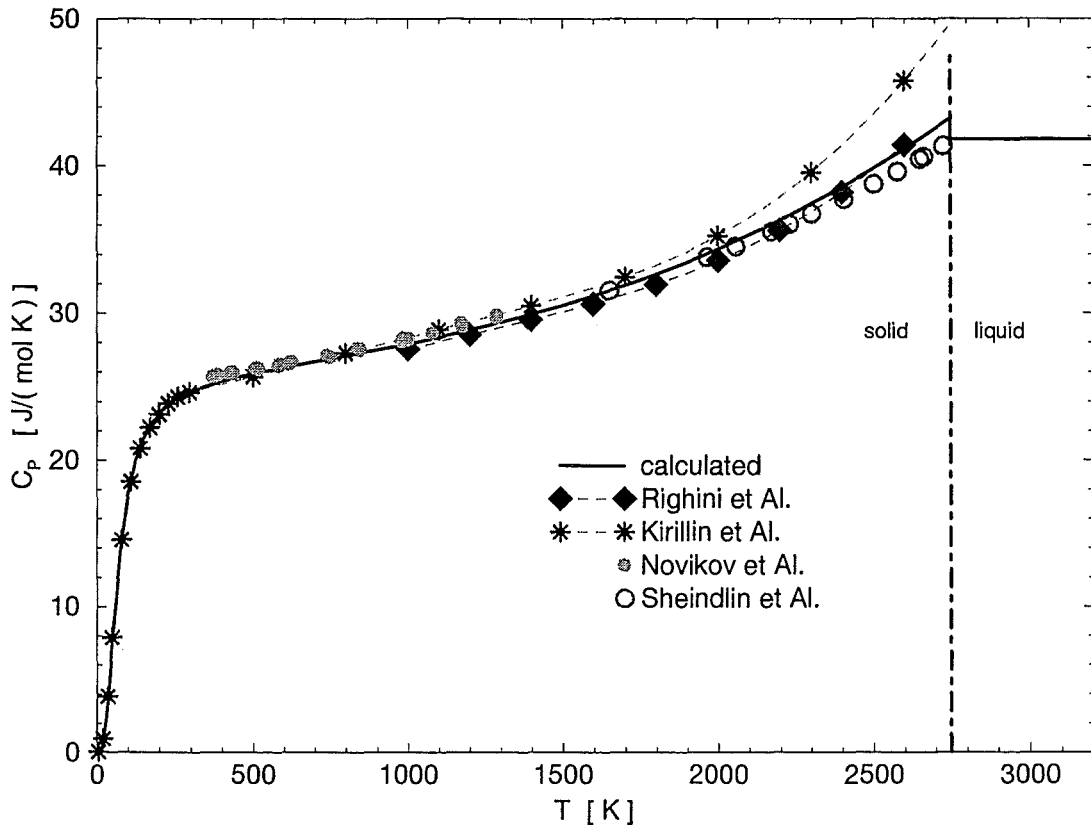


Figure 11.2: Niobium. Heat capacity C_P as a function of the temperature.

Mozgovoi and Semashko, [119] and of Righini, Roberts and Rosso, [140] (s. figure 11.2).

In solid niobium one needs only the Debye- (eq. 2.3) and the Hoch- descriptions (eq. 2.5) to describe the heat capacity.

$$C_{PS} = C_{PD} + C_{PH} \quad \text{for} \quad T \leq T_M . \quad (11.7)$$

The parameters of the best Debye- and Hoch- functions are:

$$\Theta_D = 280 \text{ K} , \quad b = 0.0025 \frac{\text{J}}{\text{mol K}^2} , \quad d = 5.5 \cdot 10^{-10} \frac{\text{J}}{\text{mol K}^4} . \quad (11.8)$$

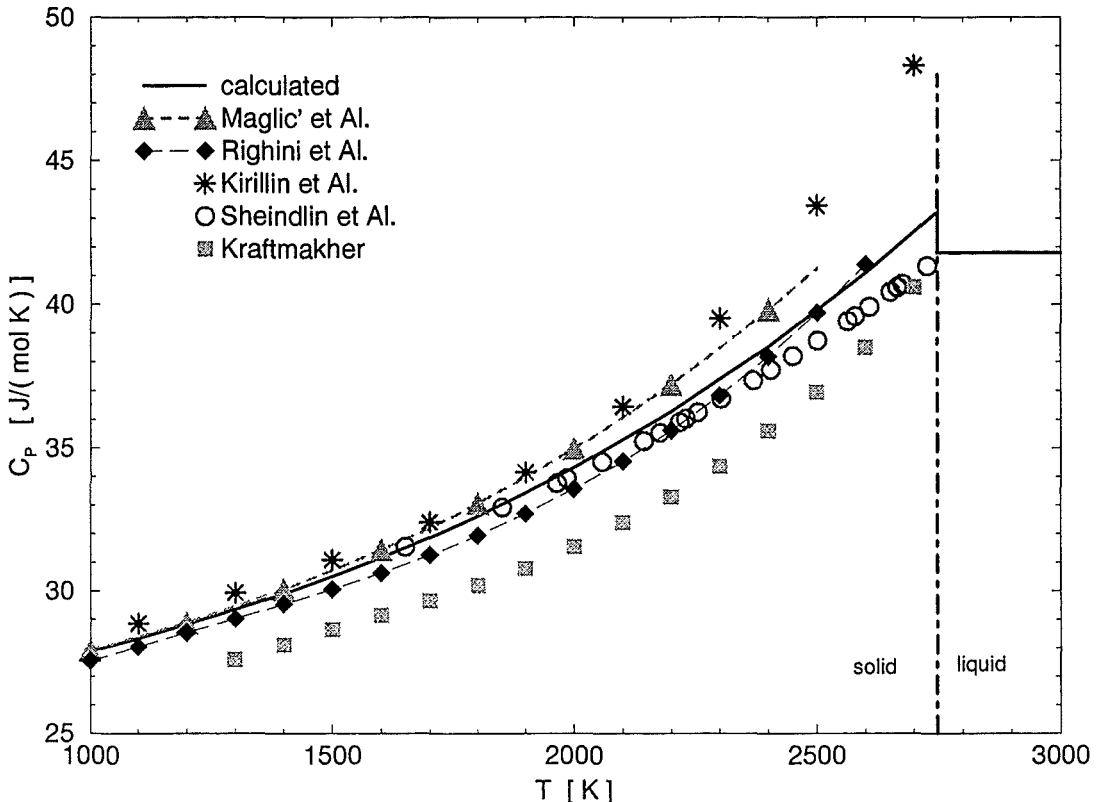
In the liquid state I use the heat capacity of Betz and Frohberg, [108]:

$$C_{PL} = 41.8 \text{ J/(mol K)} , \quad \text{for} \quad T_M < T , \quad (11.9)$$

since only this C_{PL} - value describe correctly the enthalpy increase of liquid niobium with the temperature (cf. figure 11.4 on page 82).

Figure 11.2 shows the heat capacity calculated by eq.s 11.7 - 11.9. Figure 11.3 on page 81 displays the heat capacity of niobium in the vicinity of the melting point. The measured values of Kraftmakher, [60] and of Maglič, Perović, and Vuković, [182] are also shown.

To the C_P equations 11.7 - 11.9 corresponds the following set of enthalpy - equations:

Figure 11.3: Niobium. C_P change at the melting-transition.

$$H_S(T) = H_D(T) + H_H(T) \quad \text{for } T \leq T_M \quad (11.10)$$

$$H_L(T) = H_S(T_M) + \Delta H_{fus} + C_{PL} \cdot (T - T_M) \quad \text{for } T_M < T .$$

The enthalpy calculated by equations above can be seen on figure 11.7 on page 85. 11.7 shows also the enthalpy-measurements of Gallob, Jäger and Pottlacher, [134], of Berezin, [64] and of Betz and Frohberg, [108]. The zero-point enthalpy in this figure is $H_0 = -5.25460 \text{ kJ/mol}$.

Figure 11.4 on page 82 shows the enthalpy - change at the melting transition. The data of Conway and Hein, [17] are also displayed.

11.4 Thermal expansion and density

In the solid state I developed a description for the coefficient of the linear thermal expansion by using the low-temperature data of Lebedev, Mamalui, Pervakov, Petrenko, Popov and Khotkevich, [39] (given in [69]) and the high-temperature measurements of Righini, Roberts and Rosso, [144] (s. figure 11.5 on page 83).

To fit a function to the α_L - data in solid niobium one needs only the Debye- and the Hoch-descriptions (eq.s 2.3, 2.5):

$$\alpha_{LS} = e \cdot (c_D + c_H) \quad \text{for } T \leq T_M . \quad (11.11)$$

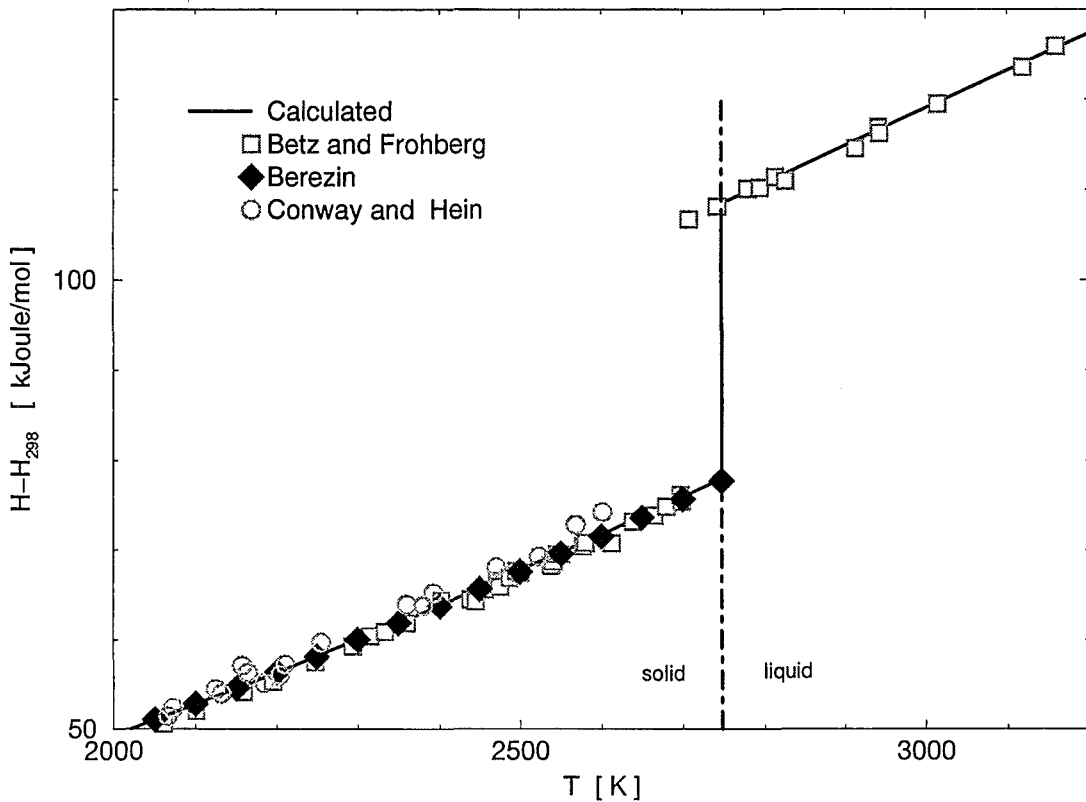


Figure 11.4: Niobium. Enthalpy change at the melting-transition

The scaling factor is here

$$e = 2.9 \cdot 10^{-7} \frac{\text{mol}}{J} \quad (11.12)$$

and the Debye- and the Hoch- parameters are

$$\Theta_D = 280 \text{ K} , \quad b = 0.0028 \cdot 10^{-3} \frac{J}{\text{mol K}^2} , \quad d = 8.0 \cdot 10^{-10} \frac{J}{\text{mol K}^4} . \quad (11.13)$$

Figure 11.5 on page 83 displays - besides of the basical data and the fitted function - also the data of Petukhov, Chekhovskoi, Andrianova and Mozhgovoi, [86], of Petukhov, Chekhovskoi and Mozhgovoi, [93] and of Miiller and Cezairliyan, [158].

α_L of solid niobium was converted again via eq. 3.2 into the normalised form of the volumetric thermal expansion, $V(T)/V_{298}$.

To calculate the density (eq. 3.3) - I used

$$\rho_{298} = 8571 \text{ kg/m}^3 \quad (11.14)$$

as standard density. This value I got by extrapolating the density - $\rho(293 \text{ K}) = 8572 \text{ kg/m}^3$ - measured by Righini, Roberts, and Rosso, [140] for niobium at 293 K.

Ming and Manghani, [92] report a Nb-density of $\rho_{298?} = 8575 \text{ kg/m}^3$. I had chosen the value of 8571 kg/m^3 as standard density, because the density function - calculated by it fits better to the density data recommended by Touloukian in [23], 1966, as a function calculated by the standard density of 8575 kg/m^3 .

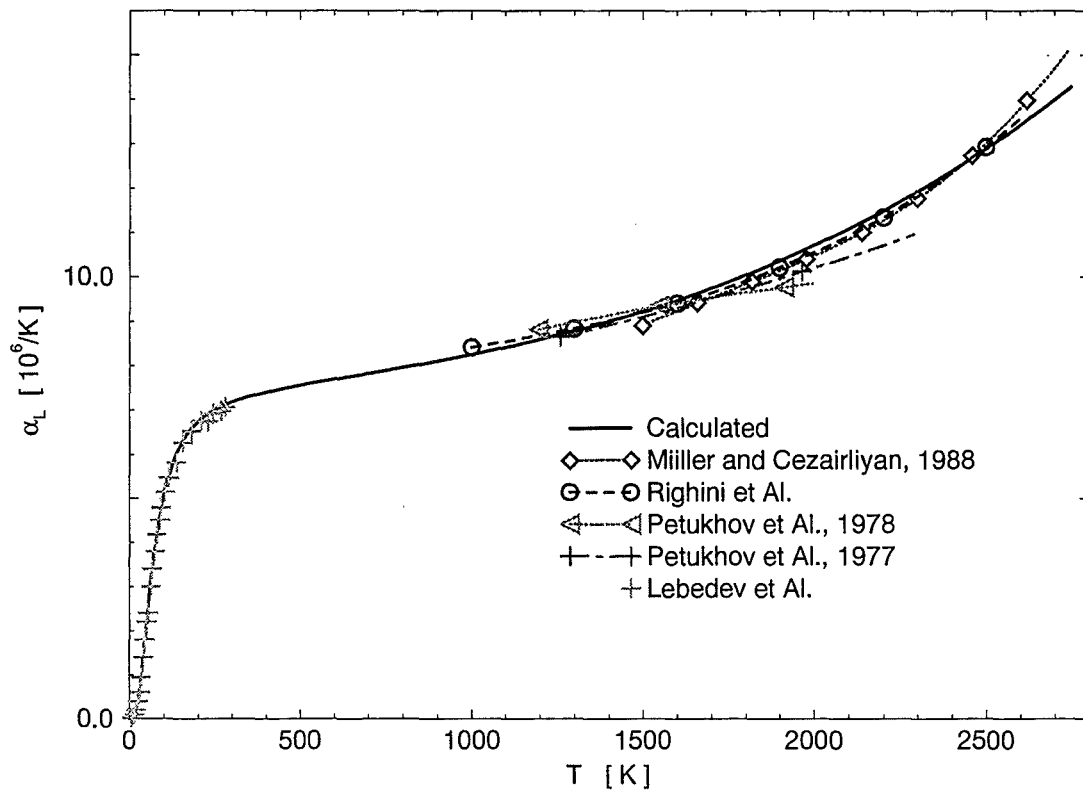


Figure 11.5: Niobium. Coefficient of the linear thermal expansion in the solid state.

In the liquid I had only the V/V298 ($H - H_{298}$) - measurements of Shaner, Gathers and Hogson, [83], and of Gallob, Jäger, Pottlacher, [134] (s. figure 11.6 on page 84) to depend on. I converted both datasets with the enthalpy - temperature relation 11.10 into a thermal expansion - temperature - relation, and then - with the standard density, to density - temperature sets (s. figure 11.8 on page 86). As a liquid density I had taken a linear density - temperature dependence,

$$\rho_L(T) = 9160.14 - T \cdot 0.54 \quad (11.15)$$

lying between the two sets of measured values.

Figure 11.8 on page 86 displays the whole density - temperature function of niobium. The melting density of Eremenko, Ivashchenko and Martsenyuk, [133] is also marked. The coefficients of the corresponding set of density polynomials are given in table 11.3 on page 84.

Figure 11.6 on page 84 shows the thermal expansion as a function of the enthalpy. The limiting enthalpy values of the solid resp. of the liquid are 77.987 and 108.487 kJ/mol.

A_0	A_1	A_2	A_3
$T \leq 360 \text{ K}$			
8610.42	0.00646907	$-7.73107 \cdot 10^{-4}$	$1.01975 \cdot 10^{-6}$
$360 \text{ K} < T \leq 2748 \text{ K}$			
8630.80	-0.197332	$6.43302 \cdot 10^{-6}$	$-7.72742 \cdot 10^{-9}$
$2748 \text{ K} < T$			
9160.14	-0.540000	0.0	0.0

Table 11.3: Niobium. Coefficients of the density description

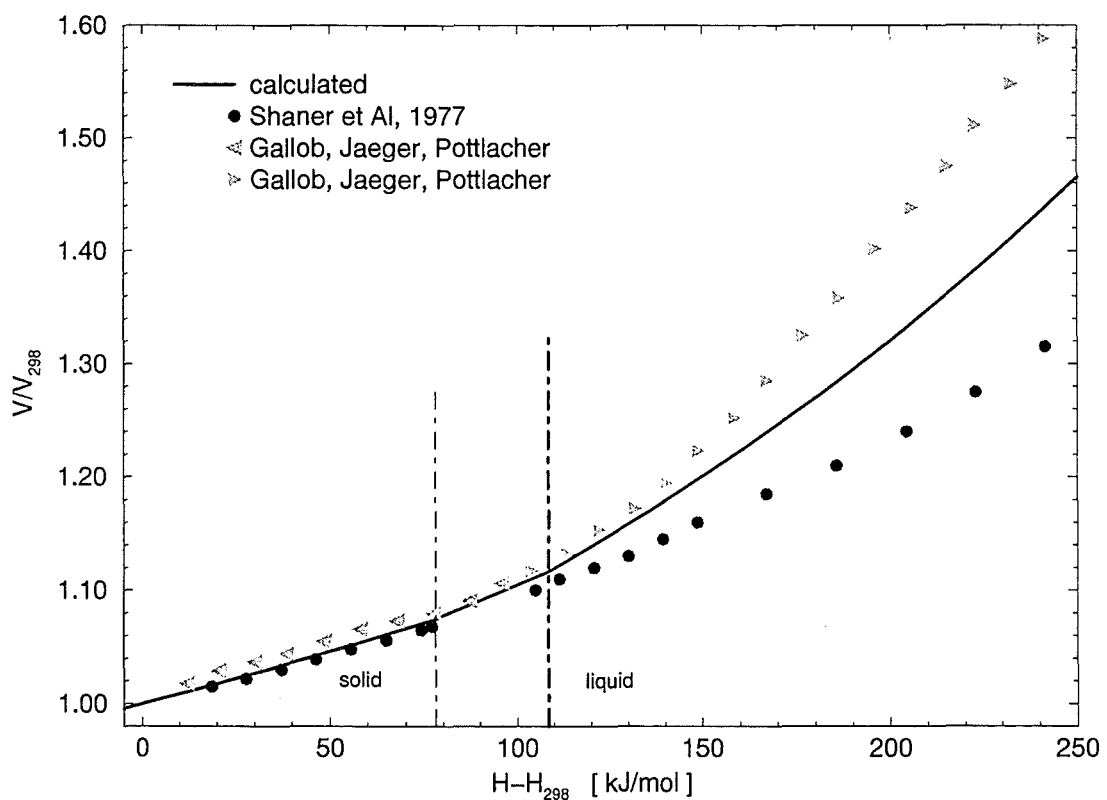


Figure 11.6: Niobium. Thermal expansion as a function of the enthalpy.

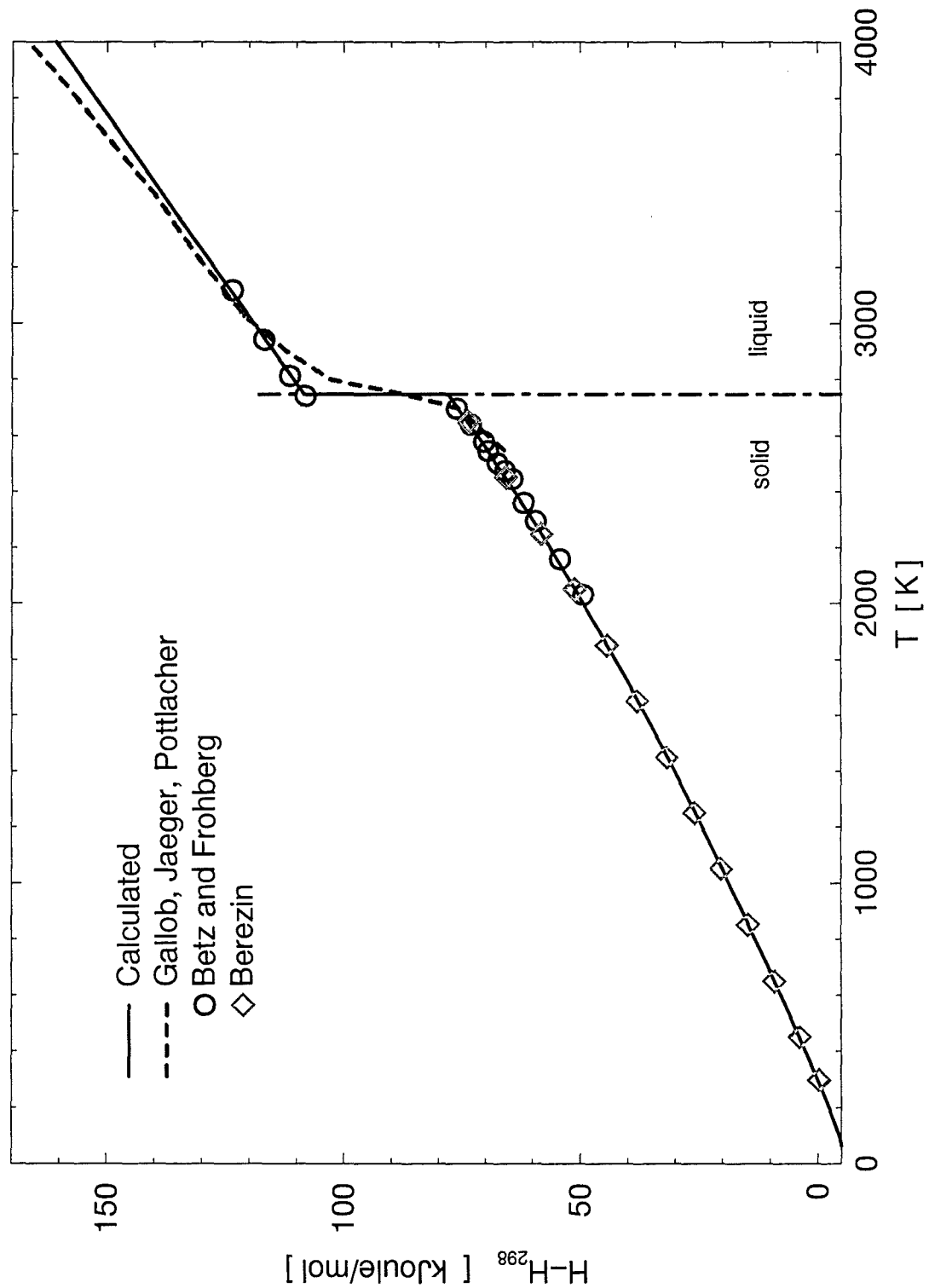


Figure 11.7: Niobium. Enthalpy as a function of the temperature

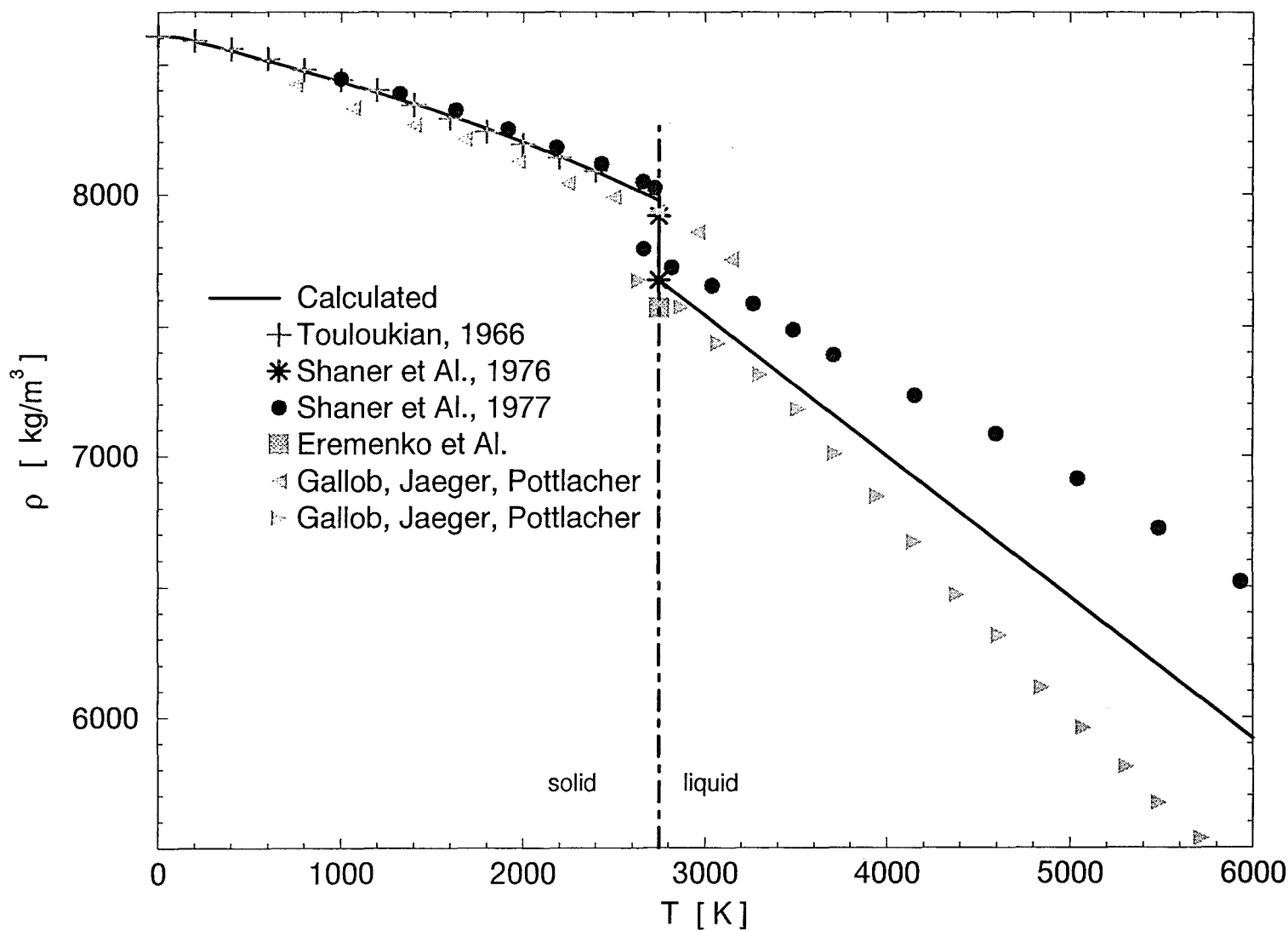


Figure 11.8: Niobium. Density as a function of the temperature.

Chapter 12

Molybdenum

12.1 Phase transitions

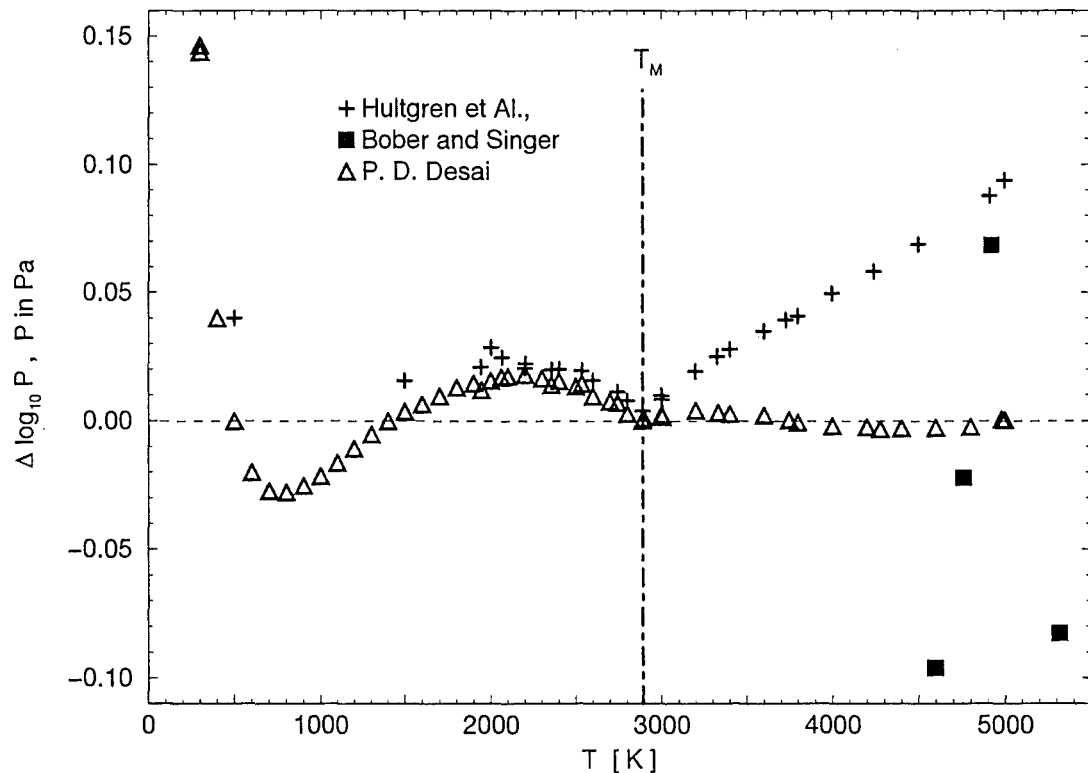


Figure 12.1: Molybdenum. Deviations of the vapor pressure data from the Dupré-Rankine description.

Molybdenum is a silvery white, very hard metal, often used for high-temperature crucibles. As an alloying agent it contributes to the hardenability of the steel and to its strength at high

temperatures. Its atomic weight and zero-point enthalpy of sublimation are (s. [3])

$$\mu = 95.940 \frac{g}{mol} \quad (12.1)$$

resp.

$$\Delta H_{sub} = 657.3 \frac{kJ}{mol} . \quad (12.2)$$

Reference	T_M	year
Worthing	2889	1925
Chiotti	2894	1950
Edwards and Johnstone	2898	1956
Knapton et al	2886	1960
Allen et al	2895	1960
Riley	2896	1964
Rudy and Progulski	2897	1967
Cezairliyan et al.	2894	1970
Latta and Fryxell	2896	1970
Kenisarin et al.	2896	1972
Bonnel et al	2895	1972
Shaner et al	2883	1977
Betz and Frohberg	2892	1981
Chekhovskoi et Kats	2898	1981
Hiernaut et al.	2890	1988

Table 12.1: Molybdenum. Measured melting points

Fortov, Dremin and Leont'ev, [74] estimate the critical temperature of molybdenum as

$$T_c \sim 16100 \text{ K} ,$$

whereas Seydel, Bauhof, Fucke and Wadle, [103] approximate it with

$$T_c \sim 14300 \text{ K} .$$

Melting point Table 12.1 lists - after [65], [149] and [160] - measured melting points of molybdenum. As the melting point of molybdenum I use the value of Betz and Frohberg, [106]:

$$T_M = 2892. \text{ K} \quad (12.3)$$

Reference	ΔH_{fus} kJ/mol	Year
Lebedev et al.	41.250	1970
Treverton and Margrave	34.814	1970
Chekhovskoi and Berezin	36.650	1971
Berezin et al.	36.585	1971
Dikhter and Lebedev	40.295	1971
Martynyuk et al.	38.0	1975
Gerasimov et al.	37.240	1977
Shaner et al.	35.786	1977
Betz and Frohberg	39.116	1980
Chekhovskoi and Kats	36.459	1981
McClure and Cezairliyan	36.4	1990

Table 12.2: Molybdenum. Measured heats of fusion

Heat of fusion Table 12.2 presents recently measured data, reported in the papers [136], [149] and [168]. As the heat of fusion of the molybdenum I selected

$$\Delta H_{fus} = 37.5 \text{ kJ/mol} , \quad (12.4)$$

for it compares well with the enthalpy data measured at the melting transition (see figure 12.4 on page 92).

12.2 Vapor pressure

The most recent vapor pressure data of molybdenum are in the critical evaluations of P. D. Desai, [149]. In approximating the data with a Dupré-Rankine equation I dropped the 3 coldest points of Desai, for they didn't fit to the other points (s. figure 12.1 on page 87). The best vapor pressure equation describing the remaining points is

$$\log_{10} p^\circ = 17.1267 - \frac{34705.1}{T} - 1.30429 \cdot \log_{10} T \quad \text{for } T \leq T_M$$

and

$$\log_{10} p^\circ = 12.7527 - \frac{30954.3}{T} - 0.415262 \cdot \log_{10} T \quad \text{for } T \geq T_M . \quad (12.5)$$

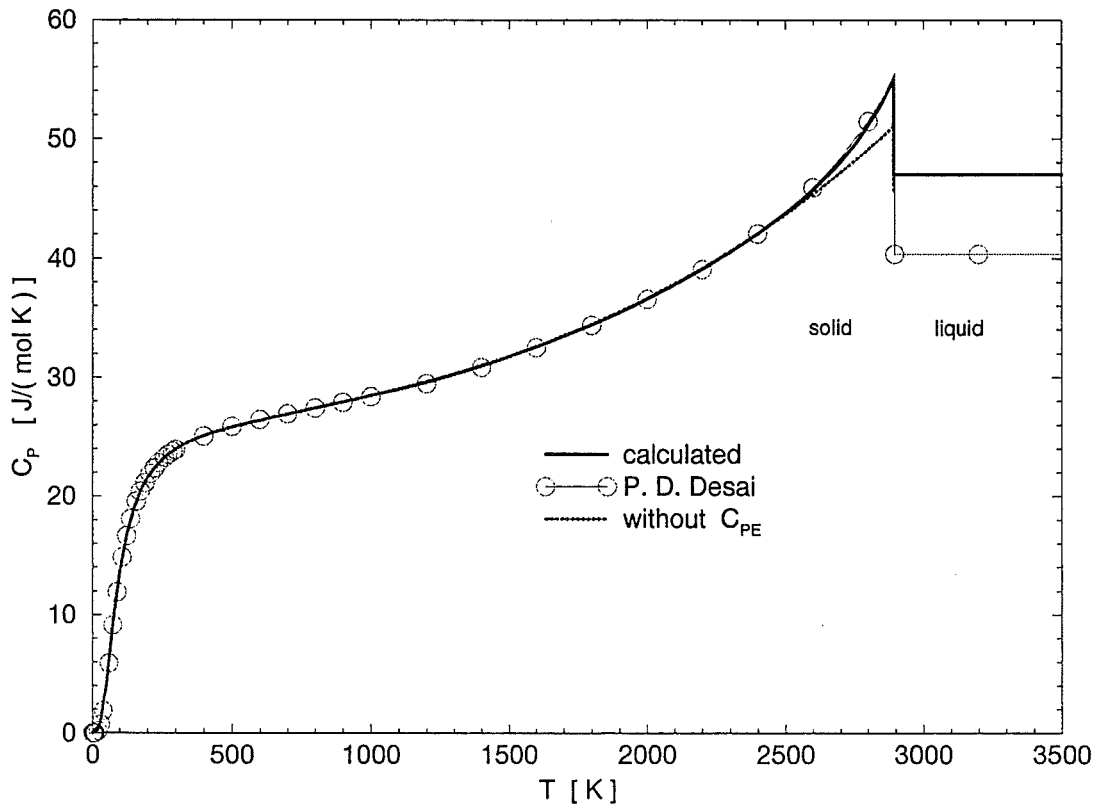


Figure 12.2: Molybdenum. Heat capacity C_P as a function of the temperature.

Figure 12.1 on page 87 compares different datasets with vapor pressure values from the Dupré-Rankine equation. Besides of the data of Desai, [149], the data recommended by Hultgren et al, [56] and the high-temperature measurements of Bober and Singer, [135] are also shown.

The vapor pressure equation, described above calculates a boiling point of

$$T_B = 4983.35 \text{ K} \quad . \quad (12.6)$$

12.3 Heat capacity and enthalpy

As the base for fitting a heat capacity - temperature function in solid molybdenum I selected the low-temperature ($T < 1500 \text{ K}$) recommendations of P. D. Desai, [149], all the measured points of Righini and Rosso, [127] and the high temperature data of Cezairliyan, [126].

At first I tried to describe the C_P data - as in the case of the niobium - solely with the Debye- and the Hoch- descriptions (eq.s 2.3, 2.5):

$$C_{PS} = C_{PD} + C_{PH} \quad \text{for} \quad T \leq T_M \quad . \quad (12.7)$$

The best description of the data with the above function I got with the parameters

$$\Theta_D = 380 \text{ K} \quad , \quad b = 0.003 \frac{\text{J}}{\text{mol K}^2} \quad , \quad d = 7.2 \cdot 10^{-10} \frac{\text{J}}{\text{mol K}^4} \quad . \quad (12.8)$$

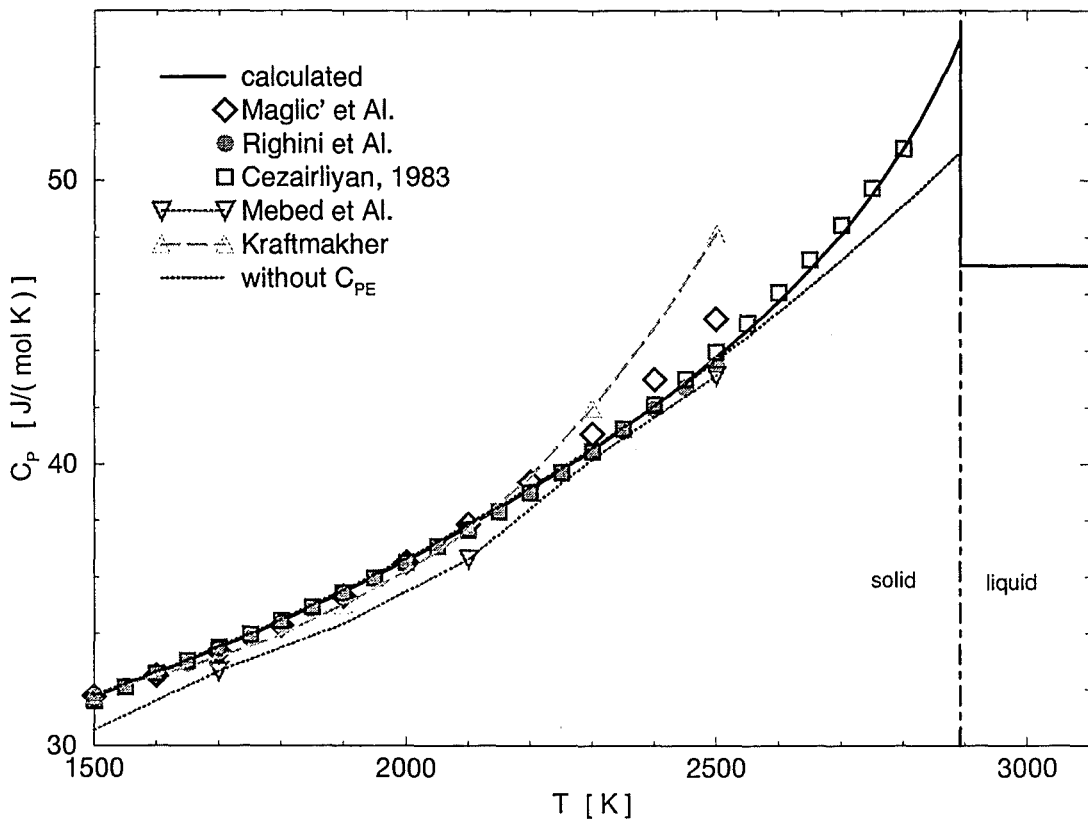


Figure 12.3: Molybdenum. C_P change at the melting-transition.

As the figure 12.2 on page 90 resp. fig. 12.3 shows, formula 12.7 is not satisfying in the vicinity of T_M , the C_P -values it calculates here are too low.

To get a better description I replaced the Hoch-function (eq. 2.5) with an extended version of C_{PH} in the heat capacity equation:

$$C_{PS} = C_{PD} + C_{PH*} \quad \text{for} \quad T \leq T_M \quad (12.9)$$

with

$$C_{PH*} \equiv b \cdot T + c \cdot T^2 + d \cdot T^3 \quad . \quad (12.10)$$

The parameters of the best C_P -function were in this case

$$\Theta_D = 380 \text{ K} \quad , \quad b = 0.00400846 \frac{\text{J}}{\text{mol K}^2} \quad , \quad (12.11)$$

$$c = -1.33099 \cdot 10^{-6} \frac{\text{J}}{\text{mol K}^3} \quad , \quad d = 1.12064 \cdot 10^{-9} \frac{\text{J}}{\text{mol K}^4} \quad .$$

The extended Hoch-function gives a somewhat better description at high temperatures as the simple one, but its C_P -course is equally too low in the vicinity of the melting point.

Finally, I had to use the additional exponential term in the heat capacity equation to get a correct description of the C_P -points approaching T_M :

$$C_P = C_{PD} + C_{PH} + C_{PE} \quad \text{for} \quad T \leq T_M \quad . \quad (12.12)$$

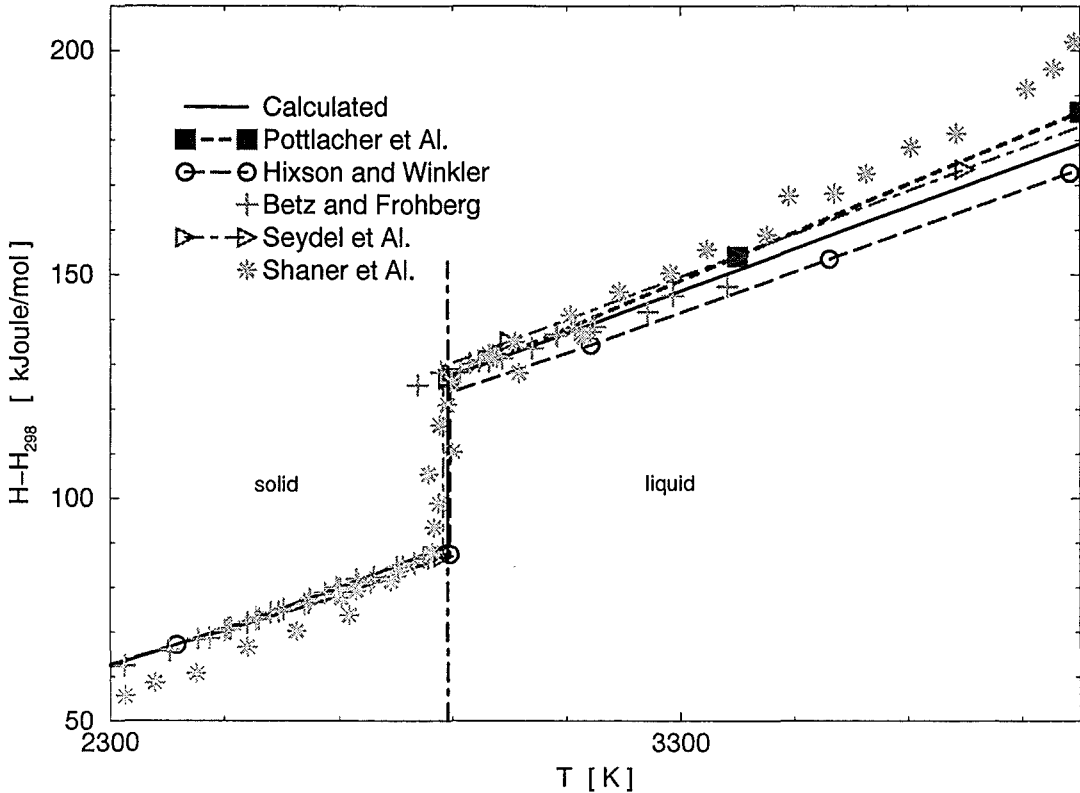


Figure 12.4: Molybdenum. Enthalpy change at the melting-transition

As best parameters of this ultimate C_P -description I got

$$\Theta_D = 380 \text{ K} , \quad b = 0.003 \frac{\text{J}}{\text{mol K}^2} , \quad d = 7.1 \cdot 10^{-10} \frac{\text{J}}{\text{mol K}^4} , \\ g = -18.8 , \quad h = 0.007 \text{ 1/K} . \quad (12.13)$$

In liquid molybdenum I use a mean value, which fits as well to the data of Seydel et al., [103] as to the points of Betz and Frohberg and to the points of Hixson and Winkler, [179]:

$$C_{PL} = 47. \text{ J/(mol K)} , \quad \text{for } T_M < T \quad (12.14)$$

(cf. figure 12.4).

Figure 12.2 on page 90 displays the heat capacity calculated by eq.s 12.12 - 12.14. Figure 12.3 on page 91 shows calculated und measured heat capacities in the vicinity of the melting point. The experimental data are from the reports Ya. A. Kraftmakher, [60], M. M. Mebed, R. P. Yurchak, L. P. Filippov, [59], A. Cezairliyan, [126], F. Righini, and A. Rosso, [127] and K. D. Maglić, N. Lj. Perović, and G. S. Vuković, [185].

To the $C_P(T)$ - description of molybdenum - eq. 12.12 - 12.14 - corresponds the following set of $H(T)$ equations:

$$H_S(T) = H_D(T) + H_H(T) + H_E(T) \quad \text{for } T \leq T_M \quad (12.15)$$

$$H_L(T) = H_S(T_M) + \Delta H_{fus} + C_{PL} \cdot (T - T_M) \quad \text{for } T_M < T .$$

Figures 12.7 and 12.4 show the enthalpy in the solid and liquid molybdenum calculated by eq.s 12.15. Figure 12.7 on page 96 displays also the enthalpy-measurements of Bondarenko, Fomichev, and Kandyba, [57], of Berezin, [64], of Berezin, Chekhovskoi and Sheidlin, [46] and of Kirillin, Sheindlin, Chekhovskoi and Petrov, [31]. The zero-point enthalpy on this figure equals $H_0 = -4.64376 \text{ kJ/mol}$.

Figure 12.4 on page 92 shows, besides of the calculated enthalpy, also the data of G. Pottlacher, E. Kaschnitz, and H. Jäger, [177], R. S. Hixson, M. A. Winkler, [179], of Betz and Frohberg, of Seydel et.al. and of Shaner, Gathers and Minichino, [85].

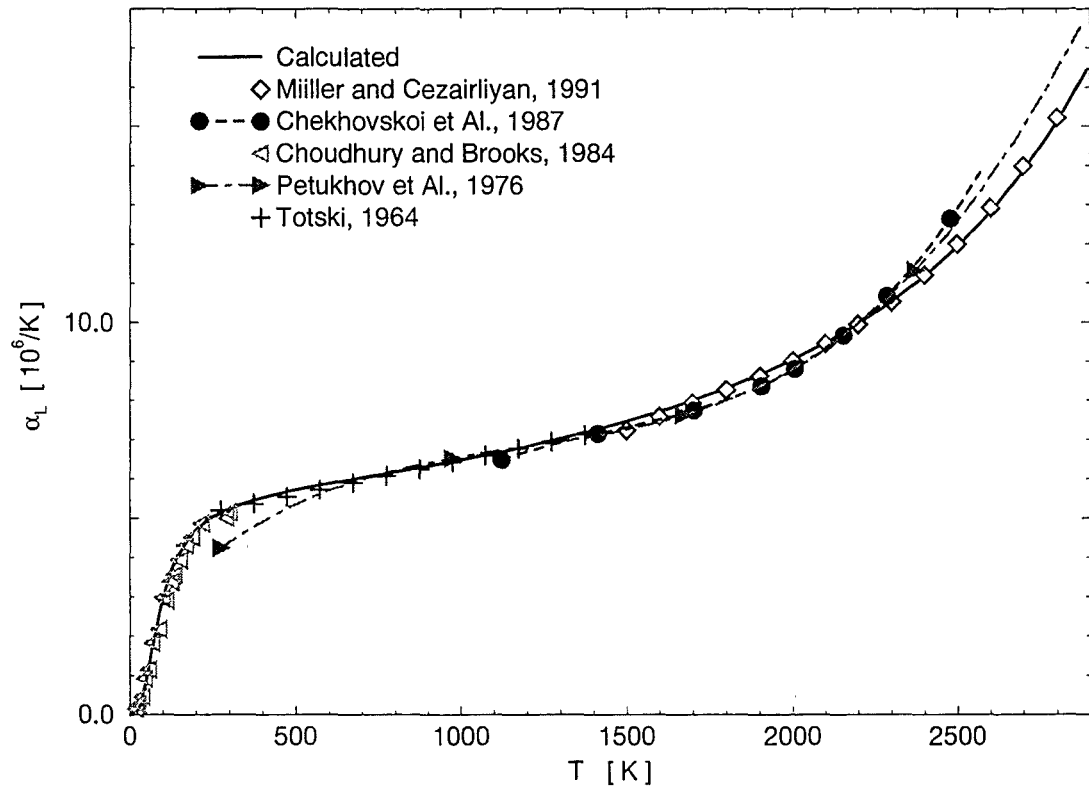


Figure 12.5: Molybdenum. Coefficient of the linear thermal expansion in the solid state.

12.4 Thermal expansion and density

In the solid state the description of the density begins by fitting a function to the measured values of $\alpha_L(T)$. As base for the fitting I selected the low-temperature data reported by

Choudhury and Brooks, [132], the data of Totskii, [16] and the high-temperature measurements of Miiller and Cezairliyan, [176] (s. figure 12.5).

To fit a function to the α_L - data I had to use - as in the case of the heat capacity - the Debye- the Hoch- and the exponential-descriptions (eq.s 2.3, 2.5, 2.7):

$$\alpha_{LS} = e \cdot (c_D + c_H + c_E) \quad \text{for } T \leq T_M \quad . \quad (12.16)$$

The scaling factor of molybdenum is

$$e = 2.15 \cdot 10^{-7} \frac{\text{mol}}{J} \quad (12.17)$$

and the Debye- Hoch- and exponential parameters are

$$\Theta_D = 380 \text{ K} , \quad b = 0.0045 \frac{J}{\text{mol K}^2} , \quad d = 7.4 \cdot 10^{-10} \frac{J}{\text{mol K}^4}$$

$$g = -4.2 , \quad h = 0.0025 \frac{1}{K} . \quad (12.18)$$

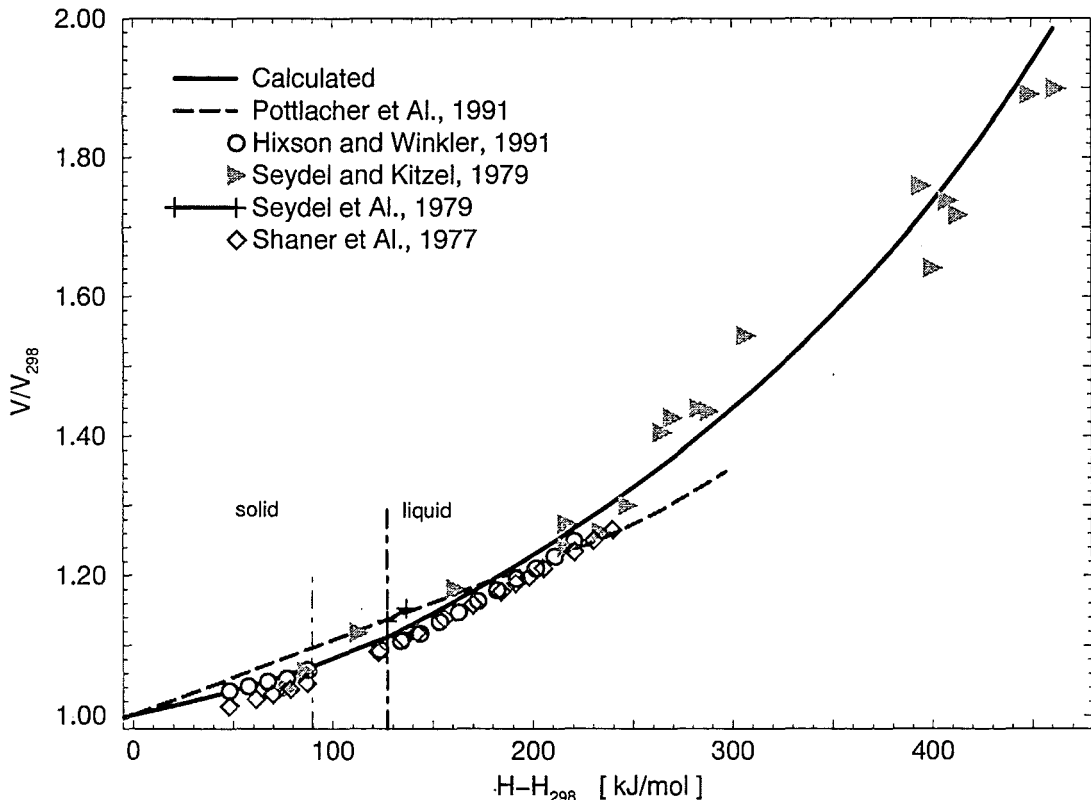


Figure 12.6: Molibdenum. Thermal expansion as a function of the enthalpy.

The volumetric thermal expansion was then evaluated from α_L by eq. 3.2 and normalized to 1 at 298 K. To calculate the density of solid molybdenum via eq. 3.3 the standard density

$$\rho_{298} = 10220. \text{ kg/m}^3 \quad (12.19)$$

reported by Hixson and Winkler was used.

In the liquid state one can depend now on a number of volumetric thermal expansion - enthalpy measurements. Figure 12.6 on page 94 shows the data of Hixson and Winkler, [179], of Pottlacher, Kaschnitz, Jäger, [177], of Seydel and Kitzel, [99] and of Shaner, Gathers and Minichino, [85].

As a density - temperature function for liquid molybdenum a linear description was chosen (s. last row of the table 12.3) which follows more or less the points of Seydel and Kitzel.

Figure 12.8 shows molybdenum densities - the measured points (converted to ρ - T functions) and the proposed density - temperature function. The liquid density departure of Seydel, Bauhof, Fucke and Wadle, [103] is also marked. The "calculated" density is again expressed by temperature polynomials, 3 polynomials are needed for the solid density, calculated from α_L , the fourth is the linear relation for the liquid (s. table 12.3).

A_0	A_1	A_2	A_3
$T \leq 300 \text{ K}$			
10250.8	0.0270421	$-7.11052 \cdot 10^{-4}$	$9.19426 \cdot 10^{-7}$
$300 \text{ K} < T \leq 1900 \text{ K}$			
10269.4	-0.160909	$-1.04368 \cdot 10^{-5}$	$-4.82037 \cdot 10^{-9}$
$1900 \text{ K} < T \leq 2892 \text{ K}$			
10641.5	-0.708874	$2.61956 \cdot 10^{-4}$	$-5.06669 \cdot 10^{-8}$
$2892 \text{ K} < T$			
10848.0	-0.569838	0.0	0.0

Table 12.3: Molybdenum. Coefficients of the density description

Figure 12.6 shows the proposed density shape as a volumetric thermal expansion in the enthalpy - dependence. To get the enthalpy, needed here by the "calculated" V/V_{298} as the independent variable the temperatures were converted by eq. 12.15. The thermal expansion was calculated from the density with the standard density, 10 220. kg/m^3 .

The experimental points are the original V (H) - relations, described by equations or picked from the diagrams supplied. Only the function of Seydel, Bauhof, Fucke and Wadle was recalculated from density - temperature to a thermal expansion - enthalpy function.

The limiting enthalpy values of the solid resp. of the liquid are 89.602 and 127.102 kJ/mol .

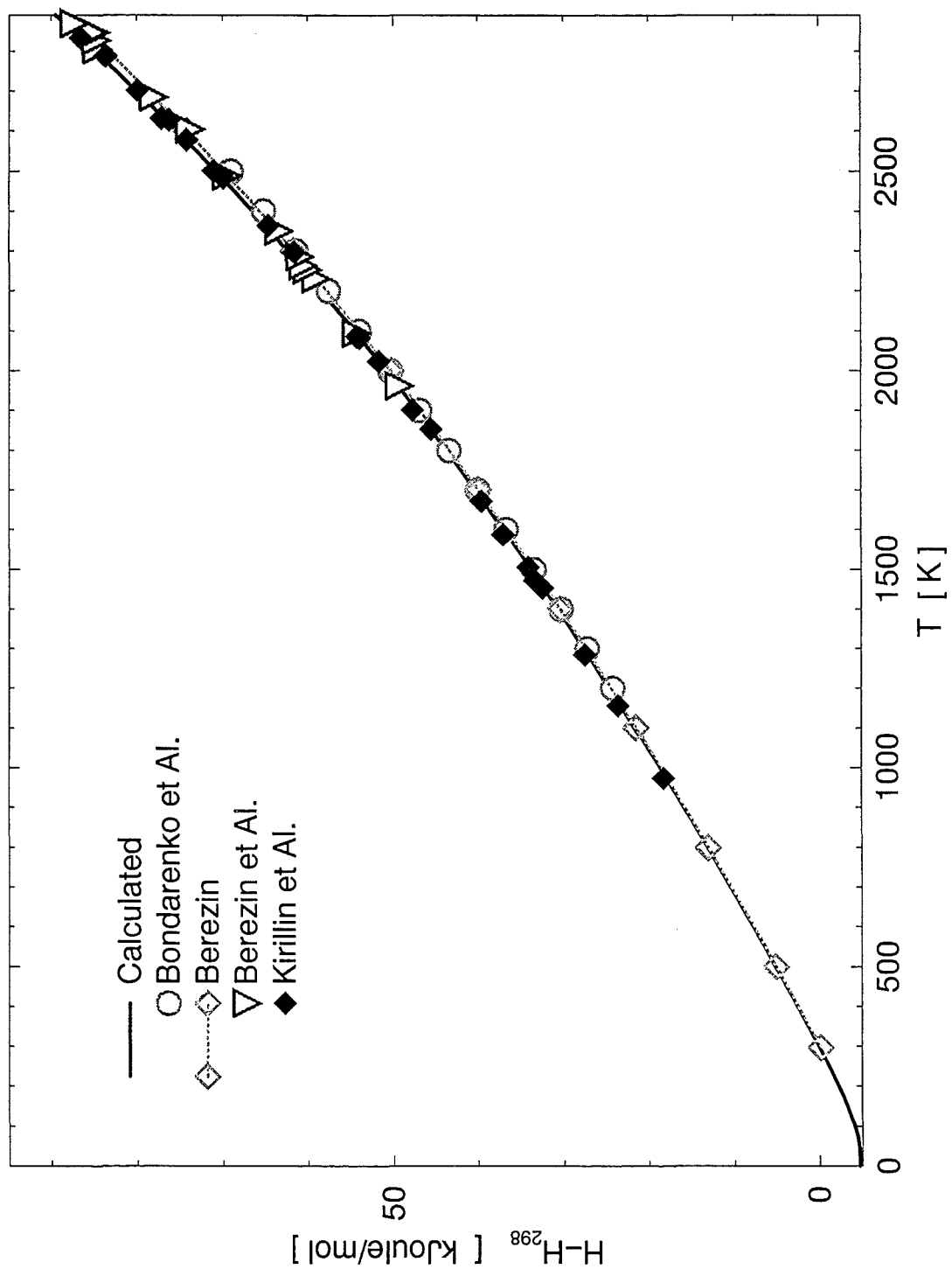


Figure 12.7: Molybdenum. Enthalpy in the solid state

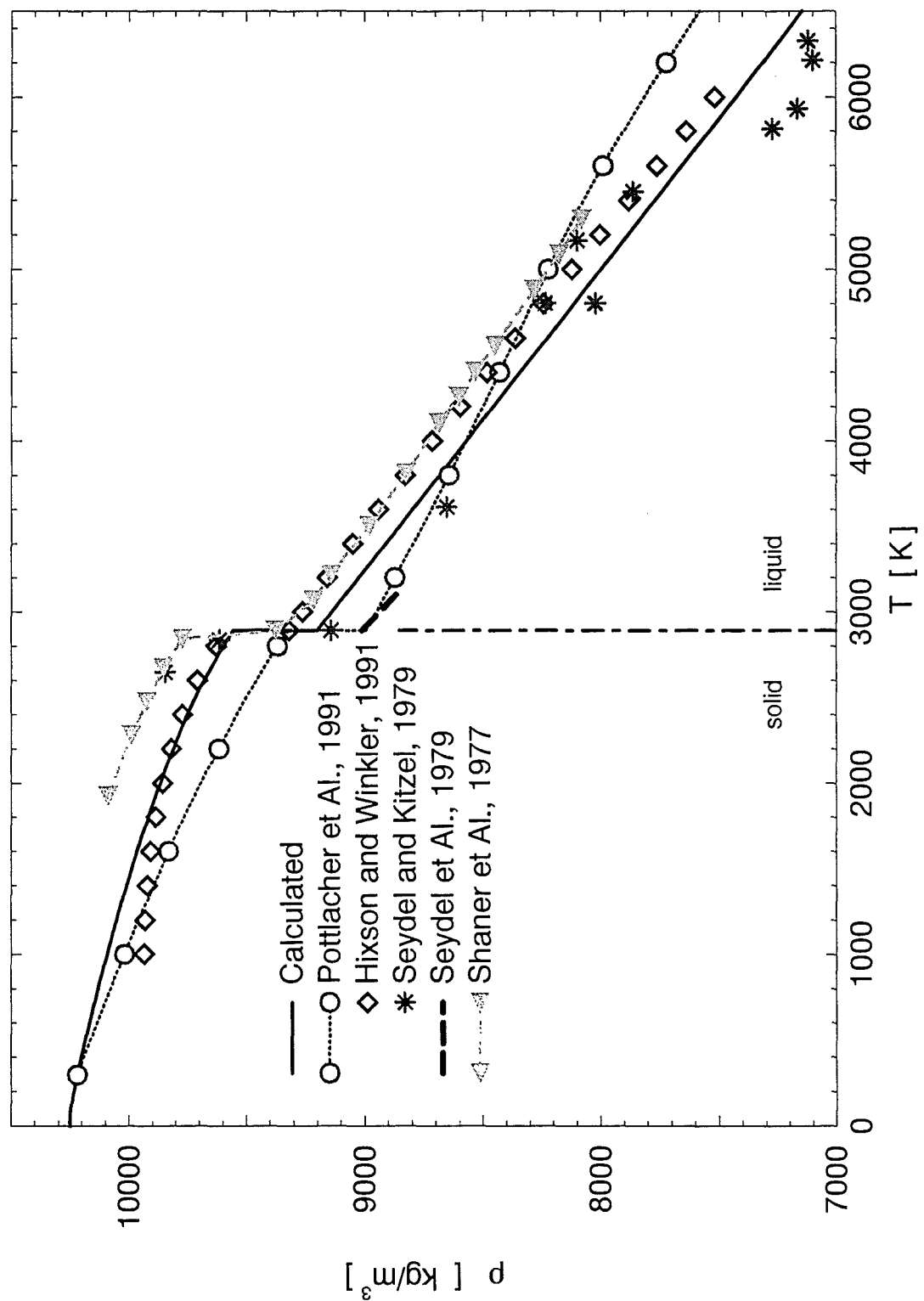


Figure 12.8: Molybdenum. Density as a function of the temperature.

Bibliography

[General properties of matter]

- [1] B. C. Allen, The Surface Tension of Liquid Metals, in Liquid Metals, Chemistry and Physics
Marcel Dekker, Inc., New York, 1972.
- [2] D. J. Steinberg, Density of Liquid Metals and Their Boiling Temperatures
Metallurgical Transactions, Vol. 5 , June, p. 1341-1343, 1974.
- [3] K. D. Garvin, Thermodynamic Properties of the Elements,
Bulletin of Alloy Phase Diagrams, 2, p. 261, 1981.
- [4] H. W. King, Atomic Size Parameters for the Elements,
Bulletin of Alloy Phase Diagrams, 2, p. 527, 1982.

[Properties of transition metals]

[b. c.]

- [5] F. Wüst, A. Meuthen, and R. Durrer,
Forsch. Geb. Ing., Heft 204, Springer, Berlin, 1918.
- [6] S. Umino,
Sci. Rep. Tohoku Univ., Ser. I. 15:597, (1926) and 16:593, (1927).
- [7] B. F. Naylor, The Heat Content of Manganese at High Temperatures
Journal of Chemical Physics, 13, pp. 329-332, 1945.
- [8] L. D. Armstrong, H. Grayson-Smith, High Temperature Calorimetry. II. Atomic Heats of Chromium, Manganese, and Cobalt between 0 and 800 C.
Canadian Journal of Research, 28A, pp. 51-59, 1950.

[1960]

- [9] F. Krauß, Die Messung der Spezifischen Wärme von Metallen bei hohen Temperaturen
Zeitschrift für Metallkunde, Vol. 49, No. 7, pp. 386-392, 1958.
- [10] A. V. Grosse, The Temperature Range of Liquid Metals and an Estimate of their Critical Constants
J. Inorg. Nucl. Chem., 22, pp. 23-31, 1961.
- [11] S. A. Bradford et O. N. Carlson
Transactions of the American Society for Metals, Vol. 55, p. 169, 1962.

- [12] A. D. Kirshenbaum, J. A. Cahill, The Density of Liquid Iron from the Melting Point to 2500 K
Transactions of The Metallurgical Society of AIME Vol. **224**, p. 816, 1962.
- [13] A. D. Kirshenbaum, J. A. Cahill, The Densities of Liquid Nickel and Cobalt and an Estimate of Their Critical Constants
Transactions of the American Society for Metals, Vol. **56**, p. 281, 1963.
- [14] R. Hultgren, R. L. Orr, P. D. Anderson, K. K. Kelley, Selected Values of the Thermodynamic Properties of Metals and Alloys
John Wiley & Sons, 1963.
- [15] M. G. Frohberg, R. Weber, Dichtemessungen an Eisen-Kobalt- und Eisen-Kupfer-Legierungen
Archiv für das Eisenhüttenwesen, Vol. **35**, No. 9, p. 877, 1964.
- [16] E. E. Totskii, Measurement of the coefficient of the linear thermal expansion of metals and alloys
High Temperature, Vol. **2**, No. 1, p. 181, 1964.
- [1965]
 - [17] J. B. Conway and R. A. Hein, Enthalpy Measurements of Solid Materials to 2400 C by Means of a Drop Technique. P. 131 in
Advances in Thermophysical Properties at Extreme Temperatures and Pressures Proceedings of the Third Symposium on Thermophysical Properties, ASME, 1965.
 - [18] V. A. Kirillin, A. E. Sheindlin, V. Ya. Chekhovskoi, I. A. Zhukova, Thermodynamic Properties of Niobium from 0 K to the Melting Point, 2740 K. P. 152 in
Advances in Thermophysical Properties at Extreme Temperatures and Pressures Proceedings of the Third Symposium on Thermophysical Properties, ASME, 1965.
 - [19] A. Cezairliyan, A High-Speed (Milliseconds) Method for The Simultaneous Measurement of Enthalpy, Specific Heat, and Resistivity of Electrical Conductors at High Temperatures. P. 253 in
Advances in Thermophysical Properties at Extreme Temperatures and Pressures Proceedings of the Third Symposium on Thermophysical Properties, ASME, 1965.
 - [20] S. Müller, P. Scholten, Die Gitterstruktur des Kobalts bei hohen Temperaturen
Zeitschrift für angewandte Physik, Vol. **20**, pp. 498-502, 1965.
 - [21] R. Kohlhaas, M. Braun und O. Vollmer, Die Atomwärme von Titan, Vanadin und Chrom im Bereich hoher Temperaturen
Zeitschrift für Naturforschung, Vol. **20a**, pp. 1077-1079, 1965.
 - [22] Ju. L. Pliner, G. F. Ignatenko, S. I. Lapko, Metallurgia chroma
Metallurgia, 1965
 - [23] Y. S. Touloukian (Editor), Recommended Values of the Thermophysical Properties of Eight Alloys, Major Constituents and their Oxides
Thermophysical Properties Research Center, Purdue University,
Lafayette, Indiana, February, 1966.
 - [24] E. Rapoport and G. C. Kennedy, Phase diagram of manganese to 40 kbars
J. Phys. Chem. Solids, Vol. **27**, pp. 93-98, 1966.

- [25] O. Vollmer, R. Kohlhaas, und M. Braun, Die Schmelzwärme und Atomwärme im schmelzflüssigen Bereich von Eisen, Kobalt und Nickel
Zeitschrift für Naturforschung, Vol. **21a**, pp. 181-182, 1966.
- [26] S. Müller, P. Scholten, Die Gitterstruktur des Kobalts bei hohen Temperaturen
Zeitschrift für angewandte Physik, Vol. **20**, pp. 498-502, 1966.
- [27] Y. S. Touloukian (Editor), Thermophysical Properties of High Temperature Solid Materials, Volume I: Elements
The Macmillan Company, New York, 1967.
- [28] Mechanische und thermische Eigenschaften des Vanadins, S. 414 ff. in
GMELIN V, Teil A System-Nummer **48**, 1968.
- [29] S. Müller, P. Dünner, and N. Schmitz-Pranghe, Bestimmung der Gitterparameter von Kobalt und Chrom im Temperaturbereich von 20 C bis 180 C
Zeitschrift für angewandte Physik, Vol. **22**, pp. 403-406, 1967.
- [30] R. Kohlhaas, P. Dünner, and N. Schmitz-Pranghe, Über die Temperaturabhängigkeit der Gitterparameter von Eisen, Kobalt und Nickel im Bereich hoher Temperaturen
Zeitschrift für angewandte Physik, Vol. **23**, pp. 245-249, 1967.
- [31] V. A. Kirillin, A. E. Sheindlin, V. Ya. Chekhovskoi, V. A. Petrov, Enthalpy and Heat Capacity of Molybdenum at Extremly High Temperatures. P. 54 in
Proceedings of the Fourth Symposium on Thermophysical Properties, ASME, 1968.
- [32] R. Adams and C. Altstetter, Thermodynamics of the Cobalt Transformation,
Transactions of the Metallurgical Society of AIME Vol. **242**, January, p. 139, 1968.
- [33] M. J. Ferrante, F. E. Block et J. L. Schaller
U.S. BUR. of Mines, Rept. Invest. Nr. **7145**, 1968.
- [34] M. Braun, R. Kohlhaas und O. Vollmer, Zur Hochtemperatur-Kalorimetrie von Metallen
Zeitschrift für angewandte Physik, Vol. **25**, pp. 365-372, 1968.
- [35] N. Schmitz-Pranghe and P. Dünner, Gitterstruktur und thermische Ausdehnung der Übergangsmetalle Scandium, Titan, Vanadin und Mangan
Zeitschrift für Metallkunde, Vol. **59**, No. 5, pp. 377-382, 1968.
- [36] F. L. Yaggee, E. R. Gilbert, and J. W. Styles, Thermal Expansivities, Thermal Conductivities, and Densities of Vanadium, Titanium, Chromium, and Some Vanadium-Base Alloys (A Comparison with Austenitic Stainless Steel)
J. Less-Common Metals, **19**, No. 1, pp. 39-51, 1969.
- [37] T. Saito, Y. Shiraishi, Y. Sakuma, Density Measurement of Molten Metals by Levitation Technique at Temperatures between 1800 and 2200 C
Transactions ISIJ, **9**, pp. 118-126 1969.
- [38] M. Hoch, The high temperature specific heat of body-centered cubic refractory metals
High Temperatures - High Pressures, **1**, pp. 531-542, 1969.
- [39] V. P. Lebedev, A. A. Mamalui, V. A. Pervakov, N. S. Petrenko, V. P. Popov, and V. I. Khotkevich, Thermal Expansion of Niobium, Molybdenum, and Their Alloy at Low Temperatures,
Ukrainskii Fizicheskii Zhurnal, Vol. **14**, No. 5, pp. 746-750, 1969.

- [40] E. Rudy, Compendium of Phase Diagram Data
U.S. Air Force Report AFML-TR-65-2, Pt. IV, 1969.
- [41] W. Kurz und B. Lux, Die Schallgeschwindigkeit von Eisen und Eisenlegierungen im festen und flüssigen Zustand
High Temperatures - High Pressures, **1**, pp. 387-399, 1969.
- [1970]
- [42] J. A. Treverton and J. L. Margrave, Thermal Properties of Liquid Mo by Levitation Calorimetry. P. 489 in
Proceedings of the Fifth Symposium on Thermal Properties, Boston, 1970.
- [43] J. L. Margrave,
High Temperatures - High Pressures, **2**, p. 583, 1970.
- [44] S. Watanabe, Densities and Viscosities of Iron, Cobalt and Fe-Co Alloy in Liquid State
Transactions of the Japan Institute of Metals, Vol. **12**, p. 17, 1971.
- [45] V. E. Peletskii, V. P. Druzhinin, Ya. G. Sobol', Thermophysical properties of vanadium at high temperatures,
High Temperatures - High Pressures, **3**, pp. 153-159, 1971.
- [46] B. Ya. Berezin, V. Ya. Chekhovskoi, A. E. Sheindlin, Enthalpy of solid and liquid molybdenum by levitation calorimetry. Heat of fusion of molybdenum
High Temperatures - High Pressures, **3**, pp. 287-297, 1971.
- [47] J. A. Treverton and J. L. Margrave, Thermodynamic properties by levitation calorimetry III. The enthalpies of fusion and heat capacities of the liquid phases of iron, titanium, and vanadium
J. Chem. Thermodynamics, Vol. **3**, pp. 473-481, 1971.
- [48] A. V. Arutyunov, S. N. Banchila, and L. P. Filipov, Properties of Titanium at Temperatures Above 1000 K.
High Temperature, Vol. **9**, No. 3, p. 487, 1971.
- [49] L. D. Lucas, Densité de métaux à haute température (dans les états solide et liquide).
Première partie
Mémoires Scientifiques de Revue de Metallurgie, **69**, pp. 395 - 409, 1972.
- [50] L. D. Lucas, Densité de métaux à haute température (dans les états solide et liquide).
Deuxième partie
Mémoires Scientifiques de Revue de Metallurgie, **69**, pp. 479 - 492, 1972.
- [51] A. Cezairliyan, Measurement of melting point, normal spectral emittance (at melting point), and electrical resistivity (above 2650 K) of niobium by a pulse heating method
High Temperatures - High Pressures, **4**, pp. 453-458, 1972.
- [52] B. Ya. Berezin, V. Ya. Chekhovskoi, and A. E. Sheindlin, The Enthalpy and Specific Heat of Molten Vanadium
High Temperature Science, **4**, pp. 478-486, 1972.
- [53] A. E. Sheindlin, B. Ya. Berezin, V. Ya. Chekhovskoi, Enthalpy of niobium in the solid and liquid state
High Temperatures - High Pressures, **4**, pp. 611-619, 1972.

- [54] M. M. Kenisarin, B. Ya. Berezin, V. Ya. Chekhovskoi, The melting point of molybdenum as a secondary fixed point on the International Practical Temperature Scale
High Temperatures - High Pressures, **4**, pp. 707-713, 1972.
- [55] W. C. Hubbel and F. R. Brotzen, Elastic Constants of Niobium-Molybdenum Alloys
in the Temperature Range -190 to 100 C
J. Appl. Phys., **43**, No. 8, pp. 3306-3312, 1972.
- [56] R. Hultgren, P. D. Desai, D. T. Hawkins, M. Gleiser, K. K. Kelley, D. D. Wagman,
Selected Values of the Thermodynamic Properties of the Elements
American Society for Metals, Metals Park, Ohio, 1973.
- [57] V. P. Bondarenko, E. N. Fomichev, V. V. Kandyba, Experimental study of the thermodynamic properties of refractories at high temperatures
High Temperatures - High Pressures, **5**, pp. 5-7, 1973.
- [58] S. Watanabe, T. Saito, Thermal expansion of Liquid Iron,
Transactions of the Japan Institute of Metals, Vol. **14**, pp. 120-122, 1973.
- [59] M. M. Mebed, R. P. Yurchak, L. P. Filippov, Measurement of the thermophysical properties of electrical conductors at high temperatures (Mo).
High Temperatures - High Pressures, **5**, pp. 253-260, 1973.
- [60] Ya. A. Kraftmakher, The modulation method for measuring specific heat
High Temperatures - High Pressures, **5**, pp. 433-454, 1973.
- [61] V. Ya. Chekhovskoi and R. G. Kalinkina, The true specific heat of vanadium in the temperature range 300 - 900 K
High Temperature, Vol. **11**, No. 4, p. 796, 1973.
- [62] M. J. Laubitz and T. Matsumura, Transport Properties of the Ferromagnetic Metals.
I. Cobalt
Canadian Journal of Physics, Vol. **51**, No. 12, pp. 1247-1256, 1973.
- [63] A. I. Savvatimskii,
High Temperature, Vol. **11**, p. 1057, 1973.
- [64] B. Ya. Berezin, Candidate thesis,
Institute of High Temperatures, Moscow, USSR, 1973.
- [65] V. Ya. Chekhovskoi, B. Ya. Berezin, M. M. Kenisarin, Proceedings of the International Symposium on Metrology, pp. 79-94
Bratislava, Nov. 5-8, 1974.
- [66] B. I. Yavoiskii, A. A. Ezhov, V. F. Kravchenko, B. S. Uckov, Yu. I. Nebosov, Yu. A. Chernov, G. A. Dorofeev, Density measurement of liquid metals using gamma-radiation
Metally, Izwestiya Akademii Nauk S.S.R., No. 4, pp. 61- 66, 1974.
- [67] B. Ya. Berezin, S. A. Kats, M. M. Kenisarin, and V. Ya. Chekhovskoi, Heat and melting temperature of titanium
High Temperature, Vol. **12**, No. 3, p. 450, 1974.
- [68] I. G. Kozhevnikov, Enthalpy and heat capacity of niobium
High Temperature, Vol. **12**, No. 4, p. 785, 1974.
- [1975]

- [69] Y. S. Touloukian, C. Y. Ho (Editors), Thermophysical properties of Matter. The TPRC Data Seies, Volume 12. Thermal Expansion - Metallic Elements and Alloys. Plenum Press, 1975
- [70] A. Cezairliyan and J. L. McClure, Subsecond Pulse Heating Technique for the Study of Solid-Solid Phase Transformation at High Temperatures: Application to Iron High Temperature Science, **7**, pp. 189-196, 1975.
- [71] Y. Waseda, S. Tamaki, Structural study of platinum and chromium in the liquid state by x-ray diffraction High Temperatures - High Pressures, **7**, pp. 215-220, 1975.
- [72] Y. Waseda, K. Hirata, M. Ohtani, High-temperature thermal exspansion of platinum, tantalum, molybdenum and tungsten measured by x-ray diffraction High Temperatures - High Pressures, **7**, pp. 221-226, 1975.
- [73] I. Ya. Dekhtyar, V. N. Kolesnik, V. I. Patoka, and V. I. Silant'ev, Investigation of the vaporization of molybdenum in an ultrahigh vacuum High Temperature, Vol. **12**, No. 5, p. 870, 1975.
- [74] V. E. Fortov, A. N. Dremin, A. A. Leontev, Evaluation of the Parameters of the Critical Point High Temperature, Vol. **13**, No. 5, p. 984, 1975.
- [75] M. M. Martynyuk, I. Kharimkhodzhaev, and V. I. Tsapkov Sov. Phys. Tech. Phys., **19**, p. 1458, 1975.
- [76] M. J. Laubitz, T. Matsumura, and P.J. Kelly, Transport Properties of the Ferromagnetic Metals. II. Nickel Canadian Journal of Physics, Vol. **54**, pp. 92-102, 1976.
- [77] M. M. Kenisarin, V. Ya. Chekhovskoi, B. Ya. Berezin, S. A. Kats, Transfer of the ITPS above 2000 K High Temperatures - High Pressures, **8**, pp. 367-376, 1976.
- [78] J. W. Shaner, G. R. Gathers, C. Minichino, A new apparatus for thermophysical measurements above 2500 K High Temperatures - High Pressures, **8**, pp. 425-429, 1976.
- [79] A. N. Amatuni, T. I. Malyutina, V. Ya. Chekhovskoi, V. A. Petukhov, Standard samples for dilatometry High Temperatures - High Pressures, **8**, pp. 565-570, 1976.
- [80] V. A. Petukhov, V. Ya. Chekhovskoi, and V. M. Zaichenko, Thermal Expansion of Molybdenum High Temperature, Vol. **14**, No. 4, p. 645, 1976.
- [81] M. I. Lesnaya, G. G. Volotkin, and V. A. Kashchuk, Effect of Addition of Transition Metals on the Temperature Coefficient of Linear Expansion of Titanium and Vanadium High Temperature, Vol. **14**, No. 6, pp. 1072-1074, 1976.
- [82] J. W. Shaner, Thermal expansion of metals over the entire liquid range, Thermal Expansion **6**, pp. 69-81, Proceedings of the Sixth International Symposium on Thermal Expansion Aug. 29-31, 1977, Hecla Island, Manitoba, Canada.

- [83] J. S. Shaner, G. R. Gathers, W. H. Hogson, Thermophysical Measurements on Liquid Metals Above 4000 K. P. 896 in
Proceedings of the Seventh Symposium on Thermophysical Properties, ASME, 1977.
- [84] A. Cezairliyan and A. P. Müller, Heat capacity and electrical resistivity of titanium in the range 1500 - 1900 K by a pulse heating method,
High Temperatures - High Pressures, **9**, pp. 319-324, 1977.
- [85] J. W. Shaner, G. R. Gathers, C. Minichino, Thermophysical properties of liquid tantalum and molybdenum
High Temperatures - High Pressures, **9**, pp. 331-343, 1977.
- [86] V. A. Petukhov, V. Ya. Chekhovskoi, V. G. Andrianova, and A. G. Mozgovoi, Experimental Investigation of Thermal Expansion of a Number of Construction Materials, Niobium and Niobium Alloy 5VMTs1
High Temperature, Vol. **15**, No. 3, pp. 561, 1977.
- [87] B. Ya. Berezin and V. Ya. Chekhovskoi, Enthalpy and heat capacity of niobium and vanadium in the region from 298.15 k to the melting point
High Temperature, Vol. **15**, No. 4, p. 651, 1977.
- [88] U. Seydel and W. Fucke, Sub-Microsecond-Pulse-Heating Measurements of High Temperature Electrical Resistivity of the 3d-Transition Metals Fe, Co, and Ni
Zeitschrift für Naturforschung, Vol. **32a**, pp. 994-1002, 1977.
- [89] T. G. Kollie, Measurement of the thermal-expansion of nickel from 300 to 1000 K and determination of the power-law constants near the Curie temperature
Phys. Rev. B, Vol. **16**, pp. 4872-4881, 1977.
- [90] V. E. Peletskii and E. B. Zaretskii, Thermophysical Properties of Group IV Transition Metals Near Polymorphous Transformations. P. 83 in
Proceedings of the Eighth Symposium on Thermophysical Properties, ASME, 1978.
- [91] A. Cezairliyan and A. P. Müller, Thermodynamic Study of the $\alpha \rightarrow \beta$ Phase Transformation in Titanium by a Pulse Heating Method
J. Res. Natl. Bur. Stand., **83**, p. 127, 1978.
- [92] L. Ming and M. H. Manghani, Isothermal compression of bcc transition metals to 100 kbar
J. Appl. Phys., **49**, No. 1, pp. 208-212, 1978.
- [93] V. A. Petukhov, V. Ya. Chekhovskoi and A. G. Mozgovoi, Experimental Investigation of the Thermal Expansion of Niobium at High Temperatures
High Temperature, Vol. **16**, No. 2, p. 353, 1978.
- [94] S. V. Boyarskii and I. I. Novikov Nature of the temperature dependence of the heat capacity near a polymorphic transition
High Temperature, Vol. **16**, No. 3, p. 453, 1978.
- [95] S. A. Kats, Candidate thesis,
Institute of High Temperatures, Moscow, USSR, 1978.
- [96] W. D. Drotning, Thermal expansion of nickel to 2300 K.
pp. 17-28 in the Proceedings of the Seventh International Thermal Expansion Symposium, held Nov. 7-9, 1979, Chicago, Ill.

- [97] T. I. Muradov, R. I. Pepinov, and M. Z. Alizade, Thermal Conductivity and Electrical Resistivity of Ni - Mn Alloys
High Temperature, Vol. **17**, No. 1, p. 64, 1979.
- [98] E. B. Zaretskii, V. E. Peletskii, A Device for Coordinated Study of Thermophysical Properties of Metals and Alloys
High Temperature, Vol. **17**, No. 1, p. 104, 1979.
- [99] U. Seydel and W. Kitzel, Thermal volume expansion of liquid Ti, V, Mo, Pd and W
Journal of Physics, F. Metal Physics, Vol. **9**, No. 9, pp. L153-L160, 1979.
- [100] I. S. Williams, E. S. R. Gopal and R. Street, The specific heat of strained and annealed chromium
Journal of Physics, F. Metal Physics. Vol. **9**, No. 3, p. 431, 1979.
- [101] A. S. Basin, Ya. L. Kolotov, S. V. Stankus, The density and thermal expansion of iron and ferrous alloys
High Temperatures - High Pressures, **11**, pp. 465-470, 1979.
- [102] S. Sato, O. J. Kleppa, The enthalpy of fusion of γ -manganese at 1386 K
J. Chem. Thermodynamics, Vol. **11**, pp. 521-525, 1979.
- [103] U. Seydel, H. Bauhof, W. Fucke, H. Wadle, Thermophysical data for various transition metals at high temperatures obtained by a submicrosecond-pulse-heating method
High Temperatures - High Pressures, **11**, pp. 635-642, 1979.
- [104] G. R. Gathers, J. S. Shaner, R. S. Hixson, D. A. Young, Very high temperature thermophysical properties of solid and liquid vanadium and iridium
High Temperatures - High Pressures, **11**, pp. 653-668, 1979.
- [1980]
- [105] V. Ya. Chekhovskoi, I. A. Zhukova, Enthalpy and Heat Capacity of Chromium in the Region from 273.15 - 2133 K
Metally, Izvestiya Akademii Nauk S.S.R., No. 3. p. 67, 1980.
- [106] G. Betz and M. G. Frohberg, Enthalpy measurements on solid and liquid molybdenum by levitation calorimetry
High Temperatures - High Pressures, **12**, pp. 169-178, 1980.
- [107] A. Cezairliyan and A. P. Müller,
International Journal of Thermophysics, Vol. **1**, No. 4, p. 195, 1980.
- [108] G. Betz and M. G. Frohberg, Enthalpy Measurements on Solid and liquid Niobium by Means of Levitation Calorimetry
Zeitschrift für Metallkunde, Vol. **71**, No. 7, pp. 451-455, 1980.
- [109] O. I. Ostrovskii, V. A. Ermachenkov, B. M. Popov, V. A. Grigoryan, L. V. Kogan, Thermophysical properties of liquid iron, cobalt and nickel
Zhurnal Fizicheskoi Chimii, **54**, pp. 1291-1295, 1980.
- [110] G. M. Barrow, *Physical Chemistry*
McGraw-Hill, New York, 1980.
- [111] C. Kittel, H. Kroemer, *Thermal Physics*, 2nd edition,
W. H. Freeman and Company, San Francisco, 1980.

- [112] A. P. Müller and A. Cezairliyan, Thermal Expansion of Iron During the $\alpha \rightarrow \gamma$ Phase Transformation by a Transient Interferometric Technique
pp. 245-258 in the Proceedings of the Eighth International Thermal Expansion Symposium, held June 15-17, 1981, Gaithersburg, Md.
- [113] C. R. Brooks, Contributions to the Cp of Alpha (HCP) Titanium from 200 - 1000 K
International Journal of Thermophysics, Vol. 2, No. 4, p. 371, 1981.
- [114] N. N. Oleinikov, Thermal Conductivity of Pure Iron
High Temperature, Vol. 19, No. ?, p. 382, 1981.
- [115] W. D. Drotning, Thermal expansion of iron, cobalt, nickel, and copper at temperatures up to 600 K above melting
High Temperatures - High Pressures, 13, pp. 441-458, 1981.
- [116] V. Ya. Chekhovskoi, S. A. Kats, Investigation of the thermophysical properties of refractory metals near the melting point
High Temperatures - High Pressures, 13, pp. 611-616, 1981.
- [117] V. E. Peletskii, E. B. Zaretskii, Investigation of the thermal transport properties and temperature anomalies near the Curie points of the classical ferromagnets cobalt and iron
High Temperatures - High Pressures, 13, pp. 661-664, 1981.
- [118] G. I. Mozharov and A. I. Savvatimskii, Specific Heat of Solid and Liquid Niobium up to 5000 K
High Temperature, Vol. 19, No. 5, p. 691, 1981.
- [119] I. I. Novikov, V. V. Roshchupkin, A. G. Mozgovoi, and N. A. Semashko Specific heat of nickel and niobium in the temperature interval 300-1300 K
High Temperature, Vol. 19, No. 5, p. 694, 1981.
- [120] Y. S. Touloukian, C. Y. Ho (Editors), Properties of Selected Ferrous Alloying Elements
McGraw-Hill Book Company, 1981.
- [121] N. V. Bodrov, G. I. Nikolaev, A. M. Nemec, Vapor pressure of iron
Metally, Izwestiya Akademii Nauk S.S.R., No. 2. p. 35, 1982.
- [122] J. L. Margrave,
Mater. Res. Soc. Symp. Proc. 9. p. 39, 1982.
- [123] N. V. Bodrov, G. I. Nikolaev, A. M. Nemec, Vapor pressure of nickel
Metally, Izwestiya Akademii Nauk S.S.R., No. 5. p. 77, 1982.
- [124] Y. Takahashi, J. Nakamura, and J. F. Smith, Laser-flash calorimetry III. Heat capacity of vanadium from 80 to 1000 K
J. Chem. Thermodynamics, Vol. 14, pp. 977-982, 1982.
- [125] L. V. Gurvich, I. V. Veits, and V. A. Medvedev, Calculations of Thermodynamic Properties
Nauka, Moscow, pp. 9-12, 1982.
- [126] A. Cezairliyan, Measurement of the Heat Capacity of Molybdenum (Standard Reference Material) in the Range 1500 - 2800 K
International Journal of Thermophysics, Vol. 4, No. 2, p. 159, 1983.

- [127] F. Righini, and A. Rosso, Heat Capacity and Electrical Resistivity of SRM Molybdenum (1000 - 2500 K)
International Journal of Thermophysics, Vol. 4, No. 2, p. 173, 1983.
- [128] A. Cezairliyan and A. P. Müller, Heat capacity and Electrical Resistivity of Nickel in the Range 1300 - 1700 K Measured with a Pulse Heating Technique
International Journal of Thermophysics, Vol. 4, No. 4, p. 389, 1983.
- [129] G. R. Gathers, Electrical Resistivity and Thermal Expansion of Liquid Titanium and Zirconium
International Journal of Thermophysics, Vol. 4, No. 3, p. 411, 1983.
- [130] R. E. Bedford, G. Bonnier, H. Mass and F. Pavese,
Metrologia, Vol. 20, p. 145, 1984.
- [131] A. Cezairliyan and A. P. Müller, Melting Temperature of Nickel by Pulse Heating Technique
International Journal of Thermophysics, Vol. 5, No. 3, p. 315, 1984.
- [132] A. Choudhury and C. R. Brooks, Contributions to the Cp of Solid Molybdenum in the Range 300 - 2890 K
International Journal of Thermophysics, Vol. 5, No. 4, p. 403, 1984.
- [133] V. N. Eremenko, Yu. N. Ivashchenko and P. S. Martsenyuk, Melting Point Density and Surface Energy for Liquid Vanadium, Niobium, and Tantalum
High Temperature, Vol. 22, No. 4, pp. 567-570, 1984.
- [1985]
- [134] R. Gallob, H. Jäger, G. Pottlacher, Recent results on thermophysical data of liquid niobium and tantalum
High Temperatures - High Pressures, 17, pp. 207-213, 1985.
- [135] M. Bober, J. Singer, High Temperature Vapor Pressures of Metals from Laser Evaporation
High Temperature Science, 19, pp. 329-345, 1985.
- [136] A. F. Guillermet, Critical Evaluation of the Thermodynamic Properties of Molybdenum
International Journal of Thermophysics, Vol. 6, No. 4, p. 367, 1985.
- [137] J. O. Andersson, Thermodynamic Properties of Chromium
International Journal of Thermophysics, Vol. 6, No. 4, p. 411, 1985.
- [138] A. S. Dobrosavljević, K. D. Maglić, N. Lj. Perović, Specific heat measurements of ferromagnetic materials by the pulse-heating technique
High Temperatures - High Pressures, 17, pp. 591-598, 1985.
- [139] A. F. Guillermet, P. Gustafson, An assessment of the thermodynamic properties and the (p,T) phase diagram of iron
High Temperatures - High Pressures, 16, pp. 591-610, 1985.
- [140] F. Righini, R. B. Roberts, and A. Rosso, Measurement of Thermophysical properties by a Pulse-Heating Method: Niobium in the Range 1000 - 2500 K
International Journal of Thermophysics, Vol. 6, No. 6, p. 681, 1985.

- [141] A. P. Miiller and A. Cezairliyan, Thermal Expansion of Molybdenum in the Range 1500 - 2800 K by a Transient Interferometric Technique
International Journal of Thermophysics, Vol. **6**, No. 6, p. 695, 1985.
- [142] P. D. Desai, Thermodynamic Properties of Vanadium
International Journal of Thermophysics, Vol. **7**, No. 1, p. 213, 1986.
- [143] M. Yousuf, P. Ch. Sahu, H. K. Jajoo, S. Rajagopalan, K. Govinda, Effect of magnetic transition on the lattice expansion of nickel
Journal of Physics, F. Metal Physics, Vol. **16**, pp. 373-380, 1986.
- [144] F. Righini, R. B. Roberts, and A. Rosso, Thermal expansion by a pulse-heating Method: niobium in the range 1000 - 2600 K
High Temperatures - High Pressures, **18**, pp. 573-583, 1986.
- [145] P. D. Desai, Thermodynamic Properties of Iron and Silicon
J. Phys. Chem. Ref. Data, Vol. **15**, No. 3, p. 967, 1986.
- [146] K. D. Maglič, A. S. Dobrosavljevič, N. Lj. Perovič, The Experimental Study of Transport and Thermodynamic Properties of Nickel
Thermal Conductivity 20. Proceedings of the Twentieth International Thermal Conductivity Conference, 1987
- [147] G. Pottlacher, H. Jäger, T. Neger, Thermophysical measurements on liquid iron and nickel
High Temperatures - High Pressures, **19**, pp. 19-27, 1987.
- [148] S. Yu. Glazkov, Formation of point defects and thermophysical properties of nickel at high temperatures.
High Temperature, Vol. **25**, No. 1, p. 51, 1987.
- [149] P. D. Desai, Thermodynamic Properties of Manganese and Molybdenum
J. Phys. Chem. Ref. Data, Vol. **16**, No. 1, p. 91, 1987.
- [150] V. Ya. Chekhovskoi, L. N. Latev, V. A. Petukhov, E. N. Shestakov, S. V. Onufriev, A. Z. Zhuk, Optical properties and thermal expansion of molybdenum as a thermo-physical reference standard
High Temperatures - High Pressures, **19**, pp. 397-405, 1987.
- [151] A. F. Guillermet, Critical Evaluation of the Thermodynamic Properties of Cobalt
International Journal of Thermophysics, Vol. **8**, No. 4, p. 481, 1987.
- [152] A. Cezairliyan and J. L. McClure, Microsecond-Resolution Transient Technique for Measuring the Heat of Fusion of Metals: Niobium
International Journal of Thermophysics, Vol. **8**, No. 5, p. 577, 1987.
- [153] P. D. Desai, Thermodynamic Properties of Nickel
International Journal of Thermophysics, Vol. **8**, No. 6, p. 763, 1987.
- [154] P. D. Desai, Thermodynamic Properties of Titanium
International Journal of Thermophysics, Vol. **8**, No. 6, p. 781, 1987.
- [155] G. K. White, Cp of the Transition Metals at High T (calc. Grueneisen-Fact.)
International Journal of Thermophysics, Vol. **9**, No. 5, p. 839, 1988.
- [156] M. Thiessen, An Analysis of the High-Temperature Entropy of Transition Metals, (Ti , V , Nb , Mo)
International Journal of Thermophysics, Vol. **9**, No. 1, p. 159, 1988.

- [157] M. C. Y. Lee and A. Adams, A Combination Compact Knudsen Cell-Mass Spectrometer Apparatus for Alloy Studies
High Temperature Science, **25**, pp. 103-116, 1988.
- [158] Miiler, Cezairliyan, Thermal Expansion of Niobium in the Range 1500 - 2700 K by a Transient Interferometric Technique
International Journal of Thermophysics, Vol. **9**, No. 2, p. 195, 1988.
- [159] R. Lin, M. G. Frohberg, Enthalpy measurements of solid and liquid chromium by levitation calorimetry
High Temperatures - High Pressures, **20**, pp. 539-544, 1988.
- [160] J. Hiernaut, F. Sakuma, C. Ronchi, Determination of the melting point and the emissivity of refractory metals with a six-wavelength pyrometer
High Temperatures - High Pressures, **21**, pp. 139-148, 1989.
- [161] J. W. Vandersande, A. Zoltan, and C. Wood, Accurate Determination of Specific Heat at High Temperatures Using the Flash Diffusivity Method (Nb)
International Journal of Thermophysics, Vol. **10**, No. 1, p. 251, 1989.
- [162] M. C. Y. Lee, Activity Measurement and its Use in Predicting Phase Relationships in Stainless Steels
Journal of Nuclear Materials, **167**. p. 175, 1989.
- [163] N. A. Gokcen, The Phase Transformations in Mn
Bulletin of Alloy Phase Diagrams, **10**, p. 313, 1989.
- [164] A. S. Dobrosavljević, K. D. Maglić, N. Lj. Perović, Experimental study of transport and thermodynamic properties of cobalt
High Temperatures - High Pressures, **21**, pp. 317-324, 1989.
- [165] A. S. Dobrosavljević, K. D. Maglić, Evaluation of a direct pulse heating method for measurement of specific heat and electric resistivity in the range 300 - 1900 K
High Temperatures - High Pressures, **21**, pp. 411-421, 1989.
- [166] V. V. Makeev, E. L. Demina, P. S. Popel', and E. L. Arkhangel'skii, Study of the Density of Metals by the Method of Penetrating Radiation in the Temperature Interval 290-2100 K
High Temperature, Vol. **27**, No. 5, p. 701, 1989.
- [1990]
- [167] G. A. Murray, R. J. Kematick, C. E. Myers, and M. A. Frisch, Comparison of Thermo-dynamic Data Obtained by Knudsen Vaporization. Magnetic and Quadrupole Mass Spectrometric Techniques
High Temperature Science, **26**, pp. 415-425, 1990.
- [168] J. L. McClure and A. Cezairliyan, Measurement of the Heat of Fusion of Molybdenum by a Microsecond-Resolution Transient Technique
International Journal of Thermophysics, Vol. **11**, No. 4, p. 731, 1990.
- [169] A. F. Guillermet and W. Huang, Thermodynamic Analysis of Manganese
International Journal of Thermophysics, Vol. **11**, No. 5, p. 949, 1990.
- [170] A. I. Zaitsev, M. A. Zemchenko, B. M. Mogutnov, Thermodynamic Properties and Phase Equilibria at High Temperatures in Fe-Cr and Fe-Mn Systems
High Temperature Science, **28**, pp. 313-330, 1990.

- [171] J. P. Hajra, R. Lin, M. G. Frohberg, An Analysis of High Temperature Heat Capacities and Entropies of Fusion of Chromium, Molybdenum and Tungsten,
Zeitschrift für Metallkunde, Vol. **81**, No. 5, pp. 3419-344, 1990.
- [172] V. N. Korobenko and A. I. Savvatimskii, Electrical Resistivity and Enthalpy of Nickel and its Alloys in the Solid and Liquid States
High Temperature, Vol. **28**, No. 5, p. 689, 1990.
- [173] A. Nabi, R. E. Taylor, Measurement of the specific heat capacity of solids at 300 - 1200 K by radiative step heating
Proceedings of the 12th European Conference on Thermophysical Properties, Vienna, Austria, 24-28 Sept., 1990
High Temperatures - High Pressures, **24**, pp. 723-731, 1992.
- [174] R. Lin, M. G. Frohberg, Enthalpy Measurements of Solid and Liquid Vanadium by Levitation Calorimetry
Zeitschrift für Metallkunde, Vol. **82**, No. 1, pp. 49-52, 1991.
- [175] V. V. Makeev and P. S. Popel', Density and coefficients of thermal expansion of nickel, chromium, and scandium in the solid and liquid states
High Temperature, Vol. **28**, No. 4, p. 525, 1991.
- [176] A. P. Miiller and A. Cezairliyan, Interferometric Technique for the Subsecond Measurement of Thermal Expansion at High Temperatures: Application to Refractory Metals
International Journal of Thermophysics, Vol. **12**, No. 4, p. 643, 1991.
- [177] G. Pottlacher, E. Kaschnitz, and H. Jäger, High-pressure, high-temperature thermophysical measurements on molybdenum,
Journal of Physics: Condensed Matter, Vol. **3**, pp. 5783-5792, 1991.
- [178] J. L. McClure and A. Cezairliyan, Measurement of the Heat of Fusion of Titanium and a Titanium Alloy (90Ti-6Al-4V) by a Microsecond-Resolution Transient Technique
International Journal of Thermophysics, Vol. **13**, No. 1, p. 75, 1992.
- [179] R. S. Hixson, M. A. Winkler, Thermophysical Properties of Molybdenum and Ruthenium
International Journal of Thermophysics, Vol. **13**, No. 3, p. 477, 1992.
- [180] S. V. Stankus, The Density of Vanadium and Chromium at High Temperatures
High Temperature, Vol. **31**, No. 4, p. 514, 1993.
- [181] W. Obendrauf, E. Kaschnitz, G. Pottlacher, and H. Jäger, Measurements of Thermophysical Properties of Nickel With a New Highly Sensitive Pyrometer Measurements of Thermophysical Properties of Nickel with a new highly sensitive pyrometer
International Journal of Thermophysics, Vol. **14**, No. 3, p. 417, 1993.
- [182] K. D. Maglič, N. Lj. Perović, and G. S. Vuković, Specific Heat and Electrical Resistivity of Niobium Measured by Subsecond Calorimetric Technique
Proceedings of the 12th Symposium on Thermophysical Properties, Boulder, 1994.
International Journal of Thermophysics, Vol. **15**, No. 5, pp. 963-972, 1994.
- [183] M. Beutl, G. Pottlacher, and H. Jäger, Thermophysical Properties of Liquid Iron
Proceedings of the 12th Symposium on Thermophysical Properties, Boulder, 1994.
International Journal of Thermophysics, Vol. **15**, No. 6, pp. 1323-1331, 1994.

- [184] E. Kaschnitz, J. L. McClure and A. Cezairliyan, Measurements of Thermophysical Properties of Nickel Near Its Melting Temperature by a Microsecond-Resolution Transient Technique
International Journal of Thermophysics, Vol. **15**, No. 4, p. 757, 1994.
- [185] K. D. Maglič, N. Lj. Perović, and G. S. Vuković, Specific heat and electric resistivity of molybdenum between 400 and 2500 K
High Temperatures - High Pressures, **29**, pp. 97-102, 1997.
- [186] J. Qin, M. Roesner-Kuhn, K. Drewes, U. Thiedemann, G. Kuppermann, B. Camin, R. Blume, and M. G. Frohberg, Spectral Emissivities at Wavelengths in the Range 500-653 nm, Enthalpies, and Heat Capacities of the Liquid Phases of Cobalt, Titanium, and Zirconium
High Temperature and Materials Science, Vol. **37**, pp. 129-141, 1997.

Appendix A

The Debye-function

A.1 Heat capacity at low temperatures.

The Debye-function In describing the low-temperature-behaviour of the heat capacity of a solidus a model - developed by Debye - is commonly used. According to him at low-temperatures the internal energy of a solidus can be described as

$$U - U_0 = 3 R_{gas} T \cdot D \left(\frac{\Theta_D}{T} \right) . \quad (\text{A.1})$$

Here are Θ_D the Debye-temperature and U_0 the zero-point internal energy of the substance. D , the Debye-function is the reduced version of the internal energy :

$$\frac{U - U_0}{3 R_{gas} T} = D(x) \equiv \frac{3}{x^3} \int_0^x \frac{dy y^3}{e^y - 1} \quad \text{with } x \equiv \frac{\Theta_D}{T} . \quad (\text{A.2})$$

Differentiating eq. A.1 for T results in the following heat capacity equation :

$$C_V(T) \equiv \frac{\partial U}{\partial T} = 3 R_{gas} [4 \cdot D(\Theta_D/T) - 3 \cdot P(\Theta_D/T)] . \quad (\text{A.3})$$

P in the above equation is the Planck-function (s. eq. A.6).

Using instead of eq. A.1 a different formula for the internal energy -

$$U - U_0 = \frac{9 R_{gas}}{\Theta_D^3} \int_0^{\Theta_D} \frac{dz z^3}{e^{z/T} - 1} \quad (\text{A.4})$$

results in an alternative expression for C_V :

$$C_V(T) \equiv \frac{\partial U}{\partial T} = \frac{9 R_{gas}}{x^3} \int_0^x \frac{dy e^y \cdot y^4}{(e^y - 1)^2} , \quad x = \frac{\Theta_D}{T} . \quad (\text{A.5})$$

Internal energy and heat capacity corresponding to the Debye-model can be seen in fig. A.1 on page 120.

The Planck-function

$$P(x) \equiv \frac{x}{e^x - 1} \quad (\text{A.6})$$

describes the mean energy of an oscillator and is introduced by Planck to calculate the electromagnetic radiation in a cavity (see e. g. p. 757 in [3]).

The reduced heat capacity It is convenient to calculate the heat capacity in a reduced form

$$C(x) \equiv \frac{C_V(T)}{3R_{gas}} = 4D(x) - 3P(x), \quad x = \Theta_D/T \quad (\text{A.7})$$

(cf. eq. A.3).

A.2 Expanding the functions at high temperatures

The Planck-function - Bernoulli-numbers For high temperatures - i.e. for small $x = \Theta_D/T$ values - the Planck-function can be developed as an x-polynomial. One sets

$$P(x) \equiv \sum_{n=0}^{\infty} Q_n x^n, \quad (\text{A.8})$$

then using the identity

$$\frac{e^x - 1}{x} = \sum_{m=1}^{\infty} \frac{x^{m-1}}{m!} = \sum_{n=0}^{\infty} \frac{x^n}{(n+1)!} \quad (\text{A.9})$$

one can expand 1 into a series :

$$1 = \frac{x}{e^x - 1} \cdot \frac{e^x - 1}{x} = \sum_{n=0}^{\infty} \sum_{i=0}^{\infty} Q_n \frac{x^{n+i}}{(i+1)!} \quad (\text{A.10})$$

The above Eq. can also be written as :

$$1 = \sum_{n=0}^{\infty} \sum_{i=0}^{\infty} Q_n \frac{x^{n+i}}{(i+1)!} = \sum_{k=0}^{\infty} A_k x^k, \quad (\text{A.11})$$

which gives

$$A_k = \sum_{n=0}^k \frac{Q_n}{(k+1-n)!}, \quad k = 0, 1, 2, \dots. \quad (\text{A.12})$$

Comparing the coefficients on both sides of eq. A.11 one has :

$$A_0 = 1 \quad \text{and} \quad A_k = 0 \quad \text{for} \quad \forall k > 0. \quad (\text{A.13})$$

eq. A.12 with eq. A.13 gives the following recursive way to calculate the coefficients Q_n :

$$Q_0 = 1 \quad \text{and} \quad Q_n = - \sum_{i=0}^{n-1} \frac{Q_i}{(n+1-i)!} \quad \text{for} \quad \forall n > 0. \quad (\text{A.14})$$

The "Bernoulli-numbers", B_n are closely related to the coefficients Q_n :

$$P(x) = \sum_{n=0}^{\infty} B_n \frac{x^n}{n!} \quad \text{respectively} \quad B_n = n! \cdot Q_n. \quad (\text{A.15})$$

eq. A.15 with eq. A.14 allows to calculate the Bernoulli-numbers as follows :

$$B_0 = 1 \quad \text{and} \quad (n+1) B_n = - \sum_{i=0}^{n-1} B_i \binom{n+1}{i} \quad \text{for} \quad \forall n > 0. \quad (\text{A.16})$$

Beside of B_1 all odd Bernoulli-numbers are zero (see e. g. [2], p. 405)

Inserting the first 2 Bernoulli-numbers into the eq. A.15 allows an expansion with the even - B_n -s only :

$$P(x) = 1 - \frac{x}{2} + P^x(x) \quad (A.17)$$

with

$$P^x(x) \equiv \sum_{n=2}^{\infty} B_n \frac{x^n}{n!} = \sum_{m=1}^{\infty} B_{2m} \frac{x^{2m}}{2m!} . \quad (A.18)$$

The above polynomial can be transformed to :

$$\begin{aligned} P^x(x) &= \frac{x^2}{1 \cdot 2} \sum_{m=1}^{\infty} B_{2m} \frac{2! x^{2(m-1)}}{2m!} = \\ &= \frac{x^2}{1 \cdot 2} \left[B_2 + \frac{x^2}{3 \cdot 4} \sum_{m=2}^{\infty} B_{2m} \frac{4! x^{2(m-2)}}{2m!} \right] \\ &= \frac{x^2}{1 \cdot 2} \left[B_2 + \frac{x^2}{3 \cdot 4} \left[B_4 + \frac{x^2}{5 \cdot 6} \sum_{m=3}^{\infty} B_{2m} \frac{6!}{2m!} x^{2(m-3)} \right] \right] \\ &\dots \\ &\dots \\ &\dots \end{aligned} \quad (A.19)$$

Using the first 16 B_n -values presented in the table A.1 gives :

$$\begin{aligned} P^x(x) &= \frac{x^2}{2} \left[\frac{1}{6} + \frac{x^2}{12} \left[\frac{-1}{30} + \frac{x^2}{30} \left[\frac{1}{42} + \frac{x^2}{56} \left[\frac{-1}{30} + \frac{x^2}{90} \left[\frac{5}{66} \right. \right. \right. \right. \right. \\ &\quad \left. \left. \left. \left. \left. \left. + \frac{x^2}{132} \left[\frac{-691}{2730} + \frac{x^2}{182} \left[\frac{7}{6} + \frac{x^2}{240} \frac{-3617}{510} \right] \right] \right] \right] \right] \right] . \end{aligned} \quad (A.20)$$

Setting $y = x^2/12$ turns P^x into :

$$\begin{aligned} P^x(x) &= y \left[1 - \frac{y}{5} \left[1 - \frac{2y}{7} \left[1 - \frac{3y}{10} \left[1 - \frac{10y}{33} \right. \right. \right. \right. \right. \\ &\quad \left. \left. \left. \left. \left. \left. \cdot \left[1 - \frac{691y}{2275} \left[1 - \frac{210y}{691} \left[1 - y \frac{3617}{11900} \right] \right] \right] \right] \right] \right] \right] , \\ \text{with } y &= \frac{x^2}{12} . \end{aligned} \quad (A.21)$$

The Debye-function The expansion of $P(x)$, eq. A.15 allows also a developement for the Debye-function:

$$D(x) = \frac{3}{x^3} \int_0^x dy \frac{y^3}{e^y - 1} = \frac{3}{x^3} \int_0^x dy y^2 P(y) =$$

$$\begin{aligned}
&= \frac{3}{x^3} \int_0^x dy y^2 \sum_{n=0}^{\infty} B_n \frac{y^n}{n!} = \frac{3}{x^3} \int_0^x dy \sum_{n=0}^{\infty} B_n \frac{y^{n+2}}{n!} = \\
&= \frac{3}{x^3} \sum_{n=0}^{\infty} \frac{B_n}{n!} \int_0^x dy y^{n+2} \equiv \sum_{n=0}^{\infty} B_n \frac{3}{n+3} \frac{x^n}{n!}
\end{aligned} \tag{A.22}$$

so in the consequence one has

$$D(x) = \sum_{n=0}^{\infty} d_n \frac{x^n}{n!} \quad \text{with} \quad d_n = \frac{3}{n+3} B_n \tag{A.23}$$

D can be described also with the help of an "even"-polynomial (compare eq. A.17):

$$D(x) = 1 - \frac{3}{8} x + D^x(x) \tag{A.24}$$

with

$$D^x(x) \equiv \sum_{m=1}^{\infty} d_{2m} \frac{x^{2m}}{2m!} . \tag{A.25}$$

Using the first 16 d_n -values presented in the table A.1 gives :

$$\begin{aligned}
D^x(x) &= \frac{x^2}{2} \left[\frac{1}{10} + \frac{x^2}{12} \left[\frac{-1}{70} + \frac{x^2}{30} \left[\frac{1}{126} + \frac{x^2}{56} \left[\frac{-1}{110} + \frac{x^2}{90} \cdot \right. \right. \right. \right. \\
&\cdot \left. \left. \left. \left. \left[\frac{5}{286} + \frac{x^2}{132} \left[\frac{-691}{13650} + \frac{x^2}{182} \left[\frac{7}{34} + \frac{x^2}{240} \frac{-3617}{3230} \right] \right] \right] \right] \right] \cdot
\end{aligned} \tag{A.26}$$

This can be transformed into :

$$\begin{aligned}
D^x(x) &= \frac{3y}{5} \left[1 - \frac{y}{7} \left[1 - \frac{2y}{9} \left[1 - \frac{27y}{110} \left[1 - \frac{10y}{39} \right. \right. \right. \right. \\
&\cdot \left. \left. \left. \left. \left[1 - \frac{691y}{2625} \left[1 - \frac{3150y}{11747} \left[1 - y \frac{3617}{13300} \right] \right] \right] \right] \right] \cdot \\
&\text{with} \quad y = \frac{x^2}{12} .
\end{aligned} \tag{A.27}$$

The reduced heat capacity According to eq. A.7 the heat capacity can be calculated as Using the evaluations for D , eq. A.23 and P , eq. A.15 the above Eq. can be transformed :

$$C(x) = 4D(x) - 3P(x) , \quad x = \Theta_D/T . \tag{A.28}$$

$$C(x) = 4 \sum_{n=0}^{\infty} d_n \frac{x^n}{n!} - 3 \sum_{n=0}^{\infty} B_n \frac{x^n}{n!} = \sum_{n=0}^{\infty} [4d_n - 3B_n] \frac{x^n}{n!} , \tag{A.29}$$

resulting in

$$C(x) = \sum_{n=0}^{\infty} c_n \frac{x^n}{n!}$$

with (A.30)

$$c_n = 4 d_n - 3 B_n = - 3 B_n \frac{n-1}{n+3} = -(n-1) d_n .$$

For the reduced heat capacity there exists a complete "even"-evaluation :

$$C(x) = 1 + C^x(x) (A.31)$$

with

$$C^x(x) \equiv \sum_{m=1}^{\infty} c_{2m} \frac{x^{2m}}{2m!} . (A.32)$$

Using the first 16 c_n -values presented in the table A.1 results in :

$$\begin{aligned} C^x(x) = & \frac{x^2}{2} \left[\frac{-1}{10} + \frac{x^2}{12} \left[\frac{3}{70} + \frac{x^2}{30} \left[\frac{-5}{126} + \frac{x^2}{56} \left[\frac{7}{110} + \frac{x^2}{90} \right. \right. \right. \right. \\ & \left. \left. \left. \left. + \frac{-45}{286} + \frac{x^2}{132} \left[\frac{7601}{13650} + \frac{x^2}{182} \left[\frac{-91}{34} + \frac{x^2}{240} \frac{10851}{646} \right] \right] \right] \right] \right] . \end{aligned} (A.33)$$

Inserting $y = x^2/12$ transforms C^x into :

$$\begin{aligned} C^x(x) = & -\frac{3y}{5} \left[1 - \frac{3y}{7} \left[1 - \frac{10y}{27} \left[1 - \frac{189y}{550} \left[1 - \frac{30y}{91} \right. \right. \right. \right. \\ & \left. \left. \left. \left. + \frac{7601y}{23625} \left[1 - \frac{40950y}{129217} \left[1 - y \frac{10851}{34580} \right] \right] \right] \right] \right] , \\ \text{with } y = & \frac{x^2}{12} . \end{aligned} (A.34)$$

A.3 Expanding the functions at low temperatures

The Planck-function The Planck-function can also be expanded for low temperatures - i.e. for high $x = \Theta_D/T$ values. With the help of the summation-formula for geometrical series one has (see e. g. p. 759 in [3]):

$$P(x) = \frac{x}{e^x - 1} = \frac{x}{e^x} \frac{1}{1 - \frac{1}{e^x}} = \frac{x}{e^x} \sum_{n=0}^{\infty} \left(\frac{1}{e^x} \right)^n = \sum_{n=1}^{\infty} \frac{x}{e^{nx}} . (A.35)$$

The Debye-function Using the above expansion for $P(x)$ the integral in the eq. A.2 can be evaluated :

$$\begin{aligned} \int_0^x \frac{dy y^3}{e^y - 1} = & \left[\int_0^{\infty} - \int_x^{\infty} \right] \frac{dy y^3}{e^y - 1} = \left[\int_0^{\infty} - \int_x^{\infty} \right] dy \sum_{n=1}^{\infty} \frac{y^3}{e^{ny}} = \\ = & \sum_{n=1}^{\infty} \int_0^{\infty} \frac{dy y^3}{e^{ny}} - \sum_{n=1}^{\infty} \int_x^{\infty} \frac{dy y^3}{e^{ny}} . \end{aligned} (A.36)$$

Using the relations

$$\Gamma(n + 1) \equiv n! = \int_0^\infty dy y^n e^{-y} \quad (\text{A.37})$$

and

$$\zeta(4) \equiv \sum_{n=1}^{\infty} \frac{1}{n^4} = \frac{\pi^4}{90} \quad (\text{A.38})$$

(see e. g. p. 406 in [2]) turns the first integral into

$$\sum_{n=1}^{\infty} \int_0^\infty \frac{dy y^3}{e^{ny}} = \sum_{n=1}^{\infty} \frac{1}{n^4} \int_0^\infty dz z^3 e^{-z} = \sum_{n=1}^{\infty} \frac{3!}{n^4} = \frac{\pi^4}{15} . \quad (\text{A.39})$$

The second integral can be calculated as follows :

$$\begin{aligned} \sum_{n=1}^{\infty} \int_x^\infty \frac{dy y^3}{e^{ny}} &= \sum_{n=1}^{\infty} \frac{1}{n^4} \int_{nx}^\infty dz z^3 e^{-z} = \\ &= \sum_{n=1}^{\infty} \frac{e^{-nx}}{n^4} [(nx)^3 + 3(nx)^2 + 6(nx) + 6] . \end{aligned} \quad (\text{A.40})$$

Comparing the equations eq. A.2 eq. A.39 and eq. A.40 results in the following low-temperature expansion for the Debye-function:

$$D(x) = \frac{\pi^4}{5x^3} - 3 \sum_{n=1}^{\infty} \left[1 + \frac{3}{nx} \left(1 + \frac{2}{nx} \left(1 + \frac{1}{nx} \right) \right) \right] \frac{e^{-nx}}{n} . \quad (\text{A.41})$$

The reduced heat capacity The above expansion together with the formula for $P(x)$, eq. A.35 evaluates the heat capacity at low-temperatures as follows :

$$\begin{aligned} C(x) &= 4D(x) - 3P(x) = \frac{4\pi^4}{5x^3} + \\ &- 3 \sum_{n=1}^{\infty} \left[nx + 4 \left(1 + \frac{3}{nx} \left(1 + \frac{2}{nx} \left(1 + \frac{1}{nx} \right) \right) \right) \right] \frac{e^{-nx}}{n} . \end{aligned} \quad (\text{A.42})$$

n	B_n	d_n	c_n
0	1	1	1
1	$-\frac{1}{2}$	$-\frac{3}{8}$	0
2	$\frac{1}{6}$	$\frac{1}{10}$	$-\frac{1}{10}$
4	$-\frac{1}{30}$	$-\frac{1}{70}$	$\frac{3}{70}$
6	$\frac{1}{42}$	$\frac{1}{126}$	$-\frac{5}{126}$
8	$-\frac{1}{30}$	$-\frac{1}{110}$	$\frac{7}{110}$
10	$\frac{5}{66}$	$\frac{5}{286}$	$-\frac{45}{286}$
12	$-\frac{691}{2730}$	$-\frac{691}{13650}$	$\frac{7601}{13650}$
14	$\frac{7}{6}$	$\frac{7}{34}$	$-\frac{91}{34}$
16	$-\frac{3617}{510}$	$-\frac{3617}{3230}$	$\frac{10851}{646}$

Table A.1: The first 16 coefficients of the developement of $P(x)$, $D(x)$ and $C(x)$

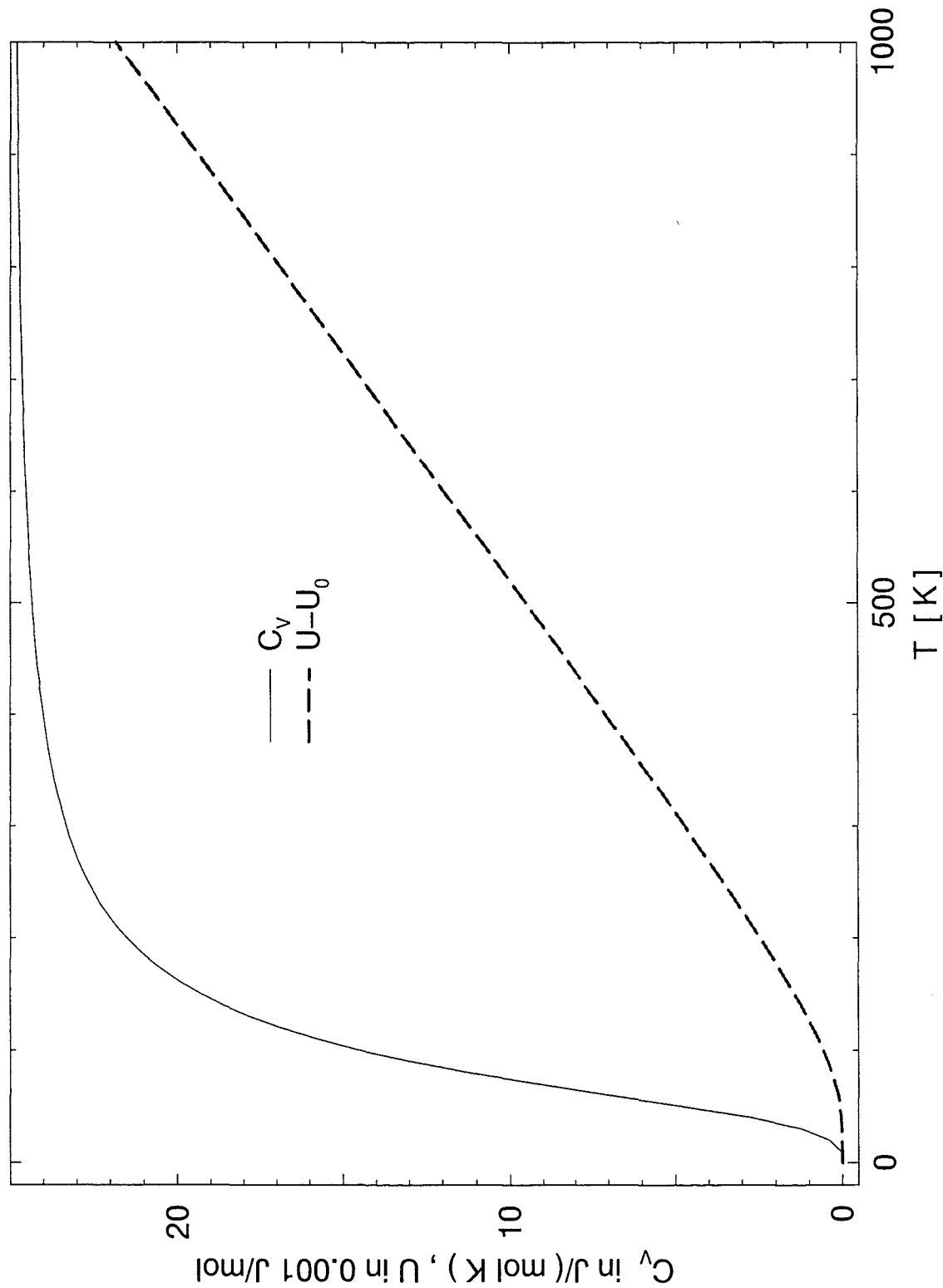


Figure A.1: Caloric properties of a material with $\Theta_D = 350$ K after Debye

Appendix B

Speakeasy routines to calculate caloric properties

B.1 Calculating the heat capacity

DEBEC calculates the reduced heat capacity, $C = FX$ as a function of $X = \Theta_D$ for all x-values.

```
1 FUNCTION DEBEC(X,RC,FP)
2 $ CV AFTER DEBYE                               90/09/27
3 FN=X-X; RC=FN+1.E-10; FP=FN+1
4 XG=2.4,2.7,3.3,4.2,5.7,8.7,18.,24.
5 DISTRI(X,XG,MY,JAM)
6 JU=LOCS(MY .LE. 0)
7 IF(SUM(JU) .LT. 1) GOTO L4
8 Z=X(JU); Y=Z*Z/12
9 FX(JU)=1+DEBECPX(Y,R)
10 RC(JU)=R
11 L4: JO=LOCS(MY .GT. 0)
12 IF(SUM(JO) .LT. 1) GOTO L9
13 Z=X(JO)
14 FP(JO)=77.92727282/(Z*Z*Z)
15 FOR K=1,JAM-1
16 JK=LOCS(MY .EQ. K)
18 IF(K .GT. 7) GOTO L7
19 M=8-K
20 W=X(JK)
21 DEBECEX(W,M,F7,R7)
22 FN(JK)=F7
24 L6: NEXT K
```

122 APPENDIX B. SPEAKEASY ROUTINES TO CALCULATE CALORIC PROPERTIES

DEBEC (cont.)

```
25 L7: FX(JO)=FP(JO)-FN(JO)
23 RC(JK)=R7
26 L9: RETURN FX
27 END
```

DEBECPX calculates the even-part of the reduced heat capacity, $C^e = FX$ as a function of X for small x-values according to the equations eq. A.31 and eq. A.34.

```
1 FUNCTION DEBECPX(Y,R)
2 $ CALCULATES CV AT HIGH TEMPERATURES , T > THETD      90/09/28
3 $ Y=X*X/12
4 FX=1-(30*Y/91)*(1-(40950*Y/129217)*(1-10851*Y/34580))
5 FX=1-(10*Y/27)*(1-(189*Y/550)*(1-(7601*Y/23625)*FX ))
6 FX=-(3*Y/5)*(1-(3*Y/7)*FX )
7 R=Y**8*(27*3617)/(49*125*11*13*17*19)
8 RETURN FX
9 END
```

DEBECEX calculates approximating members, FN for C (X) in the low-T description eq. A.42 as a function of $X = \Theta_D/T$ and M = n.

```
1 SUBROUTINE DEBECEX(X,M,FN,RN)
2 $ CALCULATES APPROXIMATING MEMBERS FOR DEBEC      90/09/27
3 N=INTS(M); N1=N; X1=X
4 MELD X1 N1
5 AX=A2D(NOELS(X),M:X1)*N
6 AY=1/AX
7 MEN=(AX+4*(1+3*AY*(1+2*AY*(1+AY)))*EXP(-AX))
8 FN=3*MEN/N
9 RN=FN(,M)
10 FN=SUMROWS(FN)
11 RETURN
12 END
```

B.2 Calculating the enthalpy

DEBEH calculates the reduced enthalpy, $D = FX$ as a function of $X = \Theta_D/T$ for all x-values.

```

1  FUNCTION DEBEH(X,RH,FP)
2  $ H AFTER DEBYE 90/09/27
3  FN=X-X; RH=FN+1.E-10; FP=FN+1
4  XG=2.4,2.7,3.3,4.2,5.7,8.7,18.,24.
5  DISTRI(X,XG,MY,JAM)
6  JU=LOCS(MY .LE. 0)
7  IF(SUM(JU) .LT. 1) GOTO L4
8  Z=X(JU); Y=Z*Z/12
9  FX(JU)=1-(3/8)*Z+DEBEHPX(Y,R)
10 RH(JU)=R
11 L4: JO=LOCS(MY .GT. 0)
12 IF(SUM(JO) .LT. 1) GOTO L9
13 Z=X(JO)
14 FP(JO)=19.48181821/(Z*Z*Z)
15 FOR K=1,JAM-1
16 JK=LOCS(MY .EQ. K)
17 IF(SUM(JK) .LT. 1) GOTO L6
18 IF(K .GT. 7) GOTO L7
19 M=8-K
20 W=X(JK)
21 DEBEHEX(W,M,F7,R7)
22 FN(JK)=F7
23 RH(JK)=R7
24 L6: NEXT K
25 L7: FX(JO)=FP(JO)-FN(JO)
26 L9: RETURN FX
27 END

```

DEBEHPX calculates the even-part of the reduced enthalpy, $D^x = FX$ as a function of X for small x-values according to the equations eq. A.24 and eq. A.27.

```

1  FUNCTION DEBEHPX(Y)
2  $ CALCULATES H AT HIGH TEMPERATURES , T > THETD      90/09/28
3  $ Y=X*X/12
4  FX=1-(691*Y/2625)*(1-(3150*Y/11747)*(1-3617*Y/11747))
5  FX=1-(2*Y/9)*(1-(27*Y/110)*(1-(10*Y/39)*FX ))
6  FX=(3*Y/5)*(1-(Y/7)*FX )
7  R=Y**8*(9*3617)/(49*625*11*13*17*19)
8  RETURN FX
9  END

```

DEBEHEX calculates approximating members, FN for D (X) in the low-T description eq. A.41 as a function of $X = \Theta_D/T$ and M = n.

124 APPENDIX B. SPEAKEASY ROUTINES TO CALCULATE CALORIC PROPERTIES

```

1 SUBROUTINE DEBEHEX(X,M,FN,RN)
2 $ CALCULATES APPROXIMATING MEMBERS FOR DEBEH          90/09/27
3 N=INTS(M); N1=N; X1=X
4 MELD X1 N1
5 AX=A2D(NOELS(X),M:X1)*N
6 AY=1/AX
7 MEN=(1+3*AY*(1+2*AY*(1+AY)))*EXP(-AX)
8 FN=3*MEN/N
9 RN=FN(,M)
10 FN=SUMROWS(FN)
11 RETURN
12 END

```

B.3 Auxiliary routines

FINOM subdivides the array X uniformly. Each point in X turns to GR points in XU. MU is the index of X in XU: XU(MU) = X.

```

1 SUBROUTINE FINOM(X,XU,MU,GR)
2 $ XU = PARTITION ( X ) ; MU = INDEX( X IN XU )          90/02/05
3 $ () => 1 () ... GR ()
4 ARMO99(X)
5 XU=X; MU=INDEXER(XU)
6 IF(GR .LE. 1) RETURN
7 NY=NOELS(X); GL=GR-1
8 R=ELIMELS(X,NY); S=ELIMELS(X,1)
9 DR=(S-R)/GR
10 FOR I=1,GL
11 XU=XU,(R+I*DR)
12 NEXT I
13 XU=RANKED(XU)
14 MU=INDEXER(R)
15 MU=1,GR*MU+1
16 END

```

DISTRI creates a step-function MY (Y) on Y according to the partition YG in Y.

```

1 SUBROUTINE DISTRI(Y,YG,MY,JAM)
2 $ MY ( Y ) = STEP-FUNCTION TO THE PARTITION YG          90/02/02
3 ARMO99(Y)
4 IF(CLASS(YG) .NE. 5) YG=A1D(2:YG,MAX(Y))
5 YG=UNIQUE(YG);YG=RANKED(YG)
6 IF(MIN(Y) .EQ. MIN(YG)) YG=ELIMELS(YG,1)
7 IF(MAX(Y) .GT. MAX(YG)) YG=YG,MAX(Y)
8 JAM=NOELS(YG);MY=Y-Y
9 FOR J=1,JAM
10 WHERE(Y-YG(J) .GT. 0) MY=J
11 NEXT J
12 END

```

ARMO99 checks the object X to be a monotonously increasing array.

```

1 SUBROUTINE ARMO99(X)
2 $ TESTING X FOR 1D-ARRAY AND MONOTONITY.      90/10/16
3 IF(CLASS(X) .EQ. 5) GOTO L1
4 ARGNAM(1) "ISN'T AN 1D-ARRAY"; MANUAL
5 L1: IF(NOELS(X) .LE. 1) RETURN
6 I=INDEXER(X);J=RANKER(X)
7 MONOTON=I-J; MONOTON=ABS(MONOTON)
8 IF(SUM(MONOTON) .EQ. 0) RETURN
9 ARGNAM(1) "ISN'T A MONOTONIC-INCREASING ARRAY !"; MANUAL
10 END

```

P1 is a routine for testing the programs DEBEC and DEBEH.

```

1 PROGRAM
2 $ TESTING DEBEC AND DEBEH                      90/09/28
3 ASK("LAST Z =: ( 0 = OLD RANGE )","ZM =")
4 IF(ZM .LE. 0) GOTO L2
5 ZG=2.4,2.7,3.3,4.2,5.7,8.7,18.,24.
6 ZGM=ZG-0.001; ZGP=ZG+0.001; ZG=1.5,ZG,ZM
7 FINOM(ZG,Z,JF,10)
8 Z=Z,ZGM,ZG,ZGP; Z=UNIQUE(Z)
9 OKO=JF,JF+1,JF-1; OKO=UNIQUE(OKO)
10 IK=LOCS(OKO .LE. 0)
11 IF(SUM(IK) .LE. 0) GOTO L2
12 OKO=ELIMELS(OKO,IK)
13 L2: CV=DEBEC(Z,RC,FC)
14 R1=RC(OKO)/FC(OKO)
15 TABULATE(Z(OKO),CV(OKO),RC(OKO),R1)
16 FZC=LOG10(RC)
17 H=DEBEH(Z,RH,FH)
18 R2=RH(OKO)/FH(OKO)
19 TABULATE(Z(OKO),H(OKO),RH(OKO),R2)
20 FZH=LOG10(RH)
21 END

```

Bibliography

- [1] S. Cohen, S. C. Pieper, The Speakeasy-3 Reference Manual,
Argonne National Laboratory, Dec. 1977.
- [2] R. Courant, Vorlesungen über Differential- und Integralrechnung, I.
Dritte Auflage. Springer-Verlag 1955
- [3] W. Weizel, Lehrbuch der Theoretischen Physik, I.
Zweite Auflage. Springer-Verlag 1955